Materials Today Bio 23 (2023) 100787

Contents lists available at ScienceDirect

Materials Today Bio

journal homepage: www.journals.elsevier.com/materials-today-bio

Applications of flexible electronics related to cardiocerebral vascular system

Runxing Lin [a,b,1], Ming Lei [a,1], Sen Ding [a], Quansheng Cheng [a], Zhichao Ma [d], Liping Wang [b], Zikang Tang [a], Bingpu Zhou [a,**], Yinning Zhou [a,c,*]

[a] Joint Key Laboratory of the Ministry of Education, Institute of Applied Physics and Materials Engineering, University of Macau, Avenida da Universidade, Taipa, Macau, 999078, China

[b] Brain Cognition and Brain Disease Institute, Shenzhen Institute of Advanced Technology, Chinese Academy of Sciences, Shenzhen, 518055, China

[c] Department of Physics and Chemistry, Faculty of Science and Technology, University of Macau, Avenida da Universidade, Taipa, Macau, 999078, China

[d] Institute of Medical Robotics, School of Biomedical Engineering, Shanghai Jiao Tong University, No.800 Dongchuan Road, Shanghai, 200240, China

A B S T R A C T

Ensuring accessible and high-quality healthcare worldwide requires field-deployable and affordable clinical diagnostic tools with high performance. In recent years, flexible electronics with wearable and implantable capabilities have garnered significant attention from researchers, which functioned as vital clinical diagnostic-assisted tools by real-time signal transmission from interested targets in vivo. As the most crucial and complex system of human body, cardiocerebral vascular system together with heart-brain network attracts researchers inputting profuse and indefatigable efforts on proper flexible electronics design and materials selection, trying to overcome the impassable gulf between vivid organisms and rigid inorganic units. This article reviews recent breakthroughs in flexible electronics specifically applied to cardiocerebral vascular system and heart-brain network. Relevant sensor types and working principles, electronics materials selection and treatment methods are expounded. Applications of flexible electronics related to these interested organs and systems are specially highlighted. Through precedent great working studies, we conclude their merits and point out some limitations in this emerging field, thus will help to pave the way for revolutionary flexible electronics and diagnosis assisted tools development.

1. Introduction

Cardiocerebral vascular system, which includes the blood, heart and blood vessels, together with heart-brain network functions as the most crucial and complex role in supporting the normal vital movement of human beings [1]. Primarily, the system triggered by the heart pumping is responsible for the transportation of nutrients [2], oxygen-rich/deoxygenated blood [3], other compulsory biomolecules [4] and metabolic waste [5]. Dysfunction, abnormalities or any injuries occurring on random parts of the cardiovascular system may lead to severe health complications [6–9]. Among the diseases with extremely high mortality worldwide, deaths due to cardiovascular diseases (CVDs) account for 31% of the global death toll each year, reaching 17 million people [10]. Besides, neurological diseases related to the heart-brain network are the second leading disease causing death and disability worldwide. Cerebroma also belongs to one of the most deadly cancer types with an extremely rare cure rate [11]. Therefore, thorough indicators monitoring of cardiac, cerebral and cardiocerebral vascular systems is of prominent significance for clinical pre-diagnosis, morbidity/mortality reduction and instant drug or intervention therapy [10]. Flexible electronics and wearable sensors functioned to reflect the real-time body signals of cardiocerebral vascular system, not only for patients with chronic and acute diseases, are emerging upon the huge market demand.

Presently, electronic devices find application in an increasingly diverse array of fields [12–14], encompassing domains such as biomedicine, where they are employed to monitor various human physiological parameters [15]. For wearable and implantable devices, the mechanical stiffness of traditional sensor devices can cause discomfort to the soft tissue in contact, due to the impassable gulf between vivid organisms and rigid inorganic units. Wearable devices with a rigid hardness that are typically mounted on the skin may cause skin discomfort and skin irritation, and even lead to rashes and allergic reactions [16–20]. The situation will get even more complicated in

* Corresponding author. Joint Key Laboratory of the Ministry of Education, Institute of Applied Physics and Materials Engineering, University of Macau, Avenida da Universidade, Taipa, Macau, 999078, China.

** Corresponding author.

E-mail addresses: bpzhou@um.edu.mo (B. Zhou), ynzhou@um.edu.mo (Y. Zhou).

[1] These two authors contributed equally.

https://doi.org/10.1016/j.mtbio.2023.100787

Received 6 June 2023; Received in revised form 14 August 2023; Accepted 28 August 2023

Available online 30 August 2023

implantable devices because rigid devices may also induce inflammatory responses. Also, after long-term integration with organs, the functionality of sensors may become unstable due to the mismatch between the chemical composition and mechanical properties of rigid devices and biological tissues. Then the resulting scar tissue may also reduce the sensing of electronic devices [16,21,22]. In addition, rigid sensors often cannot fit closely with skin or tissue which exhibit inherent curvature and surface texture, thus may affect the accurate acquisition of signals [16,23,24]. Furthermore, the performance of sensors is compromised due to the unsatisfactory biocompatibility imposed by fluidic and hydrophilic bio-tissues [25,26]. In the domain of cardiocerebral vascular systems, flexible electronic devices offer an array of distinctive advantages, effectively surmounting the challenges posed by conventional rigid counterparts in this realm. Beyond their inherent flexibility and bendability, these devices also boast attributes of wearability [27], comfort [10], implantability [28], biocompatibility [29], prolonged monitoring and treatment capabilities [30], real-time monitoring [31], heightened sensitivity, and enhanced accuracy [10]. Given the protracted nature of cardiocerebral vascular diseases, prolonged monitoring is often necessitated. However, conventional rigid devices tend to be sizeable, cumbersome, and ill-suited to conform closely to intricate biological tissue contours or wearable placement. In contrast, flexible electronic devices can be rendered thin and lightweight, adept at seamlessly conforming to bodily curves and contours, thereby lending themselves to convenient surface adherence [27]. This innate adaptability proves advantageous for medical monitoring and treatment applications, such as heart function assessment [32], brain activity observation [33], and blood flow tracking [34]. Moreover, as alluded to earlier, the utilization of implantable rigid devices may incite inflammatory responses, thereby potentially compromising sensing efficacy. In contrast, flexible sensors predominantly employ biocompatible materials characterized by low irritation and biotoxicity, consequently diminishing the likelihood of immune reactions [29]. Notably, owing to their superior resilience and stability, implanted flexible sensors circumvent the risk of damage or discomfort upon contact with the host organism. This attribute enables extended and more profound observations [35] as well as real-time monitoring [31] of physiological parameters within the intricacies of the cardiocerebral vascular system. Such attributes are particularly advantageous for patients necessitating prolonged monitoring, significantly contributing to the diagnosis, treatment, and overall management of diseases. Notably, rigid devices might contend with signal distortion or inaccuracies stemming from improper placement or individual movements. In sharp contrast, owing to their enhanced conformity to the body's contours, flexible electronic devices yield heightened sensitivity signals, thereby facilitating the discernment of nuanced physiological signal fluctuations [10]. Therefore, smart flexible and soft sensors design and materials selection provide possible solutions for aforementioned challenges. Researchers input profuse and indefatigable efforts on working principles developing and novel materials generation, while the latter needs characteristics with light weight, natural fit on tissues, and better signal quality [36–40].

Different from existing review articles [16,36,41–45] that primarily focus on the fundamentals of flexible electronics and their applications in all aspects, this review mainly summarizes recent breakthroughs of flexible electronics specifically applied to cardiocerebral vascular system and heart-brain network, aiming to provide relatively thoroughly reference. In juxtaposition with pertinent reviews within the field [28,46–48], this review stands out for its comprehensiveness concerning flexible electronic devices dedicated to the cardiocerebral vascular system. It not only delves extensively into the underlying principles and materials but also furnishes illustrative instances of their practical applications. For the first section, relevant sensor types and working principles were illustrated. Then the alternative electronic materials and treatment methods for various purposes are expounded. After that, applications of flexible electronics related to these interested organs and systems are specially highlighted. Finally, we conclude their merits and point out some limitations in this emerging field, thus will help to pave the way for revolutionary flexible electronics, diagnosis assisted tools development and human-computer interaction field.

2. Working principles

As the most crucial indicator in measuring human health condition, several parameters of the cardiocerebral vascular system and the heart-brain network, such as blood pressure (BP), blood oxygen saturation (SpO_2), blood glucose (BG), etc., need to be monitored in real-time. For instance, by tracking changes in SpO_2 over time, we can achieve seasonable alerts for heart failure, sleep apnea, and other parlous conditions. Scientists are inspired by the color-changing characteristics of the hemoglobin molecules, thus creating commercial optical oximeters to enable real-time, non-invasive testing of blood oxygen levels. Therefore, by exploiting the specific characteristics of these physiological signals, we can classify existing wearable or implantable sensors into bioelectrical, optical, mechanoelectrical, electrochemical, temperature and other types, as shown in Fig. 1. In subsequent chapters, the working principle of various sensor types will be illustrated in detail.

2.1. Bioelectrical sensors

Bioelectrical signals relating to the state of tissues or organs alive are widely used for clinical treatment, behavior analysis and disease prevention. Among the cardiocerebral vascular system and heart-brain network of human body, bioelectrical sensors based on electrocardiography (ECG) and electroencephalogram (EEG) signals provide the most critical messages for heart or brain diseases such as epilepsy, dementia, and cerebroma [53]. Therefore, we will mainly focus on the illustration of bioelectric sensors in these two areas.

2.1.1. ECG sensor

ECG is a technique for recording the heart's electrical signal during every cardiac cycle [54]. The depolarization and repolarization of cardiac cells contribute to the generation of the cardiac electrical activity. According to the standard signal image, the composition of the ECG signals includes P-wave, PR-segment, QRS-complex, ST-segment, T-wave, U-wave, PR interval and QT interval. Among them, the P-wave, which is atrial depolarization, represents atrial contraction; while QRS- complex wave means ventricular depolarization and T-wave represents ventricular repolarization. These items are used as the characteristic waveforms depicting the ECG signal in one cardiac cycle. The PR- segment connects P-wave and QRS-complex, while the ST-segment connects QRS-complex and T-wave, which is a process of slow ventricular repolarization. The U-wave is behind the T-wave. The time between the initial P-wave and the initial QRS-complex is represented by the PR interval. The time between the beginning of the QRS-complex and the end of the T-wave is represented by the QT interval [55]. Under a rest state of a human body, compared with the outer potential of cardiomyocytes, its inner membrane potential is more negative, which is called resting potential. That is, the inside is negatively polarized relative to the outside, and there are excessive potassium ions (K^+) inside the cell, while luxuriant sodium ions (Na^+) are outside. This phenomenon appears due to the high concentration of K^+ efflux in cardiac cells. When the myocardium contracts, the permeability of the cell membrane changes, Na^+ enters and K^+ effuses, thereby depolarizing the cell. Hence, when cardiac cells are excited, they depolarize and then repolarize to form an action potential (AP) [56]. As we know, the most critical part of one wearable ECG sensor is the skin electrode interface [57]. Skin electrodes measure the ECG by making direct contact with the skin surface by measuring tiny potential differences across the skin surface generated by the electrical activity of cardiac cycle. The conduction pathway and sequence of the cardiac action potential during the cardiac cycle are as follows: sinoatrial node (SA node), internodal tract,

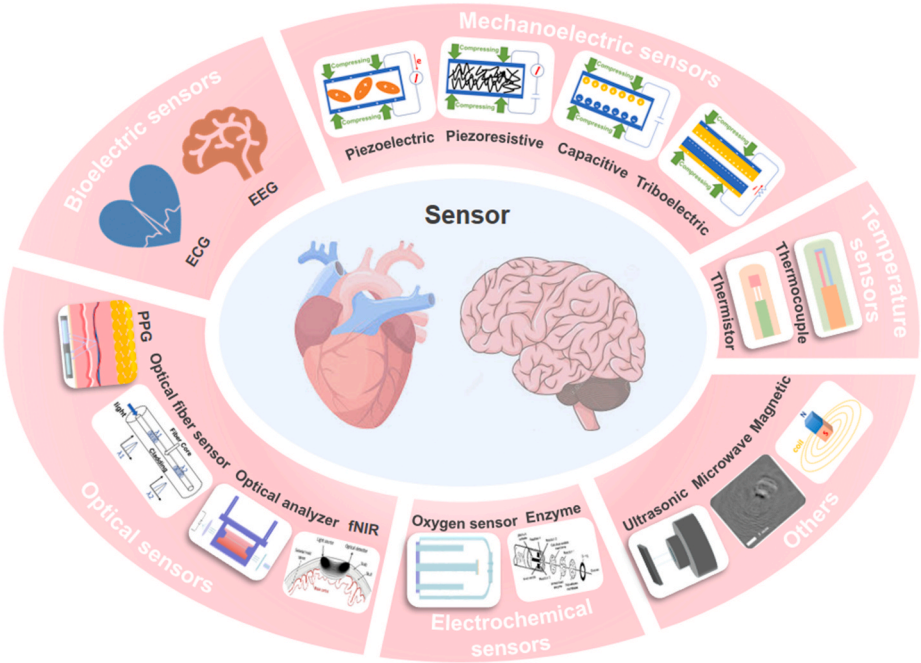

Fig. 1. Flexible sensors related to cardiocerebral vascular system. Bioelectric sensors include ECG and EEG. Mechanoelectric sensors include piezoelectric sensor, piezoresistive sensor, capacitive sensor, and triboelectric sensor (Mechanoelectric sensors possess the capability to transduce physical mechanical quantities, such as pressure, into electrical signals. Taking piezoelectric sensors as an example, the piezoelectric effect is a distinctive material characteristic observed in certain crystal materials, wherein the application of force or pressure results in a redistribution of electric charges. This alteration in charge distribution can be sensed via electrodes in contact with the crystal surface, thereby generating an electrical signal. The principles governing the remaining mechano-electric sensors bear resemblance to those of piezoelectric sensors.). Temperature sensors include thermocouple sensor (A thermocouple is integrated at the tip of a medical catheter to measure temperature. When there is a temperature change, the dissimilar metals in the thermocouple generate a current, resulting in a voltage that is related to the temperature. Through appropriate calculations, the relevant temperature information can be obtained from the voltage generated.), thermistor sensor (The tip of a medical catheter is equipped with a thermistor, which is used to measure temperature. The thermistor is located at the very end of the catheter. As the temperature fluctuates, the resistance of the thermistor will vary accordingly.). Optical sensors include PPG sensor (LEDs placed on the side of the fingertip emit a light source that travels through human tissue. After the light is partially absorbed by the tissue, the PD placed on the same side will detect the reflected light), FBG sensor (FBG sensor, which exploits the reflective spectral characteristics of a grating to gauge strain or temperature variations. When the sensor is influenced, changes in the refractive index within the grating lead to shifts in the Bragg wavelength. By analyzing the spectral changes, one can measure and interpret these wavelength shifts, thus enabling strain or temperature measurements), optical analyzer [49] (The optical analyzer used to detect the concentration of metabolites has a cuvette that can provide a site for a series of chemical reactions between the metabolites and specific oxidases, and then fluoresces under the excitation light source, and the photodiode converts the fluorescence into an electrical signal) and functional near-infrared spectroscopy (fNIR) (Diagram of optically sensitive regions (banana-shaped regions) in the human brain's near-infrared (NIR). After the near infrared light source illuminates the area, the transmitted light or reflected light is received by the detector) [50]. Electrochemical sensors include oxygen sensor (The Clark electrode, which consists of an anode and a cathode immersed in an electrolyte solution, has an oxygen-permeable membrane that allows oxygen molecules to enter, and is coated on the cathode, where the oxygen molecules undergo electrolytic reduction to generate current) and electrochemical sensors based on enzyme electrodes (The enzyme on the electrode reacts with the substance, and the resulting change is measured to obtain the concentration of the substance to be measured) [51]. Other sensors include an ultrasonic sensor (The ultrasonic sensor emit ultrasonic waves after being stimulated by voltage, which are reflected after reaching the substance and then received by the receiver), microwave sensor (Transcranial Microwave-induced thermoacoustic tomography image of the agar) [52] and magnetic sensor (When a conductor (or magnetic-sensitive material) traverses through a magnetic field, the changes in magnetic flux generate an induced electromotive force (EMF). This induced EMF is proportional to the strength of the magnetic field). Reprinted from Refs. [49][50–52] with permission.

atrioventricular node (AV node), His bundle, left and right bundle branches, and Purkinje fibers [58]. The sum of the generated electrical potential differences is conducted throughout the entire heart and subsequently transmitted to the whole body, including the body surface. By using ECG leads, a chart displaying the relationship between time and positive/negative values can be obtained. ECG leads involve placing electrodes in specific locations on the body's surface, connecting them to an ECG machine with lead wires to obtain cardiac signals from the body surface. As an internationally recognized method for collecting ECG signals, the conventional 12-lead ECG system requires a total of ten electrodes, including limb leads and chest leads. Chest leads provide a view of the heart's horizontal cross-section. The proper electrode placement and ECG-related waveforms during the cardiac cycle are shown in Fig. 2a [59]. There have been reports describing the development of devices that can wirelessly transmit signals obtained from flexible ECG patches to smartphones by combining wearable devices with near-field communication (NFC) technology [60].

2.1.2. EEG sensors

Similar to the principle of ECG commonly used in clinical fields, EEG uses electrodes to detect changes in voltage caused by human physiological electricity. Through ion conduction, the neuronal activity of the brain reaches the cerebral cortex. In general, electrodes are fixed to specific locations on the head. Physiological electrical signals from the brain are transmitted to the electrodes, and the resulting voltage changes are collected and ultimately processed and converted into EEG waves [65]. The obtained EEG records the electrical signals formed by the spontaneous and rhythmic electrophysiological activity of brain cells in a time and potential correlation form. The fundamental characteristics of EEG include cycle or frequency, amplitude (wave amplitude), waveform and phase. Due to the abnormal brain electrical signals generated during seizures in epilepsy patients, an EEG can effectively diagnose various types of epilepsy with distinct features [66]. Based on the recommendations of the American Clinical Neurophysiology Society for electrode placement on the brain, there are two standard systems available: the 10–20 system (depicted as black circles) and the 10-10 system (depicted as grey circles). The naming and location of these two systems are interrelated, and Fig. 2b illustrates the names and positions of each electrode. In clinical settings, unless it is necessary to pinpoint the exact location of the epileptic focus in patients with epilepsy, there is generally no requirement for the precise positioning of electrodes in the standard electroencephalogram for most patients [62,67,68].

Both EEG and ECG use electrodes to record the body's weak

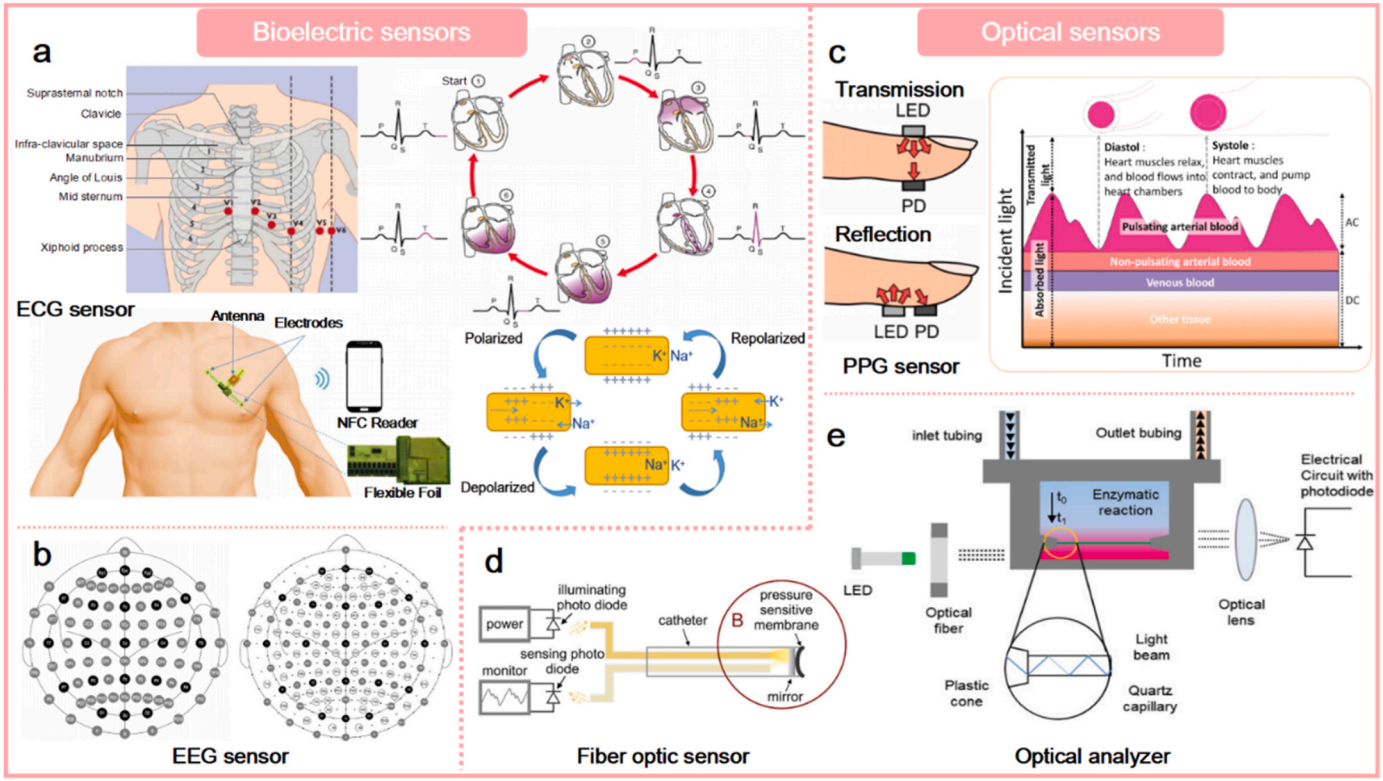

Fig. 2. The working principles of bioelectric sensors and optical sensors. a) Correct placement of 12-lead electrode (top left) [59]. The ECG signal correlates with the cardiac cycle in a single lead (top right) [61]. A drawing of an ECG patch (bottom left) [60]. The movement of potassium and sodium ions of ECG signal (bottom right) [10]. b) Electrode locations and labels in EEG-10 - 20 systems (left) [62]. Recommended electrode positions in the 10-5 system. The dots indicate positions outside the 10-10 system, the hollow circles indicate additional position selection useful for 128-channel EEG systems (right) [62]. c) Transmission and reflection modes of PPG (left) [63]. Changes in tissue light attenuation (right) [64]. d) Intensity modulation based FOS [49]. e) Optical analyzer [49]. Reprinted from Refs. [10, 49,59–64] with permission.

electrical signals. An EEG typically records the electrical activity of neurons in the brain layer by placing electrodes on the scalp [65], while ECG places electrodes mainly on the chest to record the electrical activity produced when the heart muscle is active [57]. Both methods use non-invasive techniques to convert acquired signals into visualized waveform graphs.

The ECG is mainly used for the diagnosis and monitoring of heart diseases. It records the electrical movement of the heart, including P waves, QRS complexes, and T waves [55]. These waveforms can help doctors assess the normal function of the heart or detect abnormalities. In contrast, an EEG records the electrical activity of neurons in the cerebral cortex, reflecting the functional state of the brain. EEG is often used in the diagnosis of neurological diseases such as epilepsy [66]. Its waveform features include α wave, β wave, θ wave, etc. [69] These waveforms reflect the electrical activity of the brain in different states.

2.2. Optical sensors

Since recent developments in wearable and flexible electronics have shown their potential for anti-electromagnetic interference and corrosion-resistant sensing applications with high precision and sensitivity, this has sparked research into optical sensors [70]. Here, we mainly introduce four main methods of optical sensors: photoplethysmography (PPG), optical fiber sensors, optical analyzers for metabolic monitoring and near infrared spectroscopy (NIRS) sensors.

2.2.1. PPG sensors based on optoelectronic techniques

As the non-invasive method for monitoring vital cardiovascular signals, photoplethysmography (PPG) enables the monitoring of blood volume changes by measuring the light scattering caused by blood flow [10]. Typically, the elemental composition of a PPG sensor includes a pair of photodetector (PD) and light -emitting diode (LED). When measuring certain signals of the human body as helpful information, such as fingertip blood flow, the LED is placed on the side of the fingertip to emit a light source, which penetrates the finger. The composition of the finger includes skin, tissue, blood vessels, blood and bones, etc. These parts will absorb part of the light, and then the PD is responsible for detecting the remaining light. The PD can be placed on the same side or the opposite side of the LED, which determines the detection methods of transmitted or reflected types. Therefore, PPG sensors are generally considered as classified into transmission and reflection modes (Fig. 2c) [64,71,72]. When a light beam with a certain wavelength is irradiated on the skin of the fingertip, the contraction and expansion of the blood vessels caused by heartbeat will affect the transmission or reflection of light. The transmission of light is represented by the light passing through the fingertip in transmission PPG, and the reflection of light is represented by the light reflected from the light source back to the skin surface in reflection PPG. The light will be attenuated when it penetrates the skin tissue and later reflects the photosensitive sensor. When the heart beats, there is a transient change in the blood volume of the arteries, which causes a difference in the intensity of the transmitted or reflected light [10,73]. Finally, PD converts the captured light intensity variation into electrical signal transformation, which is then processed and outputted by internal circuitry to obtain real-time information on the pulse beat.

In addition, as a crucial physiological indicator in the blood, timely blood oxygen saturation (SpO_2) monitoring can be obtained by the PPG sensor with more than one LED. The principle of this device is to analyze the difference in light absorption. Generally, the difference in light absorption between oxy-hemoglobin (HbO_2) and deoxy-hemoglobin (Hb)

in green light, red light and infra-red light is taken as the object of analysis [10].

2.2.2. Optical fiber sensors

The optical fiber sensing system comprises three parts: light source, fiber optic modulation area and light detector. The light source signal is transmitted to the modulation area through the input optical fiber. When the external parameters change (i.e., refractive index, pressure), it will cause the physical characteristics variation of the input light wave (such as intensity, wavelength, frequency and phase), and then the output light wave is analyzed and processed by a photodetector, which can further sense the alteration of an external signal.

2.2.2.1. Fluorescence detection. When a fluorescent molecule is irradiated with light of a specific wavelength, it absorbs energy to reach an excited state and emits fluorescence upon releasing the energy. The principle of a fluorescence-based optical fiber temperature sensor used for monitoring temperature is based on measuring the temperature-dependent emission decay of a fluorescent dye [74]. The light source of the sensor system is transmitted to the temperature-sensitive fluorescent substance through an optical fiber. When excited by the light signal, the temperature-sensitive fluorescent substance emits fluorescence, and its luminous intensity decreases with temperature changes [49]. Some luminescent materials used in sensors have fluorescence lifetimes that are temperature-dependent [75].As the temperature increases, the fluorescence lifetime decreases. Fluorescence lifetime measurements allow inference of temperature changes. [49] The basic method of fluorescence detection is to measure the property and intensity of a fluorescent compound emitted by light irradiation at a specific wavelength. Compared with traditional non-focused and confocal optical systems, optical fibers, owing to the miniaturized volume and flexibility, are commonly the carrier responsible for receiving fluorescence signals or transmitting excitation light in fluorescence detection systems. For example, as the most crucial parameter of the intracranial health condition, temperature monitoring attracts researchers inputting profuse and indefatigable efforts on optical fiber sensors based on fluorescence detection, trying to overcome the problem of miniaturization and implantability. In addition, with the high sensitivity and selectivity of the fluorescent material, the optical fiber fluorescence sensor provides booming application prospects in early disease diagnosis and single-molecule recognition and detection [76].

2.2.2.2. Fiber Bragg Grating. As a typical passive filter device, Fiber Bragg Grating (FBG) is a kind of diffraction grating formed by a certain method to make the refractive index of the fiber core undergo axial periodic modulation. In 1978, K·O.Haill et al. made the first fiber grating by standing wave writing method in germanium doped fiber. After more than 30 years of development, it has a broad application prospect in laser, communication, and sensing. With the continuous improvement of FBG manufacturing technology, it has gradually become one of the most promising, representative and rapidly developed fiber-passive devices.

The mode coupling mechanism of FBG is that there is a coupler between the forward and reverse core modes. By design of a periodic refractive index variation, the fiber can only reflect a specific wavelength and transmit all others, thus forming a narrow-band (transmission or reflection) filter or mirror in the core. According to the coupled-mode theory, the central wavelength (λ_B) of FBG is:

$$\lambda_B = 2n_{eff}\Lambda$$

where n_{eff} is the effective refractive index of FBG in the core region, Λ is the grating period of the FBG. In a real application, standard FBG is often used in temperature measurement due to its excellent temperature sensitivity [77].

2.2.3. Optical analyzers for metabolic monitoring

An optical analyzer setup for basic testing consists of a measuring cuvette, a sensing photodiode, and an illumination device, shown in Fig. 2e. The function of a cuvette is to support the chemical reaction between the detected metabolite and specific compounds, including specific oxidases, to produce fluorescence for indirect measurement of the amount of metabolite. Typically, the amount of the metabolite being tested is directly proportional to the fluorescence intensity. After the selected oxidase oxidizes the metabolite to be tested, hydrogen peroxide, phenol, and 4-amino-antipyrine react to form a red-purple quinone imine, which emits fluorescence under the excitation light source. The fluorescence is converted into an electrical signal related to the concentration of the metabolite being tested through a photodiode [78]. By measuring the fluorescence intensity, the concentration of the analyte can be easily obtained [49].

2.2.4. Near-infrared spectroscopy (NIRS) sensors

In the field of brain research, monitoring changes in oxygenation of the cerebral cortex is an object of interest, and optical methods based on NIRS are increasingly adopted today [79]. The functional near-infrared spectroscopy (f_{NIR}) optical brain imaging system possesses independent components, which usually include a control unit and a continuous near-infrared spectral sensor. For the latter spectral sensor, normally it is comprised of the infrared light source and a detector. The wavelengths in the spectral region of 780~2526 nm can record the frequency doubling and combined frequency absorption information of chemical bond vibrations such as C–O, O–H and N–H, which realizes the physicochemical property measurement of hydrogen group organics [80]. After the near-infrared light source irradiates the detection target, it will attenuate, and the component content of the detection target is analyzed according to the transmitted light or reflected light received by the detector. The system is capable of detecting and mapping changes in blood flow and oxygen levels in the brain's cortex, allowing for visualization and quantitative evaluation of brain activity [80]. There exist various discrepancies in the absorption characteristics of tissues upon different wavelengths of near-infrared light. The brain components with light absorption mainly include HbO_2 and Hb [81]. Using the absorption and scattering relationship between near-infrared light of multiple wavelengths and chromophore substances in brain tissue can obtain the inside concentration changes of HbO_2, Hb and total hemoglobin [82]. This enables the monitoring of neuronal activity, cellular energy metabolism, and hemodynamics [83].

2.3. Mechanoelectrical sensors

As an essential part of the cardiovascular and heart-brain network, the elastic arteries can pulsate significantly in response to the heartbeat and blood pressure changes. For example, pulse detection in traditional Chinese medicine plays a significant role in diagnosing symptoms. Clinically, Chinese medicine doctors often use pulse diagnosis to evaluate the health status of the body, which is achieved by sensing the pulse at the patient's wrist with the doctor's fingers. The finger's skin has a complex sensing network, so subtle mechanical vibrations are converted into bioelectrical signals and transmitted through the neural network to the brain for processing. Mimicking the property of human skin, scientists have designed electronic skin to capture the body's mechanical movement signals. The electrical signals generated by electromechanical sensors, such as resistance and capacitance, will change when they are stimulated by the outside world, therefore, by demodulating changes in electrical signals, sensing mechanical activity or motion can be achieved. These sensors usually consist of two electrodes sandwiching a sensitive unit, which can be divided into four categories according to the electrical characteristics of the sensitive unit: resistive, capacitive, piezoelectric, and triboelectric devices [84]. For example, one way to monitor heart rate/blood pressure is by placing sensors on the skin close to the carotid or radial arteries so that vibrations from the arteries are

transmitted to the sensors and generate a corresponding signal [85]. In the application of monitoring the cardiocerebral vascular system, seismocardiography (SCG) measures the local vibration of the chest wall caused by cardiac mechanical movements such as myocardial contraction, heart valve motion, and blood flow turbulence [86]. In addition, the center of gravity of the entire body changes slightly with each heartbeat. Ballistocardiography (BCG) measures micromotions of the body longitudinally or laterally caused by the body's recoil [87]. The detail of each mechanoelectrical sensors will be illustrated as follows.

2.3.1. Piezoelectric sensor

The principle of piezoelectric sensors is based on the electric potential generated in certain materials in response to an applied mechanical force. With the external force applied to the solid material, the variation in the separation between dipoles would lead to an accumulation of charges on the electrodes. Hooke's law and the electrical behavior of the materials govern the basic principle of the piezoelectric sensors by

$$S = sT$$

where S is the strain, s is the compliance of the material, and T is the stress which is obtained by diving the applied force with the applied area. And

$$D = \varepsilon E$$

where D is the electric charge density displacement, ε is permittivity, and E is the electric field strength in the material. The equations can be further linearly approximated to

$$S = S^E T + dE$$

$$D = \varepsilon^T E + dT$$

Here, the superscripts on the strain and permittivity indicate that the electric field (E) and stress (T) are held as constant. The above equations confirm that the change of strain will lead to the change in the output piezoelectric signal. Consequently, the applied pressure or strain can be obtained by measuring the piezoelectrical signals of the piezoelectric materials (Fig. 3a). This mechanoelectrical interaction is only present in certain types of materials with no centrosymmetric crystal structures [88].

2.3.2. Piezoresistive sensor

The piezoresistive sensors are based on monitoring the variation of electrical resistance under the different applied forces. The following equation describes the basic principle of the piezoresistive sensors.

$$R = \frac{\rho L}{A}$$

Where ρ is the resistivity of the conductive materials, L means the device's length, A represents the contact area. Generally, the resistance of piezoresistive sensors decreases with increasing pressure due to the compression and deformation of the device caused by external pressure, which in turn increases the internal conductive path and decreases the resistance. Therefore, the resistivity changes after the conductive material are subjected to the applied pressure, and through certain circuit detection the electrical signal output proportional to the force variation can be obtained. Furthermore, piezoresistive sensors are a sophisticated and suitable candidate for flexible and wearable devices because of the more comprehensive linearity detection range and the higher stability [94,95].

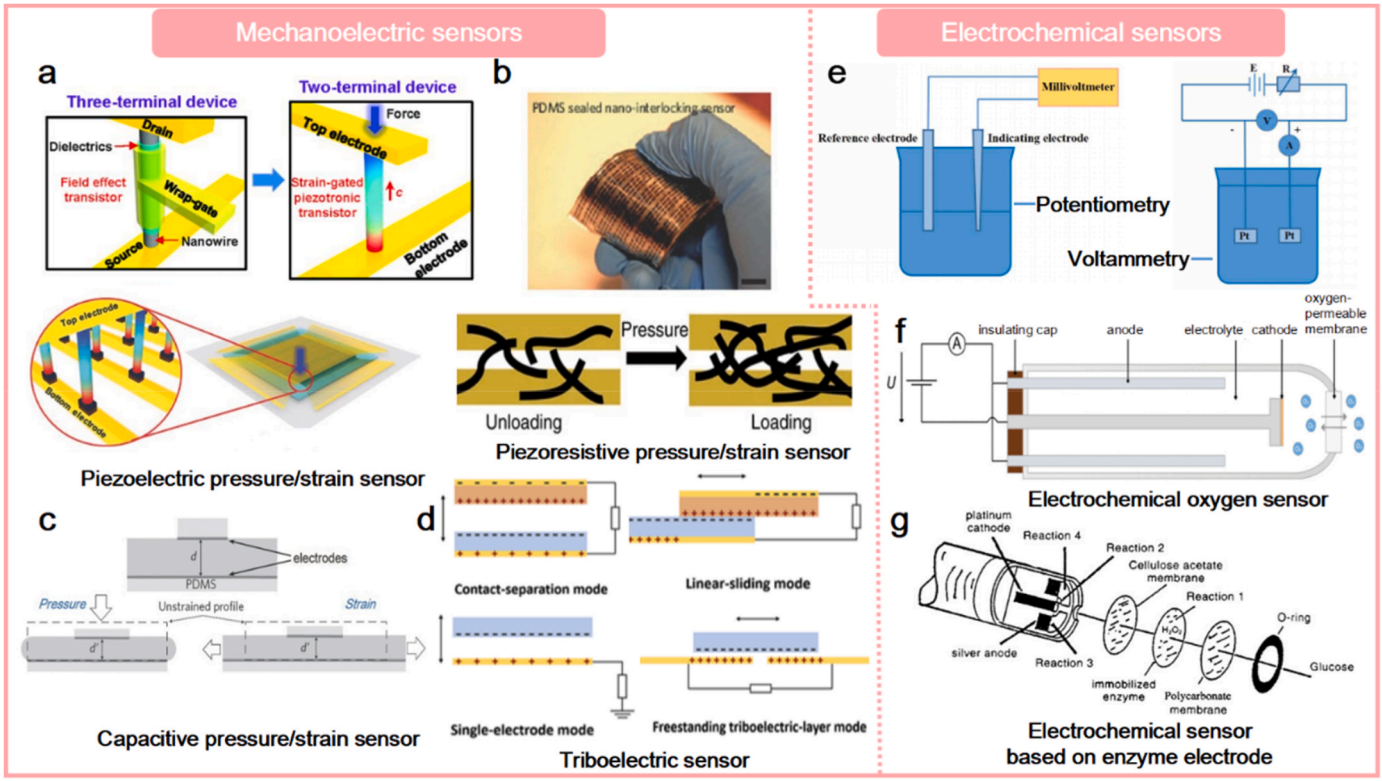

Fig. 3. The working principles of mechanoelectrical sensors and electrochemical sensors. a) Three-terminal voltage-gated NW FET (top left) and double-ended strain-gated vertical piezoelectric transistor (top right). Schematic of the piezoelectric pressure sensor (bottom) [89]. b) Piezoresistive flexible sensor constructed on a micropatterned PDMS substrate, scale bar: 1 cm (top) [90]. Diagram of the sensing mechanism of a pressure sensor based on the AuNWs coated tissue paper (bottom) [91]. c) Schematic showing the stretchable capacitor of the capacitive flexible sensor under pressure (left) and after being stretched (right) [88]. d) The working mechanism of the four basic modes of TENG [92,93]. e) Potentiometry and voltammetry in electrochemical sensors. f) The schematic of Clark Electrode [49]. g) The first generation of glucose bioenzyme sensor made by YSI Inc [51]. Reprinted from Refs. [51,89–93][49][88] with permission.

Flexible conductive materials, encompassing liquid materials and conductive composites, have gained extensive usage in wearable health-monitoring sensors based on piezoresistive principles. Liquid conductive materials are typically integrated into elastomer-based fluidic microchannels, undergoing shape changes in response to mechanical stimuli [96]. On the other hand, conductive fillers, spanning zero-dimension nanoparticles (e.g., carbon black, Ag NPs, and Au NPs), one-dimension nanowires or nanotubes (e.g., CNTs, SWNTs, AgNWs, and AuNWs), and two-dimension nanosheets (e.g., graphene, MXene, etc.), can be readily blended with polymers (e.g., PDMS, Ecoflex, etc.) to establish conductive networks capable of accommodating substantial deformations. [97]These wearable sensors capture physiological signals (heartbeat, pulse, etc.) converting them into electrical signals, thereby facilitating the assessment of patients' health status.

2.3.3. Capacitive sensors

Flexible capacitive sensors typically consist of two parallel electrodes which sandwich a dielectric layer [88]. When a certain pressure is applied to the sensor, elastic deformation occurs, and the distance and the effective area between the top and bottom electrodes change, eventually leading to a capacitance change (Fig. 3c) [88]. The following equation describes the basic principle of capacitive sensors:

$$C = \frac{\varepsilon_0 \varepsilon_r A}{d}$$

Where C is the capacitance of the device, ε_0 is the space permittivity, ε_r is the relative permittivity of the middle dielectric layer, d is the distance between the two parallel electrodes, and A is the overlapping area between electrodes. The values of effective dielectric constant and distance between two electrodes are normally dependent on the applied pressure, providing a possible solution to reflect the external pressure by monitoring the capacitance variation. Thanks to the typical and simple capacitive sensors, the parallel plate structure has a wide detection range and high stability, making them a suitable candidate for monitoring finger and wrist motion, heartbeat and respiration [42].

2.3.4. Triboelectric sensors

Triboelectric nanogenerators (TENGs) have attracted much attention in the field of flexible and wearable devices due to their simple construction and excellent biocompatibility. TENGs has the characteristics of efficient energy conversion, high sensitivity [98] and self-supplying energy [99]. They are able to capture and store energy generated by friction or mechanical motion for use in power supply. This means that even if there is no external power source, TENGs can generate its own electricity and achieve its own energy supply [99]. In addition, TENGs is very sensitive to mechanical energy changes and is able to capture and convert small amounts of motion energy, showing high sensitivity [98]. The two thin-layer materials with different triboelectric polarities in TENG have different electronegativity upon contact, which leads to charge transfer on the surfaces of the two materials, resulting in opposite charges forming a potential difference. Induced by the electric potential generated by the charge, electrons flow through the external circuit, and the mechanical force is converted into electrical energy. Self-powered triboelectric sensors convert applied pressure or strain into electrical signals by causing changes in transferred charge in response to geometric changes in pressure or strain [100]. The following equation describes the basic principle of the TENG sensor:

$$V = -\frac{1}{C(X)}Q + V_{OC}(X)$$

where V is the total voltage between two electrodes, C represents the effective capacitance of the TENG sensor, X is the distance between these two triboelectric layers, Q means the amount of transferred charges from one electrode to another, and V_{OC} is the open-circuit voltage component contributed by the polarized triboelectric charges. Similar to piezoelectric sensors, the capability of TENGs to generate electrical signals from mechanical motion makes it useful as a self-powered sensor to detect these mechanical motions [99,101,102]. TENGs has four different working modes: including contact-separation mode, linear-sliding mode, single-electrode mode and freestanding triboelectric-layer mode (Fig. 3d).

2.4. Electrochemical sensor

According to the working principles, electrochemical sensors can be divided into amperometry [103], potentiometry [104], and voltammetry [105]. Amperometry is based on the measurement of electric current. In a sensor, a potential is applied across a working electrode and a reference electrode. The target analyte (including molecules or ions) undergoes an electrochemical reaction on the surface of the working electrode, thereby generating a current proportional to the concentration of the analyte. Measurement of this current yields the concentration of the analyte [103]. Potentiometry is based on the measurement of potential or voltage. In a sensor, the working and reference electrodes are immersed in an electrolyte solution. The target analyte interacts with the electrode surface, resulting in a change in electrochemical potential or voltage. The concentration of the analyte is related to this potential change, and by measuring the value of the change, the concentration of the analyte can be determined. This method is commonly used for pH measurement and ion concentration determination (Fig. 3e) [104]. Voltammetry involves measuring the current as a function of the applied voltage. In the sensor, a potential is applied to the working electrode. By changing the applied voltage within a specified range and measuring the resulting current, a voltammogram can be obtained, which can reflect electrochemical information such as the concentration of the target analyte. The method is commonly used to detect a variety of substances, including neurotransmitters (Fig. 3e) [105].

In this section, we focus on oxygen and metabolite sensors based on electrochemical technology.

2.4.1. Electrochemical oxygen sensor

Electrochemical PO_2 sensors for medical applications were first proposed by Leland Clark in 1956 [106]. The Clark electrode operates based on the reduction reaction of oxygen. Its structure, as shown in Fig. 3f, consists of an anode and a cathode both immersed in an electrolyte solution. The charged cathode is coated with an oxygen-permeable membrane that enables the entry of oxygen molecules. Upon reaching the cathode, oxygen molecules undergo electrolytic reduction, generating a current whose strength is proportional to the number of oxygen molecules present. By computing the outcome of this process, the partial pressure of oxygen can be determined [49].

2.4.2. Electrochemical sensors based on enzyme electrodes

The enzymatic electrode combining biology and electrochemistry, proposed by Clark in 1962, laid the foundation for the development of subsequent biosensors [107]. The enzymatic catalytic reaction that occurs in the analyte is the basis for detecting the concentration of the analyte, such as glucose concentration. The analyte and the enzyme enclosed by a semipermeable membrane applied to the electrode undergo a chemical reaction, leading to changes in pH or pO_2. The measurement of these changes can be used to infer the concentration of the analyte. To measure blood glucose, the first-generation sensor based on the glucose oxidase (GO_x) electrode works by catalyzing glucose in the blood using glucose oxidase (GO_x), which forms gluconic acid and hydrogen peroxide (H_2O_2) [108]. Afterwards, the H_2O_2 is electrochemically oxidized on the electrode surface which generates electrons and produces a current. This current is directly proportional to the blood glucose concentration, thus allowing for the inference of the blood glucose concentration by measuring the resulting current [109]. The "first generation" glucose biosensor is shown in Fig. 3g [51].

The fundamental principle of modern electrochemical analyzers

used for measuring intracranial metabolites is similar to that of glucose sensing. Commonly tested metabolites include pyruvate, glucose, glycerol or lactate, and different oxidases are selected for each type of analysis based on their specificity. These metabolites react chemically with their respective immobilized oxidases, producing hydrogen peroxide molecules that are electro-oxidized at the platinum electrode to generate an electric current. To achieve better measurement results, multiple membranes are usually employed. The outermost layer is a catalase membrane that covers the electrode, which serves to oxidize hydrogen peroxide into hydrogen and oxygen and discharge them outward, preventing hydrogen peroxide from entering the measuring electrodes and reducing errors. Following this is a diffusion-limiting membrane designed to ensure that all metabolites to be tested are oxidized within the oxidase layer. Next is a membrane that immobilizes oxidases capable of specific catalytic reactions with the metabolites being tested. Finally, a membrane through which only hydrogen peroxide can pass is placed between the oxidase membrane and the platinum electrode [49].

2.5. Temperature sensors

As a common monitoring modality to assess brain health, temperature monitoring includes various temperature sensors and probes based on resistance temperature detectors (RTD) [110], thermocouples [111,112], optical fibers [113] and thermistors [114]. In the Neuro-Intensive Care Unit, it is clinically common to measure brain temperature using probes that are equipped with sensors for oxygen and pressure monitoring [110].

2.5.1. Thermistor sensor

The working principle of the thermistor is based on polycrystalline semiconductor materials with negative temperature coefficients [110]. The thermistor inside the thermistor sensor detects temperature changes based on the temperature-dependent resistance characteristics of semiconductor elements, and its resistivity varies accordingly when the temperature is different [49]. A schematic diagram of a medical catheter with a thermistor used for medical temperature measurement is shown in Fig. 4a. The catheter tip is placed with a thermistor, which can be connected to a cable for monitoring purposes [115]. In addition, there is also a study monitoring brain temperature through a temperature sensor with a thermistor, whose resistance value changes with temperature. The resistance value of the resistor is measured by a digital measuring instrument, thereby obtaining temperature and resistance variation accordingly [116].

For cerebral blood flow (CBF) sensors based on thermal diffusion flowmeter (TDF), the principle is based on the use of heat loss from the internal heating element when blood flows through the probe, and the amount of heat loss is related to the flow rate of the fluid. The composition of a TDF based CBF sensor includes two thermistors. One measures the temperature of the blood while the other acts as a heating element. An external circuit is used to maintain a constant temperature difference ΔT between the two components. As blood flows through the probe, it takes away heat from the internal heating element. The amount of heat taken away varies with CBF, resulting in a corresponding change in the power required to maintain a constant ΔT between the two thermistors. By analyzing this power requirement, we can deduce information about the CBF [121].

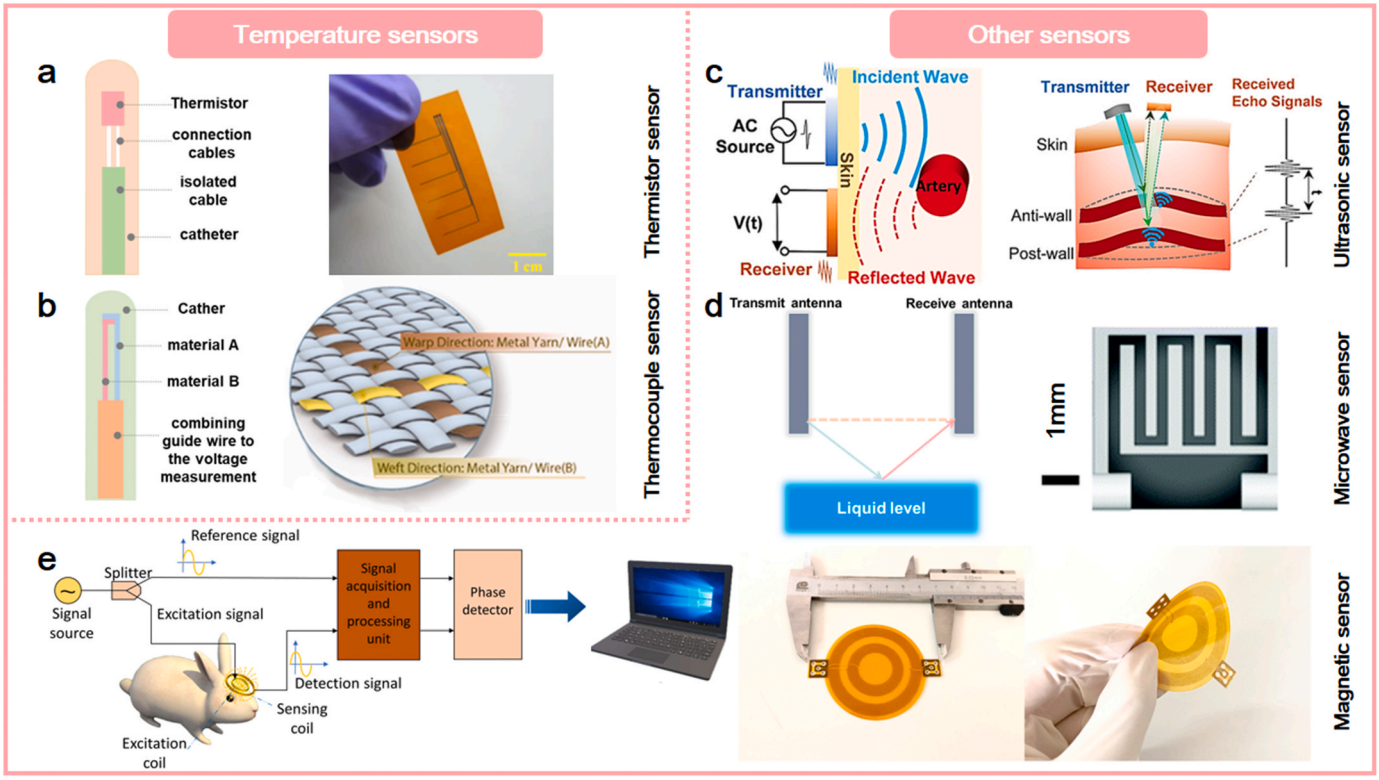

Fig. 4. The working principles of temperature sensors and other sensors. a) A medical catheter with a thermistor at the tip for temperature measurement. The thermistor is placed at the tip of the catheter. When the temperature changes, its resistivity will change. (left). Image of a thermistor array printed on the PI substrate (right) [117]. b) A medical catheter with a thermocouple at the tip for temperature measurement. When the temperature changes, a current is generated between the two materials, resulting in a voltage, which is related to the temperature, and the relevant temperature information can be obtained by calculation. (left). A Textile-based temperature sensor (right) [118]. c) The principle of ultrasonic sensors for BP estimation and arterial diameter monitoring [10]. d) The schematic diagram of an interrupted microwave sensor (left). A microwave sensor (right) [119]. e) The diagram of magnetic induction phase shift system (left) [120]. Image of a flexible conformal MIPS sensor with a geometry of approx. 60 mm × 50 mm (middle). Picture of the bending deformation of the flexible conformal MIPS sensor (right) [120]. Reprinted from Refs. [10,120,117–119] with permission.

2.5.2. Thermocouple sensors

The basic building block of a thermocouple sensor is thermocouples at the sensing tip, usually constructed of two materials with different thermal properties. Due to differences in thermal properties, a change in temperature induces a current between the two materials, creating a voltage that can be measured to infer the associated temperature [49]. For the Licox temperature sensor (LN) and the Neurotrend temperature probe (NT), the basis of their operation is the thermoelectric effect of the thermocouple element [110]. The temperature difference between the two soldering joints resulting in a voltage difference U is considered as a thermoelectric effect [122]. Fig. 4b shows a schematic diagram of a catheter with thermocouples for medical temperature measurement.

2.6. Other sensors

2.6.1. Ultrasonic sensors

In the medical field, ultrasound is mainly used for medical diagnosis and clinical treatment. The main component inside the ultrasonic sensor for medical application involves piezoelectric wafers [123]. Ultrasonic sensors can function as both transmitters and receivers of ultrasonic waves. When the ultrasonic sensor receives ultrasonic waves, it can also convert them into electrical energy [124]. The measurement or inspection of the internal structures or organs of the body through ultrasonography is successfully achieved by high-frequency ultrasonic waves generated with piezoelectric films [125]. When an ultrasonic sensor is stimulated by a certain voltage, it can emit ultrasonic waves, which are then received by the receiver. After the ultrasonic wave is transmitted into the human body, it will be reflected inside the body, due to the different structures and shapes of various tissues in the human body, the reflected direction, intensity and other information of the waves are also different [126]. Ultrasound technology is commonly used to measure arterial vessel diameter, as it operates on the principle of transmitting and reflecting ultrasound waves, illustrated in Fig. 4c. The time taken for ultrasound waves to travel across the diameter of an artery is related to its size, allowing the calculation of arterial vessel diameter based on this measurement [127]. In addition, ultrasonic sensors can be used to monitor the pulsating brain during craniotomy by the same basic principle [128].

Photoacoustic imaging, a technique akin to ultrasound imaging, has gained clinical acceptance in visualizing various human tissue structures such as breast, blood vessels, muscles, and bones. One of its key advantages is its non-invasive and contrast agent-free nature [129]. Additionally, the capability of photoacoustic imaging to visualize molecular information makes it a promising technique for detecting oxygen uptake and metabolism in biological tissues [130]. Photoacoustic imaging utilizes a pulsed laser with a short wavelength as the wave source to generate images of biological tissues. When the emitted light is absorbed by the tissue, it is converted into heat, leading to rapid temperature rise and thermal expansion. Since the heat source is time-varying, the resulting thermal expansion becomes unstable, producing ultrasound signals that can be detected and converted into images [131].

2.6.2. Microwave sensors

The fundamental principle of microwave sensor is that the system uses microwaves to irradiate the object to be detected so that the object will scatter the microwave and generate scattered fields around it. By measuring the scattered field, the complex permittivity distribution and shape of the object can be reconstructed [132]. Microwave medical imaging is now successfully adopted to detect several diseases like stroke or cancer [132,133]. The emerging technology of Microwave Induced Thermoacoustic Tomography (MI-TAT) holds great potential in the field of medical imaging due to its high resolution and contrast capabilities. The principle behind MI-TAT is to use microwave pulses to irradiate the tissue being examined. Due to dielectric loss, the energy absorbed by the tissue is rapidly converted into heat, leading to an increase in temperature and thermal expansion. This difference in temperature between tissues generates a strain force, resulting in the creation of ultrasonic waves. These waves are then detected by specialized equipment and used to create detailed images of the internal structure of the examined area [134].

2.6.3. Magnetic sensors

The principle of electromagnetic induction is the working basis of the magnetoelectric sensor. After a certain speed is applied to the sensor, the coil will convert it into a certain induced potential, which will then be outputted. As a typical passive sensor, the magnetoelectric sensor can directly realize the conversion of mechanical energy to electrical energy without an external power supply [135]. The magnetic induction phase shift (MIPS) detection system, a detection method based on a coil sensor as a sensing basis, is capable of monitoring cerebral edema (CE), which is achieved by continuous real-time measurement of changes in the electrical conductivity of objects [120]. Fig. 4e shows the basic principle of magneto-induction-based MIPS monitoring. The whole system mainly includes a signal source that generates a sinusoidal signal, an excitation coil and a sensing coil, etc. The sinusoidal signal is divided into a reference signal and an excitation signal by a separator, after which the excitation signal is conveyed to the excitation coil. The primary alternating magnetic field from the current-driven excitation coil penetrates the nearby tissue to induce eddy currents that regenerate the secondary magnetic field. The secondary and primary magnetic fields are collected by the sensing coil. There is a phase difference between the reference signal and the received detection signal. And a certain relationship exists between the secondary magnetic field and the primary magnetic field, which is related to the signal frequency, conductivity, relative permittivity and relative permeability of the sample, etc. [120] In addition, the magnetometer, a technical instrument that detects the Vout signal based on a pickup coil, has also been studied in intracranial medicine. RTD-fluxgate magnetometer sensors can be used to detect iron compounds in patients with neurodegenerative diseases [136].

3. Materials

Flexible electronics with wearable and implantable potentials have gained numerous attention from researchers. As an emerging electronic technology, flexible electronics normally are built on tenable or stretchable substrates such as plastic substrates, metal sheets, glass sheets and rubber substrates, etc., which can thus work under situations like bending, curling, compression or tension. Flexible wearable sensors used for monitoring generally consist of three components: substrates, electrodes, and sensing active components (Fig. 5) [10]. The materials of sensing components mentioned in this review and the related references are summarized in Table 1 at the end of this chapter.

3.1. Substrate materials

3.1.1. Polymers

Common organic materials used in substrates are polymers, silicone and rubbers [42]. Among them, polyethylene terephthalate (PET), polyimide (PI), polyetherimide (PEI), parylene or polyethylene naphthalate (PEN) films have exhibited excellent flexible performance [186]. In addition, polydimethylsiloxane (PDMS), poly (vinyl alcohol) (PVA), paper sheets and natural textile materials are also considered as popular flexible materials. Polymer materials are highly suitable as substrates for flexible sensors due to their unique characteristics. Here are some key advantages of using polymers in flexible sensors. Polymer substrates offer excellent flexibility and bendability, allowing the sensor to conform to curved surfaces and adapt to various shapes. This property is crucial for applications requiring flexibility, such as wearable sensors or sensors integrated into conformable devices [142]. Polymer materials generally have a lighter mass compared to traditional rigid materials, making the sensors more comfortable to wear and highly portable [187].

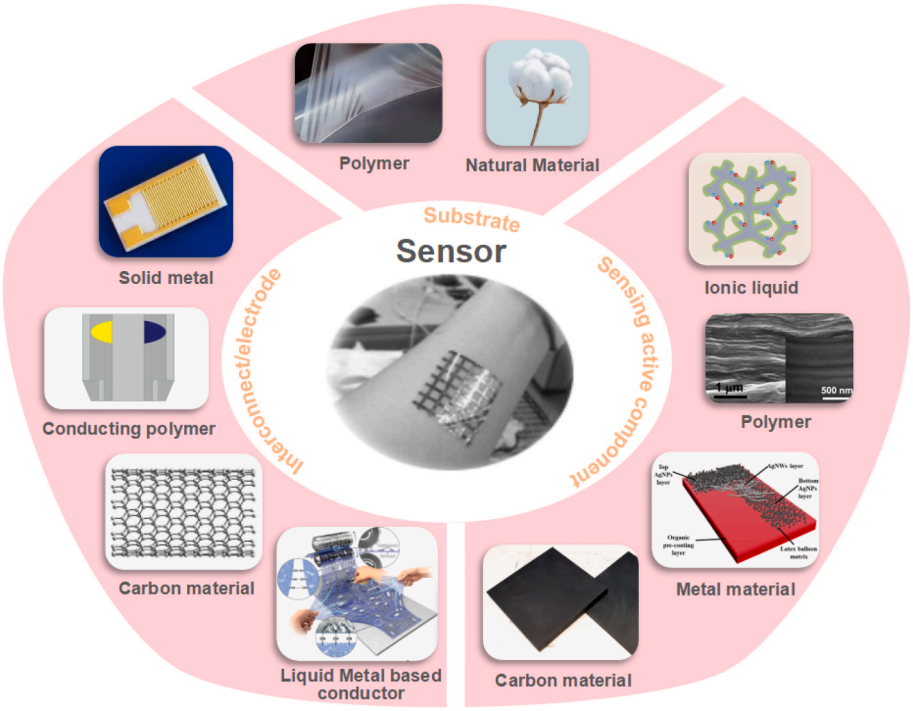

Fig. 5. Materials adopted for the flexible sensors related to the cardiocerebral vascular system. The diagram of carbon material of electrodes and interconnects: carbon nanotubes (CNTs) [137]. Diagram of liquid metal based conductor of electrodes and interconnects: eutectic gallium-indium (EgaIn) electrode on a hydrogel [138]. Schematic image shows metal material of sensing active component: the strain sensor [139]. The photography of polymer of sensing active component: PEDOT:PSS/GO composite membrane with GO concentration of 50% (v/v) [140]. The diagram of ionic liquid sensing active component: an ionic liquid-coated porous structure [141]. The photography of the sensor in the center: flexible electronics [142]. Reprinted from Ref. [137], [138], [139–142] with permission.

Table 1
The materials of components mentioned and the related references.

Component	Type	Advantages	Disadvantages	Material	Reference
Substrate Materials	Polymers	Flexibility, light weight, biocompatibility, stretchability	Low hardness, low thermal stability	PDMS, PET, PI and Polymer fiber and its textile, etc.	[143–147,148, 149,150–153, 154]
	Natural materials	Flexibility, air permeability biodegradability	Low hardness, low stability, water absorption, low chemical corrosion resistance	Cellulose paper and Natural textiles, etc.	[155,156,157]
Electrodes and Interconnect Materials	Solid metals	Electrical conductivity, high hardness, durability, high temperature stability	Low flexibility, heavy weight, low chemical resistance, low processability	Au, Pt and ITO thin films, etc.	[31,158–162]
	Conductive polymers	Flexibility, light weight, biocompatibility, high machinability	High resistivity, low stability, high fabrication cost	polyacetylene, polyindol, polythiophene, PPy, and PANI, etc.	[163–165]
	Carbon Materials	High conductivity, light weight, biocompatibility	low stability, high fabrication cost	CNT, graphene and carbon fiber, etc.	[166,167, 168–171]
	Liquid metals-based conductors	Flexibility, high conductivity, low resistance	Low stability, fabrication complexity	Galinstan, etc.	[172]
Materials of Sensing Active Component	Carbon Materials	Light weight, high sensitivity, fast response speed, wide operating temperature range, biocompatibility	low stability, high fabrication cost	Graphite, CNT, graphene, silk georgette, tissue paper, cotton fabric and even wheat bran, etc.	[143,173,174, 175,176]
	Metal Materials	Electrical conductivity, good thermal conductivity, easy processing	High weight, limited flexibility, low biocompatibility	Ga and its alloys, metal NW and NP, Galinstan, etc.	[177–180]
	Polymers	Flexibility, light weight, biocompatibility, low energy consumption	Low sensitivity, low stability	PEDOT-based polymers, PVDF and its copolymers, PANI, PPy and P3HT, etc.	[181–183,184, 185]
	IL	High electrical conductivity, high chemical stability, low volatility	High fabrication cost, viscosity, toxicity	[BMIM]•PF_6, etc.	[141]

Many polymer materials exhibit good biocompatibility, meaning they are compatible with biological tissues and do not cause adverse reactions or harm to the body. This enables the use of flexible sensors in medical applications [188]. Certain polymer substrates possess stretchable properties, allowing them to elongate or deform without permanent damage. This provides the sensors with the ability to withstand stretching or bending forces during use without affecting their performance [189]. Some polymer materials often offer excellent resistance to chemical corrosion, making them suitable for use in various environments. Sensors integrated with these polymer substrates can withstand exposure to moisture, chemicals, or harsh conditions, enhancing their durability and longevity [190].

3.1.1.1. PDMS. PDMS has been applied in multiple fields due to flexibility, good biocompatibility, thermal stability and chemical resistance and great processability, which also belongs to a hydrophobic silicone material. Owing to these excellent properties, PDMS has broad applications in various fields such as sensors [191], microfluidics [192], medicine [193] etc., among which it is mostly used as substrates in flexible sensors. For example, one of the most common methods for developing ECG electrodes is to fabricate metal electrodes on polymer

substrates, while PDMS is typically adopted as the polymer substrate [57].

Besides, Runzhi et al. [143] produced a pressure sensor using PDMS as a flexible substrate in a novel synthesis method. The process involves forming carbon nanotubes on Si/SiO_2 substrate and making the formation vertically arranged and finally partially embedded into the substrate to form a certain stability. This is achieved by the atmospheric chemical vapor deposition method. The sensor is constructed by placing two vertically aligned carbon nanotubes facing each other as electrodes. Owing to the flexibility of the substrate, the tensile effect of the substrate reached 180% in the tensile result. The overall device also maintained consistent performance in the test results, and the device has excellent potential in the wearable field, where it can be used to measure individual HR, muscle flexion and walking signals [143]. Stability and sensitivity are important for wearable sensors used in medical applications. To improve these two properties of resistive pressure, Zhou et al. [144], using unpolished silicon wafers as templates, used this simple process to fabricate carbon nanowalls (CNWs)/PDMS with irregular structures and used them as electrodes for the sensor. Similarly, the sensor uses PDMS as the substrate to ensure flexibility, and the three-dimensional structure of the electrode is displayed as a microstructure of the CNW inserted into the substrate. The experimental results show that the sensor has an excellent detection limit and can be used to detect heart rate at least [144]. As mentioned earlier, microwave imaging has corresponding applications in the medical field. Jamlos et al. [145] used the popular graphene as the radiation material of the UWB antenna, and used it as a sensor to try to apply it for tumor detection and visualization. Using PDMS and a solution of magnetic iron oxide (Fe_3O_4) nanoparticles as raw materials, the researchers combined the two to create a polymer-based substrate. As the principle described before, microwave sensors can be used as a medium to realize the imaging of objects. For the head of patients with tumors, the presence of tumors will increase the scattered signal so as to judge the existence of tumors [145]. PDMS can also be used as packaging materials for sensors, Ouyang et al. [146] Used the PDMS layer to encapsulate a self-powered ultrasensitive pulse sensor for the monitoring of cardiovascular-related signals, which is based on the operating principle of triboelectricity. Signal analysis helps diagnose arrhythmias (atrial fibrillation) with excellent performance (Fig. 6a) [146]. Koh et al. [147] used PDMS as microfluidics channels and covering material to fabricate a microfluidics measuring device, which monitors parameters related to epidermal sweat, including sweat volume and rate, glucose, creatinine, lactate, chloride and pH. The flexible, thin, multifunctional platform extracts the tested object by collecting sweat from the surface of the skin without chemical or mechanical irritation. (Fig. 6a) [147].

3.1.1.2. PET. PET is a highly crystalline polymer resin commonly found in life, which belongs to crystalline saturated polyester. It is a thermoplastic material known for its light weight, strength, and durability. Compared to other plastics, it exhibits excellent inertia and is widely used in various industries [194], such as frequently utilized as a substrate film for electrochemical sensors during their production [195].

Palit et al. [148] fabricated an indium-zinc oxide ($InZn_xO_y$) sensing film which possesses chemical stability for extended-gate field-effect transistor (EGFET) sensors, proposed according to a simple sol-gel method on flexible PET (Fig. 6b). The sensor can be applied to detect the dopamine content in biological samples including rat serum and brain [148]. Gao et al. [149] fabricated a flexible integrated sensing

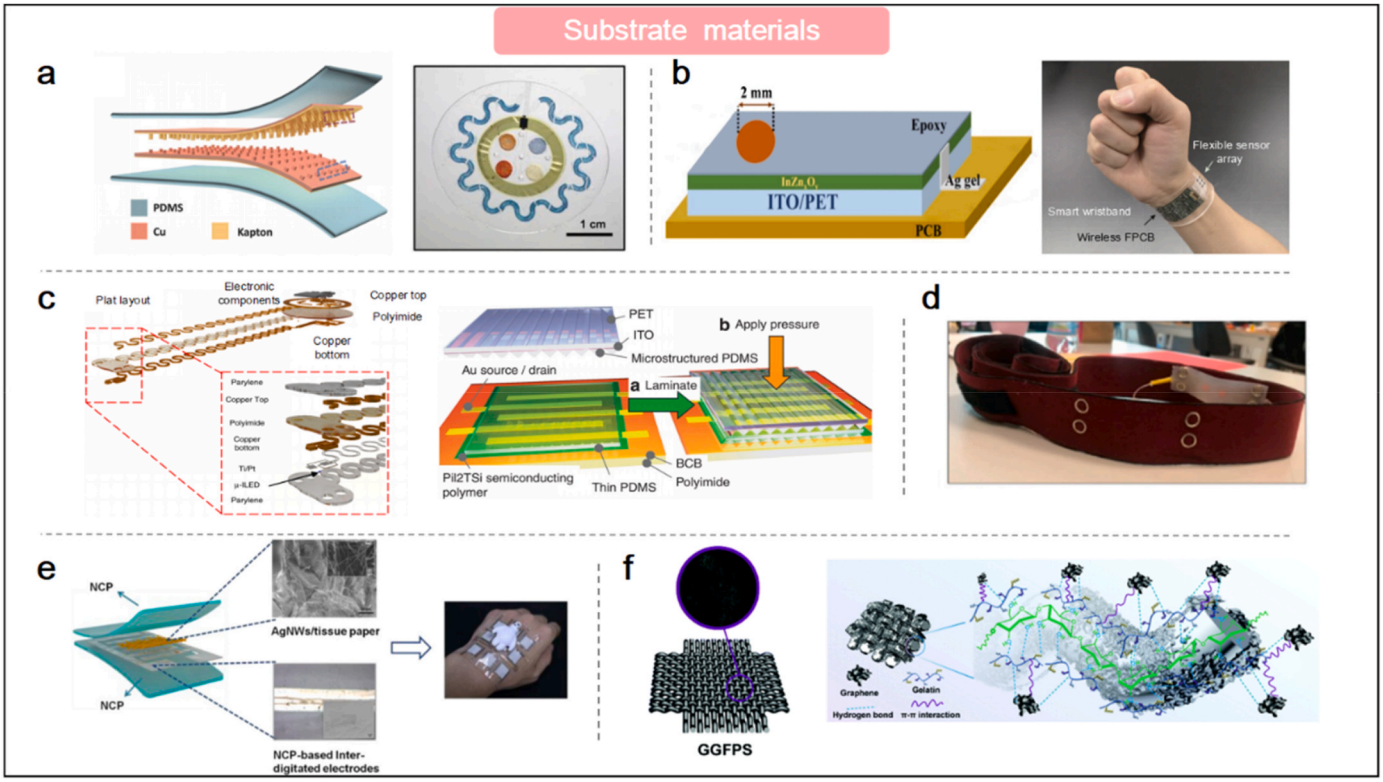

Fig. 6. The substrate materials of the flexible sensors related to cardiocerebral vascular system. a) Schematic diagram of the BD-TENG (left) [146]. Corresponding optical image of the device on PDMS under mechanical deformation of 30% strain stretch (right) [147]. b) Schematic diagram of $InZn_xO_y$ EGFET on PET (left) [148]. Photography of the wearable FISA with integrated wireless FPCB and multiplexed sweat sensor array (right) [149]. c) Rendered images of equipment configured for rats and mice (left) [152]. Schematic image of a sensor made of a layer containing a bottom source-drain electrode and a semiconductor polymer and a layer containing a gate electrode and a microstructured dielectric (right) [153]. d) Smart textile consisting of two elastic bands [154]. e) An APBP pressure sensor with a sandwich structure [155]. f) GGFPS obtained after drying, with illustration showing details. (left) [157]. Schematic diagram of graphene gelatin decorating the surface of cotton fabric (right) [157]. Reprinted from Refs. [146,147,148,149,152,153,154,155,157] with permission.

array (FISA) on a PET substrate capable of contacting the skin and enabling in situ multiplexed analysis of sweat for the detection of glucose, lactate and electrolytes, together with skin temperature measurement. The device facilitates the assessment of individual health status such as hyponatremia, hypokalemia, stress ischemia and diseases of blood glucose metabolism, etc. (Fig. 6b) [149].

3.1.1.3. PI. Properties such as light transmittance, surface roughness, and temperature resistance are usually taken into consideration when selecting materials for flexible substrates. PI is one of the organic materials with a polymer-based structure and the best comprehensive properties. It is widely employed in various fields due to its chemical corrosion resistance, high and low temperature tolerance, and excellent insulation properties. As a result, it is considered the most promising flexible electronic material [196].

PI films can be utilized in microfabrication processes to enable diversity in wearable sensor designs [42]. Kwak et al. [150] demonstrate a wearable strain-gauge sensor applied for HR detection using PI as the sensor substrate to ensure flexibility. In addition to the substrate, other materials for the sensor are sputtered nickel-chrome and electroplated copper for strain sensing. To achieve better physical motion inducing and elasticity of the artery when the sensor was installed over the radial artery, the fabricated device was attached to a silicone elastomer (Sylgard 170). The sensor can also linearly detect bend radii from 5 mm to 100 mm. It has the advantages of ultra-thin form and flexible properties, and thus can be applied to devices for heart beating detection [150]. Billard et al. fabricated a neural probe consisting of eight group sensors by depositing through-film vanadium oxide thermistors on glass and flexible 20-μm PI substrates, which can conduct long-term measurement and recording of localized temperature fields [151]. Gutruf et al. [152] proposed a wireless multisite pacemaker incorporating ECG-sensing electrodes using PI as a flexible circuit substrate with battery-free, fully implantable multimodality, long-term stability and excellent biocompatibility at the same time, it can be utilized for fully subcutaneous implantation in small animal models such as rats and mice. (Fig. 6c) [152]. Schwartz et al. [153] proposed a pressure-sensitive organic thin-film transistor, fabricated as a sensor for cardiovascular medical diagnosis such as radial artery pulse wave monitoring, comprising components with polymer semiconductors on PI films. In addition, the device features high stability and low power consumption (Fig. 6c) [153].

3.1.1.4. Polymer fiber and textile. Polymer fiber, a synthetic product made by a unique process, is often used to deposit active materials as well as its textile [197]. Presti et al. [154] proposed a facile polyamide-based smart textile (ST) for detecting chest wall excursions produced by respiration and heartbeat, which can be used to monitor respiration and cardiac activity. Two fiber Bragg grating sensors (FBGs) are encapsulated in a flexible material to form the sensor component of the equipment. To evaluate the superior ST, respiratory rate (f_R) and heart rate (HR) were used as criteria, and the results showed that the equipment was superior in f_R and HR (Fig. 6d) [154].

3.1.2. Natural materials

3.1.2.1. Cellulose paper. Cellulose paper has emerged as a popular sensor substrate due to its eco-friendliness, affordability, and biodegradability. Nanoscale cellulose is often added to enhance the paper's toughness, making it even suitable for sensor applications [198]. The high strength and density of nanocellulose paper can be attributed to the larger bonding area of its nanofibers, which allows them to form numerous bonds with adjacent fibers [199].

Generally speaking, disposable wearable pressure sensors need to solve the problem of high cost. Gao et al. [155] developed an all-paper, environmentally friendly pressure sensor, which is a piezoresistive sensor capable of measuring pulse and human vocal signals. Nanocellulose paper (NCP) is used as the base material for printing electrodes because it can guarantee the conductivity of electrodes. Silver nanowires (AgNWs) are coated on tissue paper and used as the sensing part of the sensor. The sensor not only has the advantages of green, low production cost, and environmental protection due to its all-paper manufacturing characteristics, but also has high sensitivity and excellent performance maintaining under bending state (Fig. 6e) [155]. Das et al. [156] used thermal reduced graphene oxide and a nylon-membrane (TRGO/NM) to create a high-performance sensor for bioelectrical measurements and solve the problem of biocompatibility without the usage of harmful chemicals and complex processes. The proposed epidermal sensor can be adopted to acquire ECG, electromyography (EMG), and EEG as well as monitor human motion [156].

3.1.2.2. Natural textiles. Flexible textiles can serve as a carrier for sensing electronics, and by combining the two, textiles with sensing capabilities can be developed. These functional textiles are capable of sensing the surrounding environment and transforming the data into relevant information, providing support for intelligent applications [200]. Textiles used as sensor substrates typically undergo pretreatment prior to production. It is necessary to ensure that the physicochemical properties of the textile are not significantly altered during the modification process [200]. Compared to other polymers, textiles offer the advantages of breathability and softness [201].

In pursuit of high sensitivity and convenient fabrication method of the sensor, Zhao et al. [157] made graphene nanosheets (GNs) using gelatin and graphene as raw materials and made GNs firmly fixed on the surface of cotton fiber mediated by hydrogen bond and hydrophobic interaction, thus producing a cotton-fabric based graphene/gelatin functionalized pressure sensor (GGFPS) (Fig. 6f). The device is designed to measure parameters related to movement and physiological signals, especially pulse, which shows promising applications in the medical field. The application of gelatin enhances the tensile properties of the sensor. The interwoven microstructure between the cotton fabric and GNs increases the sensitivity of the sensor because the interwoven structure increases the conductive path and reduces the resistance when subjected to pressure [157].

3.2. Electrodes and interconnect materials

Currently, electrodes and interconnects for flexible wearable electronics normally include solid metals, conducting polymers, carbon, and liquid metals-based conductors. The detailed illustration of each material will be described as follows.

3.2.1. Solid metals

Solid metals such as copper, silver and gold are commonly adopted conductor materials, which are designed as electrodes and wires. Solid metals are often fabricated into ultrathin ribbons and filaments in the form of a fractal, serpentine, and kirigami structures due to their rigidity [202]. Metal nanoparticles have good electrical conductivity and thus can be sintered into wires or thin films.

In addition, materials such as Pt, Au and indium tin oxide (ITO) thin films are also chosen as electrode materials to fabricate high-sensitivity flexible sensors [88]. For example, Li et al. [31] fabricated a flexible electrochemical sensor for real-time monitoring of nitric oxide (NO) using patterned ultrathin Au nanofilms as electrodes, which were wireless and biodegradable. Both the heart region and the joint cavity of the study animals were tested for NO in the study [31]. In addition, Peng et al. [158] fabricated an ultrasonic blood pressure (BP) sensor for BP monitoring through piezoelectric 1–3 composites and stretchable electrodes based on silver nanowires, which did not restrict body movement and exhibited great flexible properties [158]. Ion et al. [159] fabricated a flexible wearable sensor for BP monitoring with a polymer layer

covered by a metal sensor and a flexible membrane containing microfluidic channels. Microfluidic channels filled with electrolytes were aligned on the configurated metal transducers (Au), which could sense volume changes caused by the pressure applied in the channels upon the presence of electrolytes [159]. For mental health keeping, one of the main medications for preventing bipolar disorder (BD) is lithium, which acts as a mood stabilizer. Criscuolo et al. [160] proposed an electrochemical sensor that detects lithium in sweat, a device that enables drug detection monitoring in a non-invasive wearable form, which is useful for overcoming the inconvenience of regular checks to control the ideal lithium range in the blood. The whole system consists of a platinum potential sensor and a silver reference electrode (RE). The platinum potentiometric sensor has electrochemical nanostructures, which are beneficial for potential response and stability in sensing. In addition, the integrated flexible RE is chemically chlorinated and coated with IL-doped PVC film to enhance stability [160]. Wu et al. [161] fabricated a graphene-based flexible pressure sensor by converting GO to laser scribed graphene (LSG) and employed silver paste together with copper wires for creating connections. The device adopted the LSG pattern as the sensing core with wide applications, such as respiration, pulse and other physiological signal detection, also presented characteristics of high durability, high sensitivity, flexibility and so on (Fig. 7a) [161]. Lee et al. [162] proposed a flexible wearable patch with the enhanced electrochemical activity of serpentine double-layer gold mesh and gold-doped graphene, and the contained Ag/AgCl electrodes enable glucose detection in sweat. The patch of the device consists of thermally actuated heaters, humidity, temperature, glucose, pH sensors, and bioabsorbable microneedles which can release metformin to control blood sugar in diabetic mice (Fig. 7a) [162].

Solid metals can also be applied in the fabrication of conductive liquids. Conductive ink is made of conductive materials (carbon, copper, silver and gold) dispersed in binder materials. It has a certain degree of conductive properties and can be exploited for printing conductive dots or conductive lines. For modern printing processes, conductive materials are usually selected from conductive nano-inks, including nanoparticles and nanowires. Conductive inks with metal nanoparticles can be used to form electrodes for capacitive sensors by casting and annealing on the substrate surface [42].

3.2.2. *Conductive polymers*

Conductive polymers are considered promising electrodes and interconnect materials. Flexibility and stretchability can be obtained by adding nonionic and ionic small molecules and incorporating them with elastomers or hydrogels [10]. Conductive polymers such as polyacetylene, polyindol, polythiophene, polypyrrole (PPy), and polyaniline (PANI) have been reported to be used as electrode materials for rechargeable batteries [203]. Furthermore, conductive polymers are known for their lightweight nature, corrosion resistance, short response time, and high sensitivity, all of which contribute to their popularity in sensor fabrication [204].

Pressure sensor suitable for human physiological signals detection sometimes needs to embrace properties like paper-based, pure-organic,

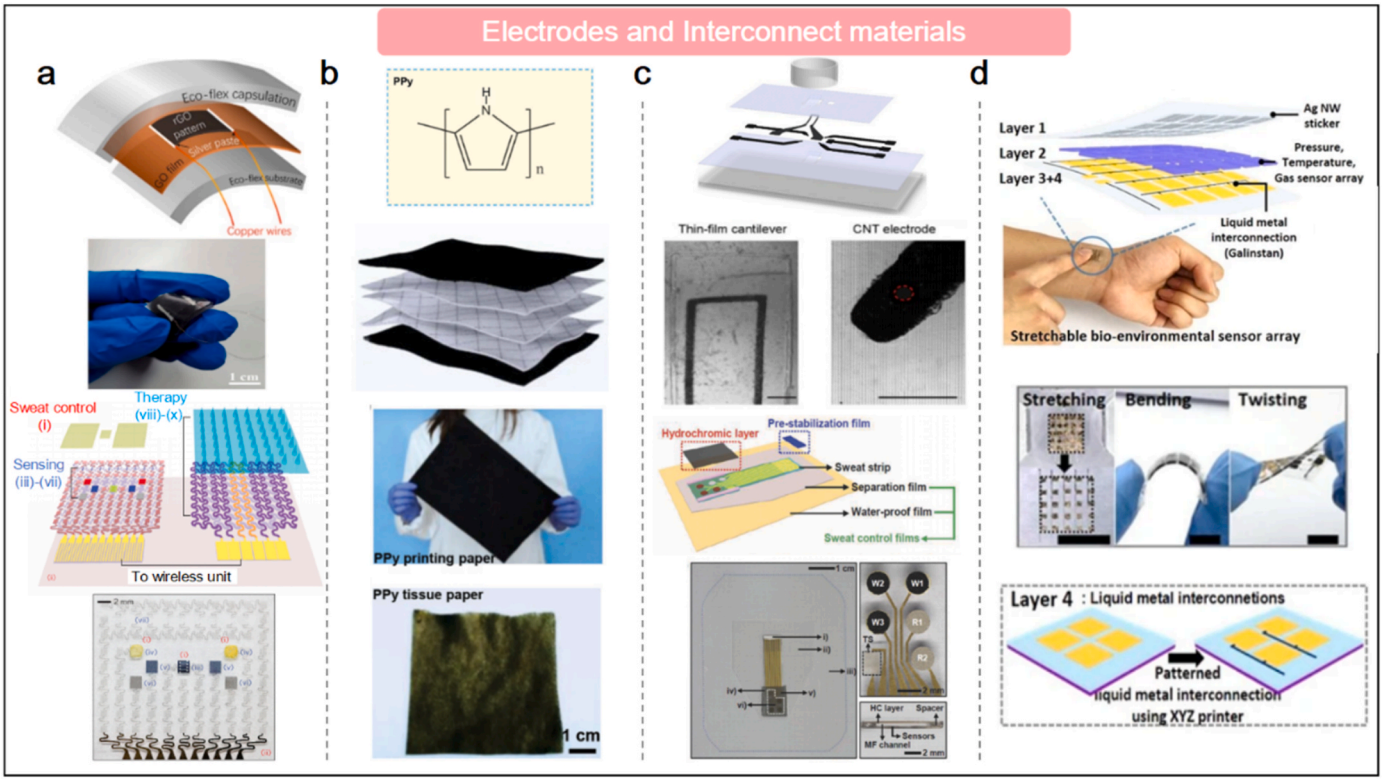

Fig. 7. The electrodes and interconnect materials of the flexible sensors related to cardiocerebral vascular system. a) Schematic of a single sandwich-like sensor containing an LSG pattern, two electrodes and a vertically integrated Eco-flex package (top 1). The triode-mimicking positive graphene pressure sensor with good flexibility (top 2) [161]. Diagram of the diabetic patch (bottom 2). Electrochemical sensor array (bottom 1) [162]. b) Molecular formula of PPy (top 1). The PPy electrode shown in black paper (printed paper) and the PPy active layer shown in white paper (tissue paper) (top 2). Photograph of printing paper (bottom 2). Photograph of tissue paper (bottom 1) [163]. c) Schematic illustration of the structural components of the carbon-based biosensing platform (top 1). An image of cantilever deflection caused by cardiomyocyte contraction and an example image of CNT electrodes. Scale bar: 500 μm (top 2) [170]. Diagram of a disposable sweat analysis strip (bottom 2). Optical image of a disposable sweat analysis strip (left), temperature Sensors (TS) and Glucose Sensors (W : WE; R : RE) (top right) and side view of the strip (bottom right) (bottom 1) [171]. d) Schematic of a skin-mounted multifunction (MF) sensor array with pressure/temperature and gas sensors which are integrated by using directly printed liquid metal interconnects (top) [172]. Stretchable multifunctional sensor array images in stretched, bent and distorted states. Scale bar: 2 cm (middle). Manufacturing process for stretchable MF sensor arrays (bottom) [172]. Reprinted from Refs. [161,162,163,170,171,172] with permission.

easy cutting and foldable, which can be achieved by choosing polypyrrole printing paper with high conductivity as an electrode, and PPy thin paper with low conductivity as the active layer (Fig. 7b). The electrical conductivity of printing or tissue paper was tuned by immersing them into reaction solutions of various concentrations of pyrrole and ferric chloride for different reaction times. In addition to the pulse, the signals monitored by the sensor also include sound, breathing, and body movement [163]. Besides, a sensor for dopamine detection with graphene oxide/poly (3,4-ethylene dioxythiophene): polystyrene sulfonate (GO/PEDOT:PSS) composites was developed, exhibiting high charge storage capacity at 100 Hz and low interfacial impedance. GO/PEDOT:PSS composites have net negative charges and the characteristic of enhanced interfacial, which optimizes both the sensitivity and detection limits of the sensor to dopamine [164]. Lo et al. [165] fabricated a polymer blend and patterned it by inkjet printing. The blend is made from PEDOT:PSS raw material and has stretchable properties. The researchers added solvents of different polarities to see the effect on the material's electrical properties. Finally, it was considered that 5 wt% ethylene glycol added as an additive to the PEDOT:PSS aqueous solution was the ideal blend among all the scenarios. In addition, further combining the blend with poly (ethylene oxide) can be used to improve the elasticity of the blend. The resulting polymer blend was inkjet printed and patterned to produce films with excellent properties, including high stretchability and electrical conductivity. In addition, the mixture can be used as an interconnect and dry electrode for medical PPG and ECG measurements [165]. Conductive polymer composites enhance durability upon mechanical action by increasing the adhesion of conductive polymers to textiles [205]. Therefore, a method to increase the flexibility of conducting polymers is to prepare composite materials, usually adopting polymers with high flexibility and stretchability (such as polyurethane).

3.2.3. Carbon materials

Carbons and nano/micro metal particles, which are made in the form of CNTs, metal plates, graphene particles and metallic nano/microwires, tend to exhibit rigidity and lack of interconnectivity [10]. Flexible conductive traces are often achieved by dispersing these materials in elastomers to create infiltrated networks for conduction [206]. Both CNTs and graphene show excellent electrical conductivity in performance, and all can be considered electrode materials for capacitive sensors [42]. The diameter of the nanowires largely determines the optical and electrical properties [207]. It has been reported that the conductivity and transparency of the nanowire networks with high aspect ratios (length/diameter) are higher than those with low aspect ratios [208]. In addition, photoelectric sensors are a classic type of heart rate monitoring, and photoelectric devices need at least one transparent electrode to transmit or collect light. By increasing the conductivity, PEDOT:PSS is thought to be useful for transparent electrodes in optoelectronics [209].

A new implantable electrochemical sensor developed by applying silica nanoporous membrane to functionalized carbon fiber microelectrode exhibits the characteristics of high current stability and quick response, which can be applied for continuous monitoring of oxygen levels in vivo [166]. In addition, graphite can be used as electrodes for developing sensor patches. Electrodes in an interdigitated pattern can be formed by casting graphite powder on a 3D-printed mold [210]. Andreotti et al. [167] developed a sensor to detect serotonin (5-HT) using nail polish and graphite powder to produce conductive inks. 5-HT imbalance is thought to be involved in BP regulation [211], depression [212], hypertension [213], and kidney diseases [211]. The sensor is convenient in the application of electrochemical sensing and biosensing [168]. There is a study to reduce the electrochemical resistance and enhance the ascorbic acid diffusion by adjusting the graphene fabrication process, which is achieved by changing the self-assembly layer and the modified region. In 500 μM ascorbic acid, the sensor exhibits an excellent low limit of detection (0.11 μM). This simple method could improve the performance of sensors that detect dopamine. At the same time, it is of great significance to further improve the sensitivity and selectivity of electrochemical sensors [167]. A study has used poly (*o*-anisidine) and CNTs (POA/CNTs) nanocomposites to modify glassy carbon electrode (GCE), and the modified electrode exhibits durable electron mediating behavior using the synergistic effect of composites for dopamine (DA) detection. The sensor was used to selectively detect the neurotransmitter DA with a wide linear range, and shows excellent sensitivity, reproducibility, and performance stability [169]. Dou et al. [170] fabricated a biosensing platform using carbon black (CB)-PDMS composites and carbon nanotubes (CNTs), where carbon black (CB)-PDMS composites exhibited piezoresistive behavior, the flexible thin-film cantilever embedded with a strain sensor of the composite is used to measure shrinkage, and carbon nanotubes (CNTs) with electrochemical sensing capabilities are made for electrodes. This platform is able to simultaneously measure iPSC contractile functions including beating rate, beating rhythm, contractile stress and extracellular field potential (Fig. 7c) [170]. Hong et al. [171] constructed a disposable sweat strip using carbon as working electrodes (WEs) and Ag/AgCl reference electrodes (REs) to form a glucose sensor. The entire device integrates sweat-based sensing and vital signs monitoring, which can combine measured glucose and physical activity data to assess post-exercise blood glucose levels. To accommodate changes in glucose sensor measurements due to temperature variations, an integrated temperature sensor (TS) is included in the strip. (Fig. 7c) [171].

3.2.4. Liquid metals-based conductors

Liquid metals are extremely stretchable (infinitely) and electrically conductive [214], combining them with polymers or elastomers will provide promising electrical conductivity or mechanical properties [10]. Hong et al. [172] fabricated a skin-like, multifunctional stretchable sensor array using directly printed Galinstan as an interconnect and a polyurethane foam coated with multi-walled carbon nanotubes/polyaniline nanocomposites as the sensing material, which can be applied to wrist pulse, ammonia gas measurement and body temperature (Fig. 7d) [172].

3.3. Materials of sensing active component

Flexible wearable sensors are divided into different types in line with the mechanism, and various sensors with multifarious sensing active element materials present great discrepancies in working principles [10]. Resistive [161], piezoelectric [215], dielectric [216], and triboelectric [217] materials are commonly adopted for sensing active components. Generally, carbon materials, metal materials and polymers are used for manufacturing [42]. Graphite, CNTs, and graphene, which are the different allotropes of carbon, are commonly applied in the fabrication of wearable sensors [42].

3.3.1. Carbon materials

Graphite exhibits properties of excellent compressive strength, corrosion resistance, electrical and thermal conductivity, and excellent biocompatibility as well. These advantages promote its frequent adoption in devices for biomedical applications [210]. Li et al. [173] fabricated a 3D graphite-polymer flexible strain sensor using 3D graphite as the key sensing element of the polymer composite strain sensor. The sensor can achieve real-time health monitoring such as human pulse, respiratory rate and throat vibration, and can also detect tiny movements with high sensitivity and durability [173]. Additionally, Lee et al. [174] mixed C_{70} based on the C active layer into TAPC in a ratio of 20:1 to make a photodetector, and proposed a reflective patch-type sensor according to the design freedom provided by organic technology. It can be applied for pulse and blood oxygen monitoring, which has the characteristic of ultra-low power consumption (Fig. 8a) [174].

Carbon nanotubes (CNTs) possess unique mechanical and physical properties, among others, that make them desirable for various

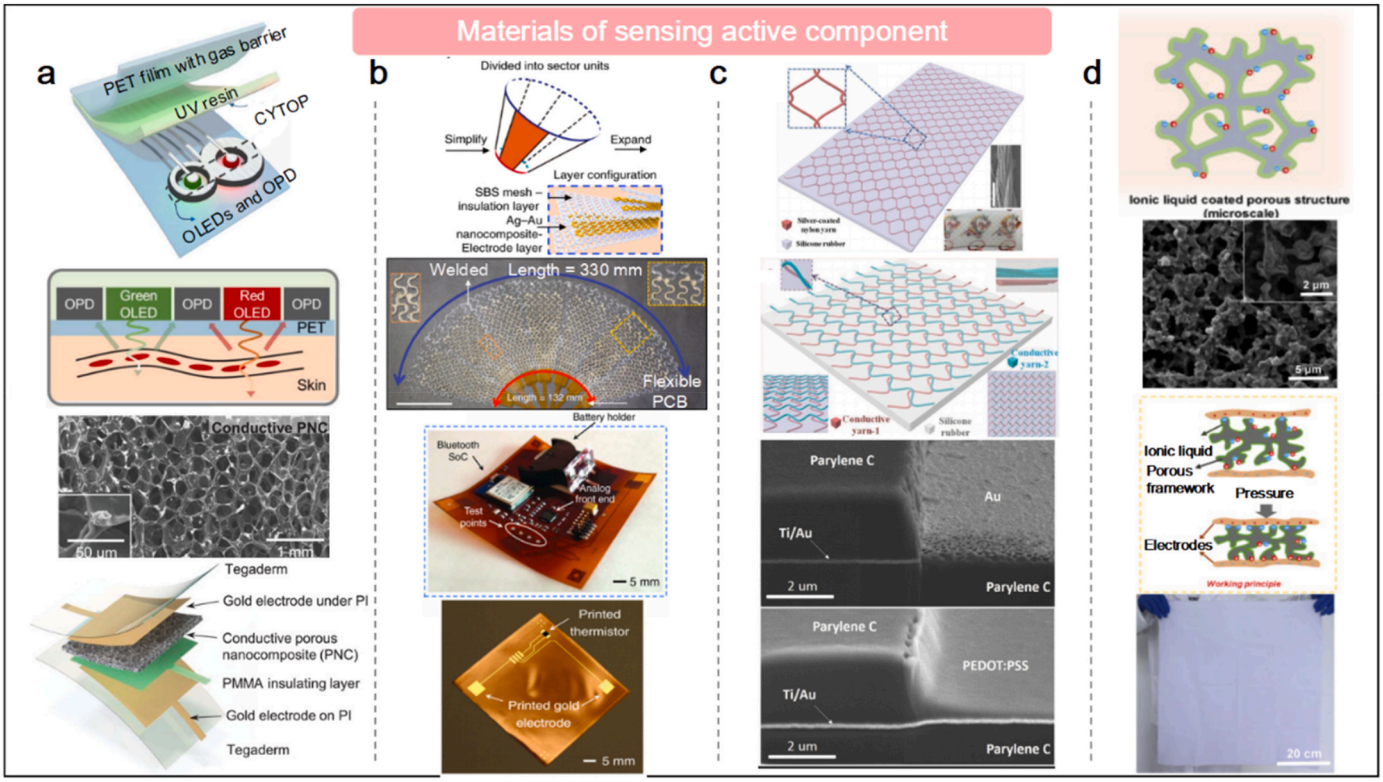

Fig. 8. The sensing active component materials of the flexible sensors related to the cardiocerebral vascular system. a) Cross-sectional illustration of the OPO sensor (top 1) and magnification depicting the arrangement of the device and the light reception process through the skin medium (top 2) [174]. SEM top view of the PNC (bottom 2). Diagram of the HRPS (bottom 1) [175]. b) The schematic illustrates the design process of an implantable cardiac mesh based on Ag–Au nanocomposites, specifically developed for monitoring and stimulating the internal functions of a porcine heart. (top 1) Optical camera image of 2D fan-shaped cardiac mesh (top 2) [179]. Photo of the component side of the patch (bottom 2). Photograph of the side of the sensor (before the assembly of the assembly) which shows the printed gold ECG electrodes and thermistor (bottom 1) [180]. c) Schematic diagram of the SI-TENG. The basic repeating diamond-shaped unit of the yarn's conductive network (top left). SEM image of the surface morphology of a triple twisted silver-plated nylon yarn (right) (scale bar: 400 μm). Transparency of SI-TENG (bottom right) (top 1). Tactile sensing array based on SI-TENG. The basic sensing pixels, profile, partially enlarged oblique and front views of the haptic sensing array are located at its top left, top right, bottom left and bottom right respectively (top 2) [181]. SEM image of a 45° cross-section view of the Au microelectrode edge after FIB sectioning, showing the poly (parylene) C encapsulating the metal lead and the exposed gold interface layer approximately 1.9 μm below the outer surface of the poly (parylene) C (bottom 2). SEM image of a 45°cross-sectional view of the PEDOT:PSS/Au microelectrode after FIB sectioning, showing the uniform coating of the PEDOT:PSS layer on top of the exposed Au contacts below (bottom 1) [183]. d) Schematic representation of the porous structure of an ionic liquid coating (top 1). Surface and cross-sectional images showing the morphology of the porous cellulose acetate film loaded with 50 wt% ionic liquid (top 2). The sensor changes the contact area between the porous dielectric layer and the electrodes in response to mechanical stimulation (bottom 2). The photo of cotton textile loaded with [BMIM]•PF_6 (bottom 1) [141]. Reprinted from Refs. [141,174,175,179,180,181,183] with permission. (For interpretation of the references to colour in this figure legend, the reader is referred to the Web version of this article.)

applications [218]. CNT has been utilized in the fabrication of percolation conducting networks for elastic strain sensors, with high aspect ratio quasi-1D structures [173]. Carbon nanotubes are known for being chemically inert and rigid, as well as having strong π-π interactions that contribute to their electronic properties. However, due to these characteristics, pure carbon nanotubes are not easily soluble in common polymers or volatile organic solvents, which can limit their processability [219]. CNTs come in two types: single-walled CNTs (SWCNTs) and multi-walled carbon nanotubes (MWCNTs), each with unique structures. Thanks to their exceptional properties, CNTs have been found used in the preparation of multifunctional composite materials [219]. Composites for humidity and touch sensing include self-healing polymers combined with CNTs [220]. A piezoresistive interlocked microdome array which uses CNT composite elastomer film as component is able to detect various mechanical stimuli such as shear force, twisting force, normal force, and bending force [143]. A hybrid-response pressure sensor (HRPS) was constructed by sandwiching a piece of highly porous nanocomposite (PNC) with two flexible electrodes, which exploited the hybrid piezoresistive and piezocapacitive responses of PNC to make itself high sensitivities in certain pressure range (Fig. 8a) [175].

Graphene is considered to be a very potential material for sensing applications. Its excellence lies in its mechanical properties and electrical properties [221], which exhibit nearly perfect thermal properties and optical transmittance. Graphene has been used to make capacitors electrodes and as fillers in the fabrication of piezoresistive composites, which are similar to the CNTs mentioned above [42]. However, it is difficult to remove the surfactant in the production process of graphene, and the cumbersome production method leads to its high production cost [222,223]. In 2014, people discovered a method of using PI films as raw materials to prepare graphene. The operation is to irradiate the film with a laser so that the PI films as carbon sources are graphitized, and finally, porous graphene can be obtained [224]. This simplifies production steps and reduces reagent consumption, thus greatly reducing production costs. The mentioned method of laser-induced graphene (LIG) was later adopted to make a variety of electronic devices [225]. Currently, piezoresistive and mechanically flexible pressure sensors with a large measurement range have been fabricated using LIG, providing promising prospects for the demand for pressure sensors [226]. In order to obtain high precision in a specific range, Zhang et al. [176] used graphene nanomaterials to attach and fill sponge-shaped melamine to prepare a piezoresistive sensor. To ensure flexibility, the

sensor used the material Ecoflex as the substrate. The sensor has a vertical structure and can collect and detect physiological signals such as heart rate (HR), blood pressure (BP) and pulse waveform [176].

3.3.2. Metal materials

Some metal materials commonly used in wearable sensors show excellent electrical conductivity [42]. Metal nanostructures have found widespread applications as conductors, and some metal nanomaterials exhibit pressure-sensitive or heat-sensitive properties. Consequently, they are increasingly being used to enhance the performance of sensors. The most commonly used metal nanostructures are silver nanostructures, gold nanostructures, and copper nanostructures. Copper nanostructures, owing to their low cost and abundance, have emerged as promising candidates for sensor applications, and researchers have shown considerable interest in them. On the other hand, gold nanostructures, despite being expensive, possess exceptional biocompatibility and oxidation resistance, making them ideal for certain sensor applications [227]. Liquid metal has a melting point that is close to room temperature. Moreover, it exhibits fluidity, flexibility, and exceptional thermal and electrical conductivity. Mercury and gallium (Ga) are the most commonly used liquid metals, but mercury is limited in its applications due to its strong toxicity. In contrast, Ga can be readily alloyed with other metals, particularly post-transition and zinc group metals. Consequently, resulting alloys exhibit lower melting points and higher entropy. Liquid metals based on Ga are considered safe and hold great promise for use in sensor applications [228].

Galinstan and PDMS were physically mixed by Oh et al. [177] to synthesize Galinstan-PDMS composites and fabricate deformable pressure-conducting rubber sensors. After the sensor is applied with force exceeding a threshold value, the composite material will change from non-conductive to conductive. The threshold is determined by the ratio of liquid metal to PDMS, which is tunable during the preparation process [177]. Cao et al. [178] utilized the cotton fiber coated with reduced graphene oxide doped with silver nanowire (rGO-AgNW@cotton fiber) to fabricate a piezoresistive sensor that can be applied for detecting signals including pulse waves. AgNWs provide a fast transport channel for charges, which improves sensitivity and reduces fast response time, among which the rGO provides protection for AgNWs from oxidation [178].

Choi et al. [179] prepared flexible Ag–Au nanocomposites with high conductivity and biocompatibility by combining a mixture of Ag–Au nanowires modified with hexylamine ligands in toluene, SBS elastomers, and additional hexylamine composite material. Composite materials fabricated wearable devices with skin-like exteriors and implantable cardiac meshes can be applied to monitor electrophysiological signals such as surface ECG, intracardiac, and surface EMG (Fig. 8b) [179]. In addition, studies have reported that the fabricated sensors integrated with conventional electronic devices through printing technology create flexible sensing platforms. Wearable sensor patch adopts printed gold electrodes to sense ECG signals and printed nickel oxide thermistors to measure skin temperature (Fig. 8b) [180].

3.3.3. Polymers

Similar mechanical properties exist between organic sensing materials and many insulating based polymers. Organic materials, such as PEDOT-based polymers with high transparency, thermal stability and tunable electrical conductivity, can also be used to construct active elements due to their great electrical properties [42]. Conductive polymer materials such as PEDOT have gained significant attention in sensor applications due to their unique properties. PEDOT fibers, gels, and films are among the widely used forms of these materials that have shown promising results in various sensing applications [229].

It has been reported that silicone rubber has been adopted as an elastic dielectric due to its ultra-soft and tough properties, inherent biocompatibility, a strong tendency to acquire electrons, and superior mechanical properties to make a triboelectric nanogenerator (SI-TENG) for possible energy harvesting and multifunctional pressure sensing. Great stretchability, detection resolution, sensitivity and fast response time are achieved by embedding silicone rubber elastomer into a continuous, planar yarn conductive network of three-layer twisted silver-coated nylon yarns in a zigzag arrangement. The device can be applied as a multifunctional electronic skin, which monitors arterial pulse and voice vibration in real time. The SI-TENG-based pressure sensor serves as a versatile tactile sensing array, offering stretchability, flexibility, and comfort when worn on the human wrist. It can be easily bent, twisted, and adjusted to accommodate different movements and activities. (Fig. 8c) [181].

The interpenetration of poly (3,4-ethylene dioxythiophene) (PEDOT) into nitrile butadiene rubber and poly (ethylene glycol) dimethacrylate crosslinked material can fabricate PEDOT-embedded hybrid electrospun fiber mats with great conductivity. Stretchable and flexible hybrid electrospun mats with adjustable fiber orientation can be designed as strain sensors to monitor body movement and muscle contraction, which exhibits high electrical conductivity. The electrospun fiber mat has been shown to support proliferation and cardiomyocyte adhesion [182]. Conductive composite poly (3,4-ethylene dioxythiophene):polystyrene sulfonate (PEDOT:PSS) is a promising polymer for conductive textile applications due to its excellent performance in water solubility, making it easy for roll-to-roll processing and compatible with many conventional processing techniques [205]. Noted that PEDOT:PSS film is unable to withstand continuous bending and stretching due to a lack of flexibility and stretchability which are necessary for flexible electronics. The bending or stretching beyond the threshold value may initiate cracks that will reduce the conductivity of the film. Therefore, printing and infiltration of PEDOT:PSS inks into porous substrates such as fabrics and cellulose papers can promote adhesion and work as a potential solution [197]. Ganji et al. [183] fabricated microelectrodes by using Au, PEDOT:PSS/Au, Pt, and PEDOT:PSS/Pt as different interface materials, and investigated the corresponding EcoG devices. By comparing the electrochemical properties of these electrodes, they found that PEDOT:PSS has better capacitive charge coupling and Faradaic charge transfer than metal electrodes. Due to this property, the electrochemical performance can be improved and the noise can be reduced at smaller electrode diameters (Fig. 8c) [183].

Poly (vinylidene fluoride) (PVDF) and its copolymers have the advantages of non-toxicity, light weight, and easy processing, thus they are the representative active materials of piezoelectric sensors [230,231]. The resulting flexible sensor fabricated from PVDF (and its copolymer PVDF-TrFE) can be used in the field of medical measurement to detect vital signals (HR and respiration), plantar pressure distribution, etc. [42] The dielectric properties can be enhanced by adding inorganic fillers with high dielectric constant, including barium titanate ($BaTiO_3$), titanium dioxide (TiO_2), zinc oxide (ZnO) and lead zirconate titanate (PZT) dispersed into the PVDF matrix [184]. Due to the increase of the piezoelectric strain constant coefficient value of PVDF, the pressure sensing capability is correspondingly improved [232,233]. Shin et al. [184] fabricated a high-sensitivity, wearable wireless pressure sensor for HR monitoring. Hybrid films based on ZnO nanoneedle/PVDF exhibit low polarization response time, high dielectric constant and excellent durability [184]. PVDF also has plenty of applications in the clinical field such as the treatment of infarcts or aneurysms. Based on the traditional catheters and guide wires methods, Takashima et al. [185] developed a catheter-type tactile sensor for minimally invasive surgery that consists of PVDF film [185].

In addition to PEDOT:PSS, PANI, PPy, poly (3-hexylthiophene) (P3HT), other semiconducting polymer organic materials are promising sensing materials in the field of flexible electronics. These polymers are also applied for making flexible electronics, such as channel materials in field effect transistors (FETs) [234].

3.3.4. Ionic liquid

In the field of electrochemical sensor research, Ionic liquid (IL), a salt

comprising organic cation and organic/inorganic anion [235], has attracted extensive attention from scholars. IL can build strain sensors by embedding them into PDMS-based microchannels, similar to liquid metals [236]. Ionic liquids are a type of solvent with a low melting point that exhibit biological activity. Some ionic liquids have been found to possess antibacterial properties, making them a potentially useful tool in the fight against bacterial infections [235]. In addition to this, a strategy for fabricating flexible tactile sensors has been studied. The sensing unit can be activated by loading the ionic liquid [BMIM]•PF_6 on the fabric backbone of commercial textiles or synthetic porous membranes, thereby the EDL capacitive interface is constructed when AgNWs or flexible silver paste are coated on the substrate (Fig. 8d) [141].

3.4. Encapsulation

The encapsulation layer is a crucial component in safeguarding the sensor element from various forms of environmental damage. Its primary function is to shield the sensor against physical and chemical harm caused by mechanical stress, humidity, dust, liquids, and other external factors. Additionally, it provides electrical insulation and protection, making it easier to install and integrate the sensor into different devices or systems [237]. The choice of material for the encapsulation layer depends on the specific application requirements. Flexible materials such as polyester film (e.g., PET) or polyimide (PI) are commonly employed due to their excellent flexibility and bending properties [238]. These materials allow the encapsulation layer to conform to different shapes and facilitate integration into complex structures. Apart from polyester film and polyimide, other materials like thermoplastic elastomers can also serve as suitable encapsulation layers for sensors. The selection of these materials depends on factors such as the desired level of flexibility, durability, temperature resistance, and compatibility with the sensor's surroundings. There are several main kinds of materials used for encapsulation in flexible sensor. Organic polymers such as epoxy resin [239], polyimide [240], offer good insulation properties, low dielectric constant, making them suitable for insulated package. Glass is often used in optical packaging due to its excellent light transmission characteristics and chemical stability [241]. It helps protect internal optical components while allowing light to pass through effectively. Encapsulants such as silica gel [242] and polyurethane [243] provide strong adhesion, chemical resistance, and mechanical strength. They play a crucial role in protecting sensors.

3.5. Characteristics of materials in flexible electronics

Polymers in flexible electronics exhibit properties such as flexibility, light weight, and biocompatibility [244], making them suitable for use as substrates. When employed as sensing active components, they also offer the advantage of low energy consumption [245]. Conductive polymers, in particular, possess excellent processability and can be utilized in electrodes and interconnects. Natural materials, with their flexibility, air permeability, and biodegradability [246], are frequently employed as substrates in wearable and flexible electronics. Solid metal materials, on the other hand, possess characteristics such as electrical conductivity, high hardness, durability, and high temperature stability [247], making them ideal for producing electrodes and interconnect materials in flexible electronics. These metals are also used as sensing active components due to their electrical conductivity [248], good thermal conductivity [249] and ease of processing. Carbon materials exhibit high conductivity [250], light weight [250], and biocompatibility [251], allowing them to serve as electrodes and interconnects. When employed as sensing active components, they demonstrate high sensitivity [252], fast response speed [253], and a wide operating temperature range [254]. Conductors based on liquid metals possess characteristics such as flexibility, high conductivity, low resistance [255], making them suitable for use as electrodes and interconnects. Lastly, ionic liquids can function as sensing active components due to their high electrical conductivity, high chemical stability, and low volatility [256].

4. Applications

In this chapter, the applications of flexible electronics applied with the cardiocerebral vascular system and heart-brain network will be elaborated on in detail. The cardiocerebral vascular network section mainly involves the sensing applications of heart rate (HR), blood oxygen saturation (SpO_2), blood pressure (BP), blood glucose and other related indicators. While the cerebral section mainly summarizes crucial detection applications related to temperature, intracranial pressure (ICP), cerebral blood flow (CBF), brain tissue oxygenation, cerebral metabolism and other targets (Fig. 9). The mentioned flexible sensors applied for indicators in the heart and brain are summarized in Table 2 at the end of this chapter , and the characteristics of the materials needed for each usage and materials commonly used in each application (including without limitation) are shown in Table 3.

4.1. Applications with cardiac and cardiovascular network

4.1.1. Heart rate

Heart rate (HR), which describes the cardiac cycle, refers to the number of times the heart beats based on the first sound within 1 min. There are individual differences in HR, at the same time, HR is also depending upon age, gender, and other physiological conditions. For instance, the HR of an adult with tachycardia can exceed 100 beats per minute [335], whereas bradycardia is common in older adults [336] or athletes [337].

For the proper detection locations of HR based on the working principles of bioelectrical, optoelectrical, mechanoelectrical and ultrasonic techniques, they are generally placed on the chest, wrist, neck and fingertips, etc. The resulting signal detected can be utilized as an indicator to judge arrhythmias, such as atrial fibrillation.

The measurement target of the bioelectric technique is biopotential, which can measure ECG signals [10]. Although plenty of wearable systems are characterized by continuous monitoring and non-invasiveness, most systems are not systematically verified for signal quality and are limited to performance demonstration. For example, textile electrodes that collect ECG signals are susceptible to skin-electrode impedance resulting in distortion of ECG data [57]. Various factors can introduce errors to the ECG signal. Motion artifacts caused by bodily movements such as breathing and voluntary muscle contractions can induce relative motion between the body surface and the electrode, as well as arterial pulses transmitted to the body surface. As a result, accurate interpretation of the ECG signal requires careful consideration and management of these potential sources of interference. More recently, with the advancement of sensor technology, a new generation of wearable sensor systems for infant monitoring has emerged. Chen et al. [260] have addressed the challenge of collecting ECG signals by proposing a replaceable electrode with a flexible connection structure. The design of the electrode resembles a small sandwich pad, where the upper layer of E-textile is connected between metal lead buttons, regular cotton is placed underneath, and another layer of E-textile forms the bottom layer. This unique design enhances the electrode's ability to withstand motion artifacts and minimizes signal errors, making it an effective solution for ECG signal collection [260]. In clinical settings, wired instruments used for monitoring the vital signs of critically ill newborns are often heavy, as most currently available equipment is rigid and wired. However, due to the fragile bodies of neonates, it can be challenging for them to tolerate these devices. In fact, the rigid components of monitoring equipment can easily damage the delicate skin of newborns [338]. Once the skin is damaged, most of the newborns with severe illness will aggravate their condition due to lower immunity than normal newborns. This is why it is crucial to prevent any secondary injuries caused by monitoring instruments.

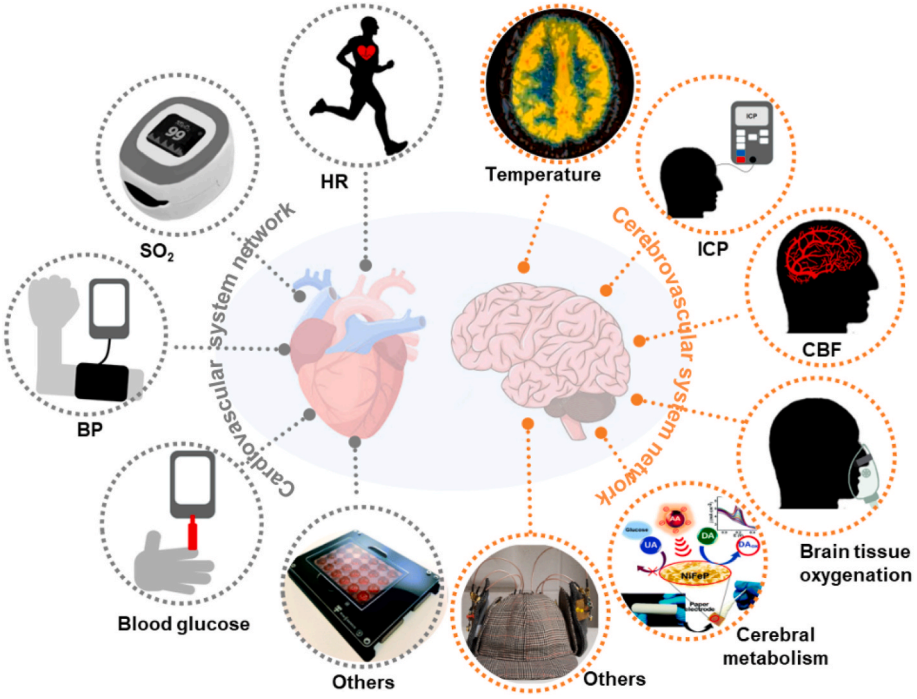

Fig. 9. The applications of flexible sensors related to cardiocerebral vascular system. Schematic diagram of cardiac parameter tests (left) and schematic diagram of brain tests (right). The photography of others applied in the heart: The 24-well cardiac microphysiological device in the recording rack, which is suitable for data acquisition within an incubator environment [257]. The diagram of cerebral metabolism applied in brain: DA detection.[258] The photography of others applied in the brain: wearable neurodegeneration monitoring device [259]. Reprinted from Refs. [257–259] with permission.

Table 2
The flexible sensors applied for indicators related to cardiocerebral vascular system.

Organ	Indicator detected	Detected locations	Working principles	Related diseases	Reference
Heart	HR	Wrist, finger, neck, chest, etc.	Bioelectric, optoelectric, mechanoelectric, ultrasonic, etc.	Arrhythmia, etc.	[32,64,88,141,143,144,150,154,155,156,157,163,165,172,173,176,178,184,260,261,262,263–267,268,269]
	SO_2	Earlobe, finger, foot, etc.	Optoelectric, etc.	Hypoxia, etc.	[269–276]
	BP	Arm, wrist, etc.	Algorithms based on PTT, PAT and ML from Bioeletric, optoelectric, mechanoelectric signal, etc.	Hypertension, etc.	[125,158,159,176,177,277,278,279–281,282–284]
	Blood glucose	Mouth, eye socket, epidermis, etc.	Electrochemical, etc.	Chronic pancreatitis, diabetes, hyperthyroidism, etc.	[119,272,285–290,291,292,293,294]
	Other applications	In vivo, in vitro, etc.	Mechanoelectric, electrochemical, etc.	Vascular bed surgery risks, etc.	[31,182,185,257,295,296,297,298,299–301]
Brain	Temperature	Forehead, ear canal, head surface, intracranial, etc.	Thermistor or thermocouple, etc.	Fever, etc.	[116,151,302–304,305,306]
	ICP	Intracranial, head surface, etc.	Mechanoelectric, optical, etc.	Infection, stroke, tumor, hydrocephalus, epilepsy, etc.	[302,303,307,308,309,310,305,311,312,313]
	CBF	Intracranial, head surface, etc.	Thermistor, optical, etc.	Cerebral arteriosclerosis, etc.	[34,314,315,316,317]
	Brain tissue oxygenation	Jugular vein, head surface, etc.	Electrochemical, optical, etc.	Cerebral hypoxia, etc.	[166,303,318,319–321]
	Cerebral metabolism	Head surface, etc.	Electrochemical, optical, etc.	Ischemia or hypoxia, etc.	[33,148,164,167,168,169,258,303,306,322,323]
	Other applications	In vivo, in vitro, etc.	Bioelectric, electrochemical, etc.	Neurodegenerative diseases, etc.	[145,156,160,185,259,324,318,319,313,325–334]

Fortunately, flexible and thin wireless monitoring equipment can address this issue, such as the wireless neonatal vital signs monitoring system developed by Chung et al. [339] This monitoring system can collect various physiological signals, including skin temperature data, ECG, and PPG, to determine HR, HR variability, blood oxygen, respiratory rate, and pulse arrival time. As the measurement module of the system closely attached to the newborn's skin, the Epidermal Electronics Systems are installed on the chest and soles of the feet to record ECG and PPG charts, respectively. The use of non-toxic ionic liquid and silicone elastomer encapsulation protects the newborn's skin from strong mechanical contact that may raise the risk of infection. Overall, this wireless monitoring system provides a safe and effective way to monitor a newborn's vital signs without compromising their delicate skin condition. (Fig. 10a) [339]. The current tattoo-like epidermal electrodes are often small in size, which limits their ability to effectively capture large-scale physiological signals. However, Wang et al. [340] have successfully developed electronic large-scale tattoo-like epidermal electrodes that can accurately record ECG signals. To ensure that the electrodes capture only the target signals and minimize errors caused by other unnecessary electrical signals, the researchers incorporated a compensation module into the design, which was validated through experiments. This large-area epidermal electrode is fabricated with a filamentous serpentine appearance through a unique "cut and paste" fabrication process. In addition to ECG signal collection, these electrodes

Table 3
The characteristics of the materials needed for each usage and materials commonly used in each application (including without limitation).

		Heart				Brain				
		HR	SO2	BP	Blood glucose	Temperature	ICP	CBF	Brain tissue oxygenation	Cerebral metabolism
Required material properties	Substrate	Softness, thin design, etc.	Softness, Durability, etc.	Softness, plasticity, etc.	Softness, etc.	Softness, thin design, high temperature resistance, etc.	High bendability, ductility, durability, stability, etc.	Softness, biocompatibility, etc.	Softness, durability, biocompatibility, etc.	Softness, biocompatibility, stability, etc.
	Interconnect/ Electrodes	Conductivity, stability, etc.	Conductivity, stability, etc.	Stability, etc.	Conductivity, durability, etc.	Conductivity, stability, etc.	Conductivity, stability, flexibility, scalability, etc.	Conductivity, elasticity, etc.	Conductivity, stability, etc.	Conductivity, corrosion resistance, etc.
	Sensing Element	Responsiveness, stability, light/force sensitivity, etc.	Fast response, stability, oxygen sensitivity, etc.	Pressure sensitivity, sensitivity, durability, etc.	Biocompatibility, high sensitivity, selectivity, stability, etc.	Sensitivity to temperature changes, etc.	Pressure responsiveness, etc.	High sensitivity, stability, etc.	High sensitivity, selectivity, stability, etc.	High sensitivity, high selectivity, stability, etc.
	Encapsulation	Abrasion resistance, water resistance, pollution resistance, etc.	Optical clarity, abrasion resistance, etc.	Flexibility, abrasion resistance, sealing, etc.	Biocompatibility, etc.	Thermal conductivity, stability, etc.	Durability, biocompatibility, etc.	Durability, biocompatibility, etc.	Durability, biocompatibility, etc.	Biocompatibility, etc.
commonly used materials	Substrate	PI, Polyurethane (PU), etc.	PI, etc.	PI film, polyester film, etc.	Polyester film (such as PET), polyimide film (such as Kapton), polyamide film, etc.	PI film, PET film, etc.	PI, PDMS, etc.	PI, etc.	Polyester film (such as polyester film PET), PI film, etc.	PI, PDMS, etc.
	Interconnect/ Electrodes	Conductive textiles, conductive Inks/ colloids, metals, etc.	Conductive polymers, conductive nanomaterials, etc.	Metals, etc.	Conductive ink, conductive polymer, etc.	Metal films, carbon nanotubes, etc.	Metal thin films, conductive polymers, etc.	Metals, carbon nanotubes, etc.	Metals, carbon nanotubes, conductive polymers, etc.	Metals etc.
	Sensing Element	Semiconductor materials, metals, etc.	Semiconductor materials, etc.	Silicon material, etc.	Glucose oxidase, etc.	Semiconductor materials, etc.	Silicon material, etc.	Polymer optical fiber, semiconductor material, etc.	Optical fiber, biological enzyme, etc.	Enzymes, etc.
	Encapsulation	Polyurethane, silica gel, etc.	Polyurethane, silica gel, glass, etc.	Polyurethane, silica gel, elastic cloth, etc.	Polyurethane, polyethylene, silica gel, etc.	Polyurethane, PDMS, etc.	Silica gel, elastic polymer, etc.	Polyurethane, silicone rubber, etc.	Polyurethane, polyester, polyethylene, etc.	Polytrifluoroethylene (PTFE), PDMS, etc.

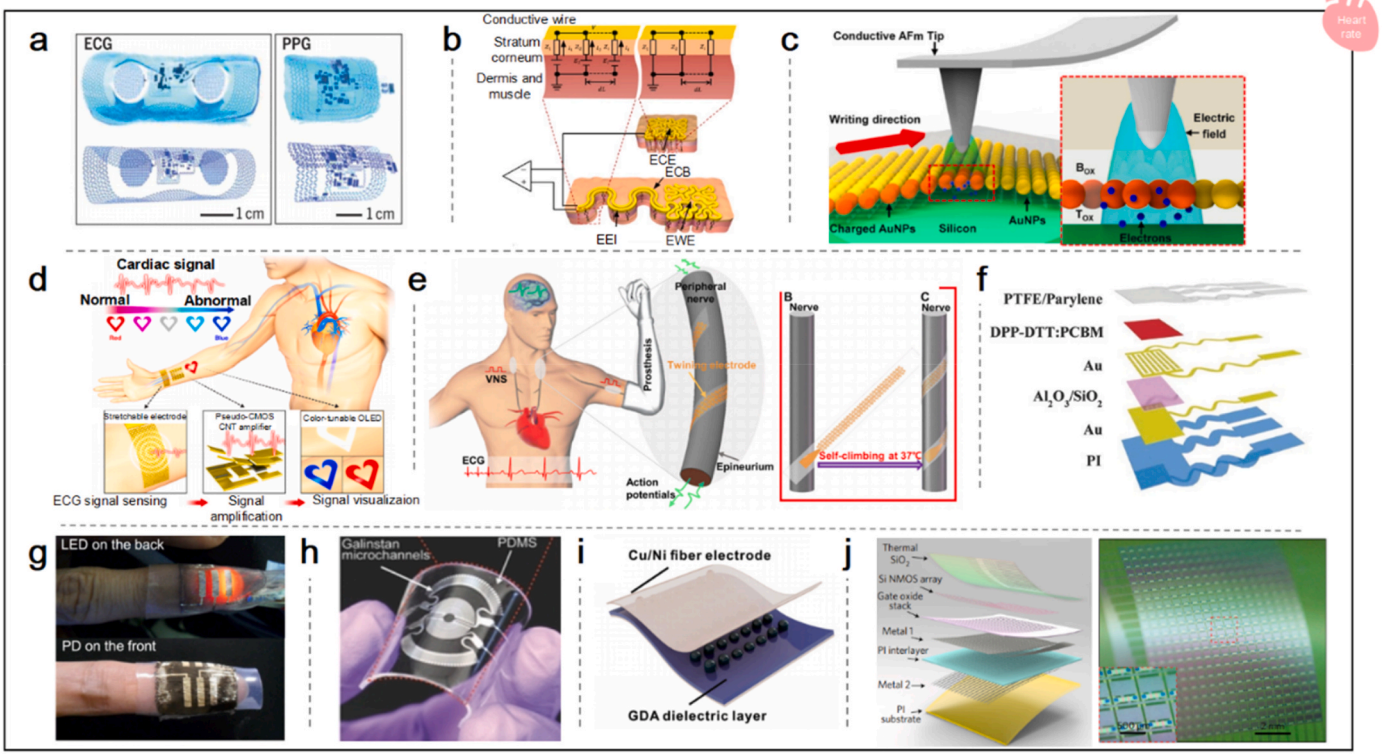

Fig. 10. The applications of flexible sensors in HR. a) Images and related finite element modelling results of ECG and PPG devices bent around a glass cylinder [339]. b) The diagram of epidermal working electrode (EWE), exposed epidermal interconnects (EEI), epidermal compensation branch (ECB), epidermal compensation electrodes (ECE) and their electrode-skin interface equivalent circuits [340]. c) The charge injection process into an AuNP FG using a conductive AFM tip. An enlarged cross-sectional structure of the FG cell (red dashed box) and the charge injection mechanism are shown in the inset [341]. d) Schematic of a real-time wearable heart monitoring system. A stretchable Au electrode measures the ECG signal, which is then amplified by a *p*-MOS CNT inverter in order to obtain a high signal-to-noise ratio. The synchronous color change of the retrieved ECG signal is displayed by a wearable CTOLED [342]. e) Schematic illustration of conceptual peripheral nervous system (PNS) neuromodulation with the function of restoring motor and physiological function (left) and the electrode-neural interface (middle), the self-climbing process driven by body temperature (right) [345]. f) Device structure diagram of the flexible OPT [32]. g) Photograph of a skin-mounted optoelectronic volumetric pulse wave sensor consisting of a QD-LED during LED operation and a QD photodetector wrapped around the subject's finger [346]. h) Optical photograph of the microfluidic diaphragm sensor [347]. i) The schematic illustration of the capacitive tactile sensor based on GDA [348]. j) Decomposition (left, key functional layers are highlighted) diagram showing a capacitively coupled flexible sensing system with 396 nodes with a slightly bent. The photograph (right) of the capacitively coupled flexible sensing system. Enlarged views of several nodes are shown in the inset [349]. Reprinted from Refs. [32,339–342,345,346, 347–349] with permission. (For interpretation of the references to colour in this figure legend, the reader is referred to the Web version of this article.)

have potential applications in prosthetic control and various other fields (Fig. 10b) [340]. Until now, a few studies have validated nanoscale experiments of charge confinement in tightly packed uniform nanocrystals, and several reports have characterized the associated device performance. Kim et al. [341] developed a wearable SiNM CTFM with a nanocrystalline floating gate, and the assembly of gold nanoparticle (AuNP) FG over a large area was achieved by the Langmuir-Blodgett method. By using a conductive AFM, charges were introduced into the AuNP floating gate (FG) following a preset procedure. Due to the potential difference between the conductive AFM tip and the bottom silicon substrate, this creates favorable conditions for the trapping of electrons in the AuNP FG between the tip and silicon. The memory device has a long retention time due to the non-existing particle-level charge confinement of charge delocalization in the packed AuNPs. The proposed device can be used for HR monitoring and long-term data storage, achieved through multiplexing of storage devices and sensor signal amplification (Fig. 10c) [341]. Carbon-based materials and materials play an important role in the fabrication of wearable sensors. A proposed device with a *p*-MOS inverter based on a CNT transistor, a stretchable electrode and a can realize the amplification of ECG signals and real-time monitoring. This wearable ECG monitor enables color visualization of ECG signals due to the integration of voltage-dependent color-tunable organic light-emitting diodes (CTOLEDs) (Fig. 10d) [342]. Stimulating the vagus nerve has been shown to inhibit the activity of the sympathetic nervous system. This can result in a reduction of the release of certain neurotransmitters, which ultimately leads to a decrease in HR, vasodilation, and a drop in blood pressure [343]. Therefore, vagus nerve stimulation (VNS) is considered to be useful in the treatment of some cardiovascular diseases such as heart failure [344]. Zhang et al. [345] have developed a shape-memory electrode that can be utilized for VNS. This flexible electrode climbs onto the nerve at body temperature, forming a wound electrode that perfectly conforms to the target nerve. The key material responsible for this behavior is a smart shape memory polymer. The unique "individual customization" of these electrodes not only enables VNS but also minimizes geometric mismatches between devices and nerves caused by individual differences and other factors, making them highly valuable for potential applications (Fig. 10e) [345].

The measurement target of the optoelectrical technique is to detect changes in light absorption, which can reflect PPG signals [10]. Extracting HR variability from PPG signals using machine learning algorithms can also be used to assess subject sleepiness. Recently, Ryu et al. [64] fabricated a flexible photosensor for detecting biosignals in PPG devices using red organic light-emitting diodes (OLEDs) and organic photodiodes (OPDs). The developed PPG sensor with a conventional driving circuit was successfully applied in detecting PPG signals. Several studies with human bodies were conducted to evaluate the performance of flexible PPG sensors in practical applications. Using a machine learning algorithm, the subject's sleepiness can be estimated

based on the HR variability extracted from the PPG signal. The conventional PPG sensor has an accuracy of 83.3% and an area under the curve (AUC) of 69%, compared to 79.2% and 72.1% of this novel flexible PPG sensor. With the experimental demonstration, the developed flexible PPG sensor achieves similar or even better performance for sleepiness estimation results [64]. Similarly, Pandey et al. [261] fabricated a novel multi-wavelength OLED-OPD flexible PPG sensor for long-term continuous monitoring of PPG signals with a time-interleaved, optimal readout system based on high order auto-tune filter. Noted that the experimental results confirm that the measurement error of the device for HR is less than 3.4 bpm [261]. Moreover, a notable sensor fabricated by Zhou et al. [262] acquires PPG signals by selecting the root of the finger as the target location for the monitoring of ring-type Surgical Pleth Index (SPI). The sensor array structure was simulated and validated by using the Monte Carlo approach. It is worth mentioning that this study provides a ring-shaped medical system that uses sensors extensively to obtain the patient's status during surgery, which has great potential in clinical applications [262]. PPG sensor is a widely used sensor for detecting cardiovascular signals as mentioned above. Xu et al. [32] have developed Near-infrared (NIR) PPG sensors that can detect HRV and BP in both disposable and reusable forms, achieved through different fabrication structures. While disposable sensors offer convenience to users, reusable sensors are more budget-friendly. The disposable sensor consists of an organic phototransistor (OPT) with a transfer function and a reflective high-efficiency inorganic light-emitting diode (LED) placed on the same side of the fingertip. An elastic acrylic adhesive creates a tight contact between these elements and the skin, forming a thin 25 μm film. In comparison, the reusable sensor uses a flexible PDMS substrate that is much thicker (300 μm) than the disposable version's adhesive film, allowing it to be utilized repeatedly. Delemintae OPT and LEDs are integrated into the substrate to form a film-like sensor that can be wrapped around the fingertip. This hybrid sensor consumes less power as it employs high-efficiency LED components (Fig. 10f) [32]. Quantum dots (QDs) have found numerous applications in various fields, such as bioimaging and biosensing, thanks to their unique electro-optic properties [350]. Kim et al. [346] have developed a photosensor that can record PPG signals. The LED in this device has a multi-layer structure with the active layer solely composed of QDs, and the anode of the LED is made from single-layer graphene. The use of PDMS or Ecoflex ensures flexibility, while the entire structure is designed to be both stretchable and foldable. The specific neutral mechanical planar design geometry embedded in the active layer minimizes mechanical stress [240], preventing performance damage caused by repeated actions like stretching during regular use. The PPG sensor is formed by placing the LED and PD on opposite sides and can be wrapped around a fingertip for PPG signal collection. (Fig. 10g) [346].

The measurement targets of the mechanoelectrical technique are strain, pressure and, acceleration, etc., which can detect seismocardiography (SCG), radial pulse, ballistocardiography (BCG) signals [10]. As a case in point, Fan et al. [263] significantly improved the response time of their previously reported MEM sensor by employing cellulose nanocrystals. Fast-response nanocomposites were obtained by adding carbon nanotube-cellulose (CNC) into PDMS, and CNC is an environmentally friendly material with excellent mechanical properties. Owing to the integration of the engineered PDMS bridge structure and CNC-concentrated flexible MEM sensors, the device enables continuous monitoring of signals such as HR from a wearable sensing platform using a pressure sensor [263]. In another reported case based on the mechanoelectrical technique, an ultrathin, ultralight and highly sensitive capacitive pressure sensor was constructed using flexible materials. A dielectric film composed of insulating microbeads contained in PVDF nanofibers was fabricated through an electrospinning process. To be specific, the microbeads optimize the sensitivity of the sensor, as stated in the study. For the application of physiological signal measurement, the fabricated sensor can be used as a wearable sensor for breathing signals and HR monitoring [264]. Furthermore, Tang et al. [265] proposed a flexible pressure sensor that possesses ultra-high sensitivity in an ultra-wide pressure range for HR detection. It is made of a sandpaper-molded multilevel microstructured PDMS and a reduced oxide graphene (rGO) film. Except for HR detection, the sensor has the potential for applications such as respiratory rate, vocal cord vibration, wrist pulse, and foot pressure sensing [265]. In addition, several excellent works related to HR monitoring are listed as follows: Josie et al. [266] reported a pressure sensor with high sensitivity and flexibility for monitoring respiration and HR by making vertically aligned, position- and dimension-controlled ZnO nanotube arrays grown on graphene layers [266]. Another reported sensor fabricated from sensing materials developed by making conductive particles in a silica matrix with non-conductivity has a similar sensitivity to existing sensors and can be cut into desired shapes. The developed wearable strain sensor has the capability for applications in the detection of HR and respiratory rates [267]. To date, wearable SCG sensors have typically upgraded from non-stretchable piezoelectric films or rigid accelerometers. Ha et al. [351] developed an ultrathin and stretchable electronic tattoo with SCG-sensing capabilities that can also measure ECG simultaneously. The researchers adhered stretchable filamentous serpentine (FS) mesh formed after PVDF film patterning with two layers of flexible medical adhesive tape Tegaderm on the top and bottom, and then integrated Au electrodes to create a highly flexible and adaptable design. Thanks to the ideal flexibility and stretchability of the materials used, this electronic tattoo can easily conform to the contours of the skin, providing a comfortable and seamless fit [351]. Gao et al. [347] proposed a high-sensitive microfluidic tactile diaphragm pressure sensor with high response linearity based on Galinstan microchannels in the formation of being embedded, which adopted an equivalent Wheatstone bridge circuit to exploit both tangential and radial strain fields. With a detection limit below 100 Pa and resolution below 50 Pa, this proposed PDMS wristband sensor can be used for wrist pulse and heart rate (HR) monitoring (Fig. 10h) [347]. Generally speaking, the sensitivity of capacitive sensors decreases with increasing pressure; although a large number of microstructured dielectrics have been studied to overcome this problem, this difficulty has not yet been resolved. Ji et al. [348] proposed a novel dielectric layer that can achieve high sensitivity and ultra-wide linear range that can be applied to capacitive tactile sensors. It can produce customizable dielectric behavior. The principle is to use the gradient micro-dome pixels of high-k micro-dome architecture (GDA), and the micro-dome and the electrode are in sequential contact with the pixels from higher to shorter, finally making the effective permittivity of the GDA dielectric layer under pressure changes linearly. The produced sensors can not only provide applications in medicine and sports, such as measuring arterial pulse, motion state, joint flexion and sound vibration but also can be applied to the transmission of morse code for information communication (Fig. 10i) [348]. Electronic devices used to monitor and treat cardiac arrhythmias may present a risk of safety events due to electrochemical reactions between biological fluid components and the device. The flexible electronic device array proposed by Fang et al. [349] does not require direct metal contact for electrophysiological measurements, and can simultaneously allow capacitive coupling between tissue and devices, thus exhibiting great properties of ultra-thin, leak-free, and biocompatible (Fig. 10j) [349].

The measurement target of the ultrasonic technique is to detect the change in arterial diameter, which can reflect pulse wave signals [10]. According to recent reports, a flexible, lightweight sensor composed of a PVDF piezoelectric film was proposed by Huang et al. [268], which could be adopted to measure changes in the brachial artery diameter. This improvement can reduce or avoid deformation of the artery under the sensor and is capable of measuring changes in arterial diameter corresponding to the cardiac cycle and minimizing measurement errors caused by motion artifacts [268].

4.1.2. Blood oxygen saturation

Blood oxygen saturation (SpO_2/SaO_2), a crucial indicator of the

respiratory cycle, refers to the percentage of the HbO_2 oxygen binding capacity in the blood to the total capacity of Hb that can be bound by oxygen. SpO_2 refers to the oxygen saturation measured by pulse oximetry, while SaO_2 means arterial oxygen saturation [352]. The difference between SaO_2 and SpO_2 may exceed three percentage points when oxygen is insufficient [353]. In a normal scenario, the value of SaO_2 of an adult is not less than 90% [354], some scholars define SpO_2 lower than 90% is considered as hypoxemia [355]. Hypoxia is a state in which insufficient oxygen at the tissue level results in an inability to maintain adequate homeostasis [356]. SaO_2 is considered to reflect the respiratory function of the patient and the changes in arterial blood oxygen to a certain extent. Therefore, the monitoring of SaO_2 possesses excellent clinical significance.

The detection location of SpO_2/SaO_2 based on the working principles of the optoelectric technique is generally placed on the fingertips, earlobes, feet, etc. The measurement target of the optoelectric technique is to detect light absorption changes, which can reflect PPG signals. The detection of the signal can be used as an indicator for hypoxia judging [10]. Low peripheral blood and pulse pressure in severe hypoxia can make SpO_2 challenging to detect accurately. There are several reported integrated compact structures of ultrathin and high-performance semiconductors that enable the convenient monitoring of SaO_2. Li et al. [270] propose a compact and highly sensitive flexible hybrid electronic that can be installed in any arterial location for monitoring hypoxia under the state of emergency treatment. The flexible device exhibits powerful capacities for convenient hypoxia monitoring and accurate SaO_2 detection with low concentration [270]. Measurement of oxygen saturation in the blood of transilluminate tissue can be performed optically, which is unfortunately not applicable to impenetrable tissue. Current methods achieve single-point measurements providing and lacking the capabilities of 2D oxygenation mapping. The sensor made by Khan et al. [271] utilized the reflected light from the tissue to monitor blood oxygen saturation. The proposed device, which achieves blood oxygen detection is an organic, flexible sensor array made by combining organic light-emitting diodes and organic photodiodes [271]. Commonly vital physiological parameters of an active individual are often monitored during exercise and fitness training, including HR, sweat pH, and SpO_2. The stretchable optical sensing patch system developed by Wang et al. [269] enables non-invasive monitoring of HR, sweat pH and continuous monitoring of SpO_2 in real-time. The system has excellent repeatability, with a deformation property of up to 35% extra extension [269]. In clinical applications, an implantable device needs to provide tight optical coupling with biological tissue and complete the detection process within a certain period, and thus is possible to realize diagnosis-assisted tools through biosorption. A bioresorbable photonic platform fabricated by Bai et al. [272] that relies on monocrystalline silicon filaments as flexible transient optical waveguides successfully realize biochemical monitoring such as glucose and oxygen saturation with near-infrared spectroscopy. As seen in this study, the platform has multiple applications in biomedicine [272].

In the field of electronics manufacturing, direct printing typically involves depositing one kind of material layer by layer. However, Han

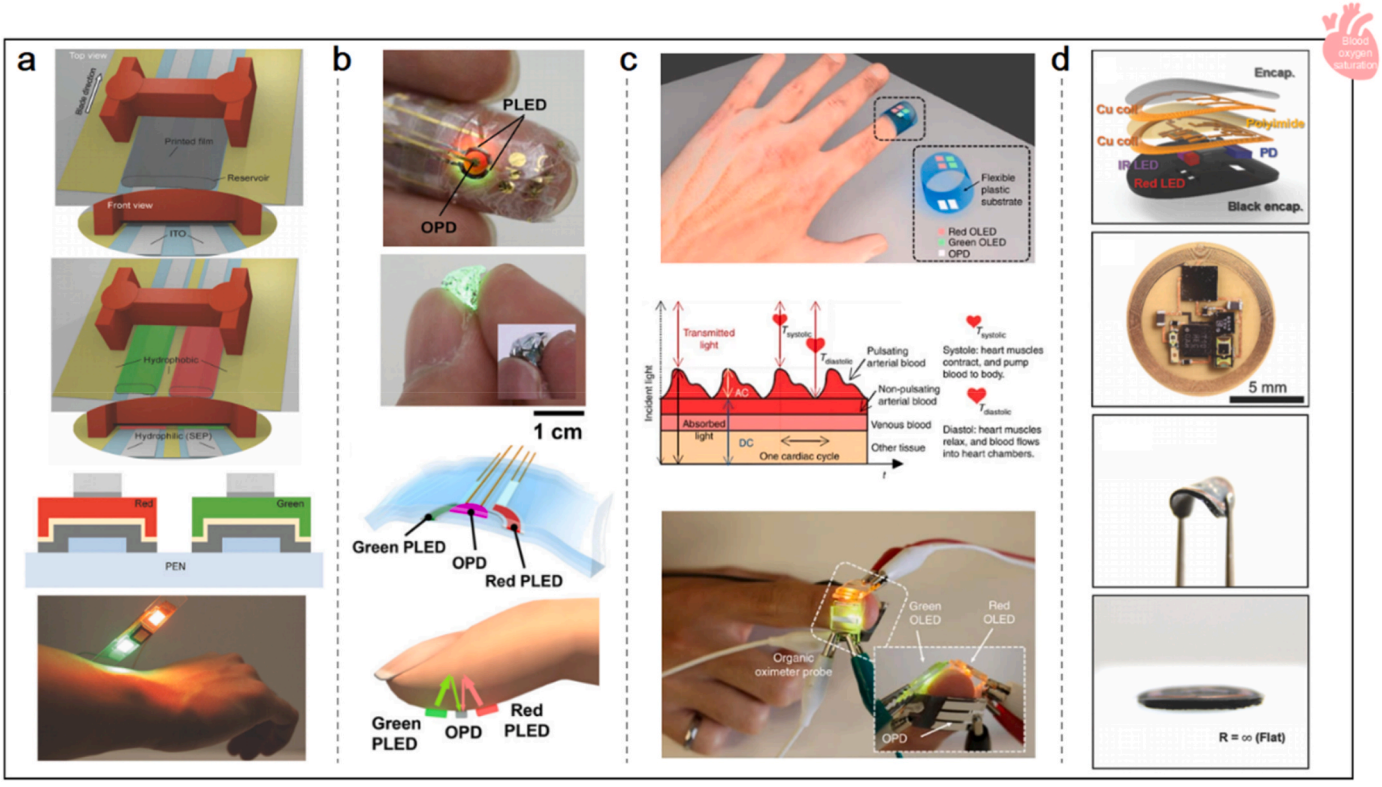

Fig. 11. Applications of flexible sensors related to blood oxygen saturation. a) Top and front views of the blade coating process using surface energy patterning (SEP) for single-color PLEDs (top 1) and multi-color PLEDs (top 2). The hydrophobic zone is indicated by the yellow area. The structure for multicolored PLED (bottom 2). Photograph of a photoelectric sensor using green and red PLEDs as light sources and a silicon PD as a photodetector (bottom 1) [273]. b) Ultra-flexible organic optical sensors (top 1). Crumpled, ultra-soft green PLED (top 2). Structure of the pulse oximeter (bottom 2). The schematic shows how reflex pulse oximetry works (bottom 1) [274]. c) A pulse oximetry sensor consisting of two OLED arrays and two OPDs (top). Light transmission paths of pulse oximetry through pulsatile arterial blood, non-pulsatile arterial blood, venous blood and other tissues over several cardiac cycles (middle). The red and green OLEDs are placed on the finger and the transmitted light is collected by an OPD pixel placed under the finger (bottom) [275]. d) The Schematic of the component layers of a millimeter pulse oximeter with NFC capability (top 1). The Unpackaged equipment (top 2). The curved device with a small radius of curvature (bottom 2). Demonstration of the conformal contact between the device and the plane (bottom 1) [276]. Reprinted from Refs. [273–276] with permission. (For interpretation of the references to colour in this figure legend, the reader is referred to the Web version of this article.)

et al. [273] proposed a unique method that allows for the printing of two different functional materials within a single step. By using this approach, they were able to fabricate a polymer light-emitting diode (PLED) that, when integrated with a photodiode (PD), was capable of measuring blood oxygen saturation through reflectance mode. Notably, the study also demonstrated the successful fabrication of PLEDs with three different colors (green, red, and near-infrared emitting properties), highlighting the versatility and potential of this innovative printing process (Fig. 11a) [273]. In addition to their potential for clinical medical applications, ultra-thin flexible electronics offer advantages such as low manufacturing cost and high throughput processing. One noteworthy example is the ultra-thin organic optical system proposed by Yokota et al. [274], which allows for measuring human blood oxygen and displaying the resulting data directly on a photoelectric skin (oe-skin) attached to the human epidermis. To achieve this, the system utilizes unique ultra-thin and flexible PLEDs and OPDs that maintain their performance despite their minimal thickness. The ultra-thin PLED includes a composite layer consisting of SiON and parylene alternately stacked as a passivation layer. This multilayer structure has a total thickness at the nanometer level, ensuring its ultra-thin properties. Remarkably, even in a crumpled state, the ultrathin PLED exhibits excellent mechanical flexibility due to its incredibly small bending radius (100 μm) (Fig. 11b) [274]. Lochner et al. [275] have proposed another pulse oximeter design that requires low fabrication cost. Their approach involves using two OLED arrays and two OPD placed on the opposite side. By combining these components with a flexible elastic substrate, the PPG sensor can be wrapped around a fingertip to capture PPG signals. The red and green OLEDs are paired together and integrated onto a flexible substrate, the resulting sensor boasts both a large sensing area and superior flexibility. Impressively, its accuracy in measuring blood oxygen saturation is nearly on par with that of a commercially available oximeter, making it a promising candidate for non-invasive healthcare monitoring (Fig. 11c) [275]. Kim et al. [276] have developed a remarkable photovoltaic sensor that is compact, lightweight, and versatile enough to collect blood oxygen, heart rate (HR), and HR variability information wirelessly across the body. The circular oximeter has a width of only 1 cm and a thickness of 5 mm, making it highly flexible and ideal for attachment to various sites almost unlimited, including nails and earlobes. Its small form factor and flexibility make it easy to apply, with the added benefit of reducing skin damage caused by mechanical friction. Moreover, unlike bulky sensors, this tiny device can be installed on solid keratinized skin, such as fingernails or toenails, almost without causing any harm to the user. This characteristic sets it apart from large sensors, making it a safer and more practical option for collecting vital signs data. For long-term nail surgery, the device minimizes the risk of irritation and motion artifacts, as discovered (Fig. 11d) [276].

4.1.3. Blood pressure

Blood pressure (BP), which refers to the lateral pressure acting on the blood vessel wall per unit area when blood flows inside the blood vessel, is a common parameter for human physiology monitoring. Hypertension is defined as systolic BP $\geq$ 140 mmHg and/or diastolic BP $\geq$ 90 mmHg in adults over the age of 18.[357] while hypotension is defined as BP below 90/60 mmHg [358]. BP is a key indicator that can be used to determine the cardiac function and peripheral vascular resistance, which plays a remarkable role in cardiovascular disease diagnosis [359].

BP measurement is typically based on the working principles of pulse transit time (PTT) and pulse arrival time (PAT). These BP-related parameters can be obtained from PPG, BCG, ECG, SCG and mechanical pulse wave signal sensing. The resulting signal detected can be used as an indicator to judge arterial diseases such as hypertension [10]. The development of oscillometric functions and algorithms for automated non-invasive BP monitoring devices requires low-cost pressure sensors with high sensitivity in clinical trials [360]. Bijender et al. [277] developed a flexible pressure sensor with hypersensitivity using a porous PDMS elastomer layer. The proposed sensor based on a capacitive switching mechanism exhibits properties of fast response, low detection limit, and a large working pressure range, which is quite suitable for application in wearable BP devices [277]. Although the existing BP monitoring devices are broadly adopted in current clinical fields, their performance is still insufficient for future developments in daily BP monitoring. A piezoelectric composite ultrasonic sensor with flexibility fabricated from silver nanowire-based and stretchable electrodes and Lead Zirconate Titanate (PZT-5A)/PDMS anisotropic 1–3 composite enables continuous monitoring of BP. According to experimental verification, as stated, the sensor has the characteristics of sufficient bandwidth and sensitivity [278]. The exploration of a comfortable, low fabricating cost and accurate wearable sensing system could help to address the current limitations of blood pressure monitoring. Luo et al. [361,362] proposed a wearable tactile sensor array attached to the temporal and ankle regions using paper substrates, and spray-deposited metal electrodes. It monitors the BP pulse waveform for HR and HR variability information [279]. Biocompatibility, high sensitivity, flexibility and stretchability are preferred for pressure sensors used for precise pulse measurement [361,362]. Porous graphene-based flexible pressure sensor for detecting HR, respiration rate, pulse wave velocity, and BP was fabricated by Peng et al. [280] through an in situ fabrication method using ink printing technology, which exhibited desirable electromechanical properties with high sensitivity, high resolution and a wide range of detection [280].

Elucidating the piezoelectric response to arterial pulses is critical for the improvement of wearable devices capable of accurate and continuous BP monitoring. Researchers investigated the correlation of BP waves and piezoelectric arterial pulse waves from the nano-to the macro-scale thickness of the piezoelectric functional layer [281]. It has reported a developed wireless wearable continuous BP monitoring system that is more portable than other traditional systems. The novel system rests on pulse wave velocity between multiple sensors by studying the correlation between piezoelectric pulse waves and BP waves. Furthermore, another wearable BP monitoring system based on a wireless data acquisition module and two piezoelectric sensors developed by Yi et al. [281] can acquire arterial pulse waves and achieve the effect of accurate and continuous recording. Blood pressure is assessed by pulse wave velocity, which can be calculated from the time difference between two arterial pulse waves. Pulsating blood flow will cause changes in blood vessels. Two sensors placed on the elbow and finger can measure the arterial pulse respectively. Since the blood flow flows from the proximal end to the distal end, there is a time difference between the two pulses. (Fig. 12a) [281].

Epidermal electronics are commonly required to achieve high-sensitivity detection of low-amplitude signals, noise reduction of motion artifacts [363,364], low manufacturing costs, and long-term comfortable wearability. Existing epidermal pressure sensing devices are often not fully equipped due to the complex multi-layered structures involved. Zhu et al. [282] successfully introduced an epidermal-ion subinterface (EII) with high sensitivity, anti-noise properties, and high adaptability capable of incorporating human skin as part of the sensor. The interface works by exploiting a novel sensing mechanism of interfacial ionic capacitance. The EII, which consists of a supporting flexible substrate, an ionic electrode layer, and an adhesive layer, has a simple structure. When subjected to an external mechanical load, the ionic electrode deforms to form an electronic-ionic contact with the skin, thereby inducing the generation of ionic capacitance. The skin-electronic contact area increases with the increase of the external load, and this change is reflected in the change of the capacitance value, which can be detected. It can obtain signals such as BP waveforms and has the characteristics of long-term stability and repeatability (Fig. 12b) [282]. Flexible electronics have become increasingly popular due to their unique properties and applications. One of the key features for optimizing flexible electronics is achieving primary energy autonomy and seamless integration. A recent study by Petritz et al. [283]

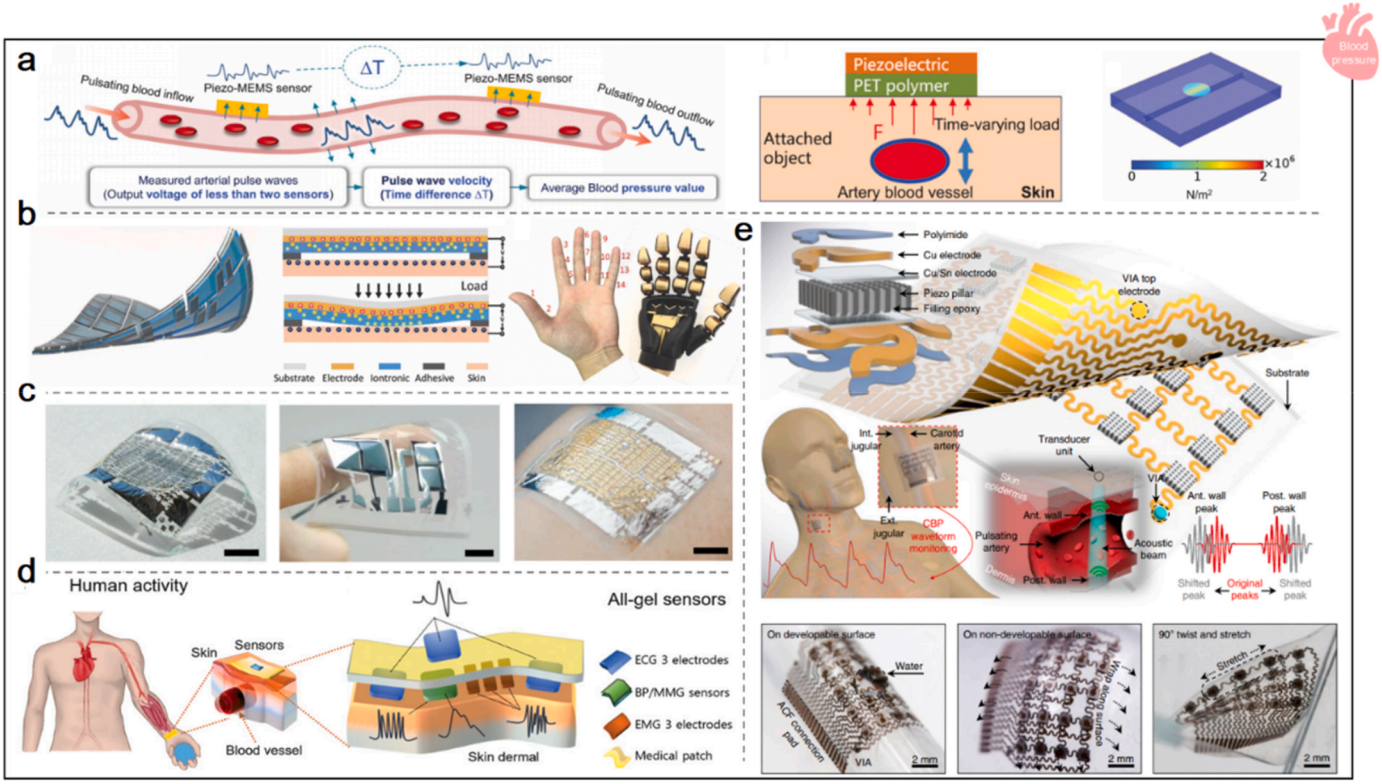

Fig. 12. The applications of flexible sensors in BP. a) Diagram of the pressure transmission mechanism (left). Diagram of the additional piezoelectric sensor (middle). Simulated stress distribution of a piezoelectric sensor due to pulsed pressure (right) [281]. b) Perspective view of the EII device (left). Cross-sectional view of an EII device including a support substrate, an ion electrode layer and an adhesive layer (middle). Photograph of a 14-unit sensing array mounted on a human and robotic hand (right) [282]. c) Ultra-flexible harvesting circuits (left). Ultraflexible ferroelectric polymer transducer for critical parameter sensing and as a piezoelectric nanogenerator (middle). Attached ultraflexible devices (right). Scale bar: 1 cm [283]. d) Artificial gel sensor modules attached to the skin capable of detecting biophysical signals related to heart of human activity [284]. e) Diagram of a stretchable ultrasonic device with key components marked (top). The device could be mounted on the human neck and monitored for CBP (middle left). Use of highly directional ultrasound beams and positioning dynamics (middle).The corresponding shifting echo radiofrequency signals are reflected from the front and rear walls (middle right). Photo of a water drop on a silicone-encapsulated hydrophobic device (bottom left). Photo of a device wrapped along the surface (bottom middle). Photo of a stretched and twisted device (bottom right) [125]. Reprinted from Refs. [125, 281,282–284] with permission.

demonstrated this by fabricating ultra-flexible ferroelectric polymer sensors and organic diodes on ultra-thin parylene plates, each only 1 μm thick. These devices were able to measure BP and pulse signals using ferroelectric polymer transducers, while also maintaining energy autonomy through the piezoelectric effect. This means that the device could collect electrical energy from mechanical pressures such as limb movements, arterial pulsation, and respiratory floating. The generated AC signal is then converted into a DC signal through a rectification circuit and stored in an energy storage device. Additionally, the use of carrier materials with excellent deformation enhances the sensitivity of the device. Overall, the integration of these key features allows for the development of highly efficient and autonomous flexible electronic devices. The advantages make the device a wireless, imperceptible electronic patch that can precisely monitor of pulse and BP (Fig. 12c) [283]. There is currently no wearable multimodal sensor capable of simultaneously measuring multiple biophysical signals using SA and RA responses at the same location as Chun et al. indicated. To solve this puzzle, Chun et al. [284] have created a wearable compact gel sensor using PVDF-TrFe gels and PANi-PVC composite gels to recognize the signals from SA and RA receptors, and the flexible, portable, compact and adherent all-gel integrated multimodal sensor combining four component sensors enables the monitoring of EMG, BP, MMG and ECG signals successfully (Fig. 12d) [284]. Wearable devices with inherent mechanical properties that record signals on superficial tissues or under the epidermis are commonly restricted by their placed locations. The ultrasound device proposed by Chonghe et al. [125] allows continuous monitoring of central blood pressure (CBP) in the deep vascular system with a wearable form while ensuring a close fit to the skin surface. The vertical interconnect access (VIA) serves as a crucial link between the upper and lower electrodes, facilitating co-planar anisotropic conductive film (ACF) bonding for bolstering the sturdiness of the device. The installation site can be the neck of the human body. The device, based on the pulse-echo method, uses a highly directional ultrasound beam to measure the pulsating vessel diameters of the carotid artery, internal jugular vein, and external jugular vein in order to obtain CBP. The ultrasound of this ultra-thin, stretchable device penetrates the body tissue to a depth of 4 cm, allowing for non-invasive, accurate monitoring of BP waveforms in deeply embedded arteries and veins (Fig. 12e) [125].

4.1.4. *Blood glucose*

Blood glucose refers to the glucose concentration inside the blood, of which the fasting value normally falls between 3.92–6.16 mmol/L [365]. As a crucial energy source, glucose is an indispensable component of the human body for various tissues and organs' daily operations [366]. When the blood glucose is pathologically increased, it is commonly clinically indicated organisms are in chronic pancreatitis [367], diabetes [368], hyperthyroidism [369], myocardial infarction [370], intracranial hemorrhage [371], etc. When blood glucose pathologically decreases, it typically reveals disorders in islet cell tumor [372], hypopituitarism [373], hypoadrenalism [374], etc. Since minor changes in blood glucose can affect the main organs, blood glucose monitoring is of great clinical significance. At present, non-invasive

techniques for measuring glucose concentration include reverse iontophoresis, Raman spectroscopy, photoacoustic spectroscopy, fluorescence, polarimetry, metabolic heat conformation, thermal emission spectroscopy, absorption spectroscopy, ultrasound etc. [285].

Blood glucose detection through electrochemical measurement aims to analyze concentrations in saliva, tears, sweat, and interstitial fluid (ISF), which can be collected to measure current or voltage. The resulting signal detected can be used as an indicator to judge diabetes [10]. Unfortunately, traditional invasive methods of measuring blood glucose will normally lead to infections in diabetes patients. Hassan et al. [285] fabricated a non-invasive glucose concentration detection sensor with low fabricating cost, which uses the glucose concentration in urine as a reference, and is able to distinguish between different levels of glucose concentration in deionized water [285]. Furthermore, a flexible sensor for non-invasive epidermal glucose monitoring through microwave means has been reported. Ordered nanostrips were fabricated with a nanoscale printing method, and glucose oxidase was doped into the nanostrips to fabricate a nanostrip-based flexible microwave enzyme biosensor. The sensor can achieve glucose detection with a low detection limit, high sensitivity, fast response, high affinity and low power detection. The function of this sensor for real-time monitoring of glucose in sweat was also validated in the study [119]. There is also a report of a two-electrode blood glucose sensor with non-invasive detection by integrating the ISF extraction module with the glucose detection module. The system consists of sensors fabricated from graphene/carbon nanotubes/glucose oxidase composite textile (graphene/carbon nanotubes/glucose oxidase composite textile) that exhibit high sensitivity to glucose in PBS and graphene/carbon nanotube/silver/silver chloride composite textile. Once the ISF is extracted by the RI process, the two electrodes are able to achieve the detection of the glucose concentration in the ISF using the amperometric method [286]. For continuous glucose monitoring with a high active surface area, Lin et al. [287] proposed a non-enzymatic glucose sensor with flexibility and high sensitivity to blood glucose monitoring. The sensor was fabricated using DVD-laser scribed graphene (LSG) as a flexible conductive substrate and copper nanoparticles (Cu-NPs) as a catalyst. For the oxidation of glucose, the sensor exhibits excellent catalytic activity, with high selectivity in the presence of other interfering substances [287].

Compared to independent equipment for monitoring various signals, electronic products that combine important metabolic parameters of the human body and physiological signals monitoring such as blood pressure are more convenient for users. This is because these integrated devices can provide a comprehensive snapshot of an individual's health status at once, making it easier to track changes over time and detect potential health issues early. In a recent study, Sempionatto et al. [288] proposed a new device that can simultaneously measure multiple signals such as blood pressure (BP) and heart rate (HR), and can also detect important biomolecules such as glucose, lactate, alcohol, and caffeine. To monitor BP, the device uses eight piezoelectric transducer arrays. An electric pulse activates the transducer, which then emits an ultrasonic wave that reaches the artery and receives an echo, allowing the device to measure relevant information from the blood vessel. For glucose monitoring, the device uses iontophoresis (IP) to extract glucose from human interstitial fluid (ISF), which is then detected using chemical sensing. The same method of IP is also used for extracting lactic acid, alcohol, and caffeine. After the current is applied, pilocarpine nitrate is

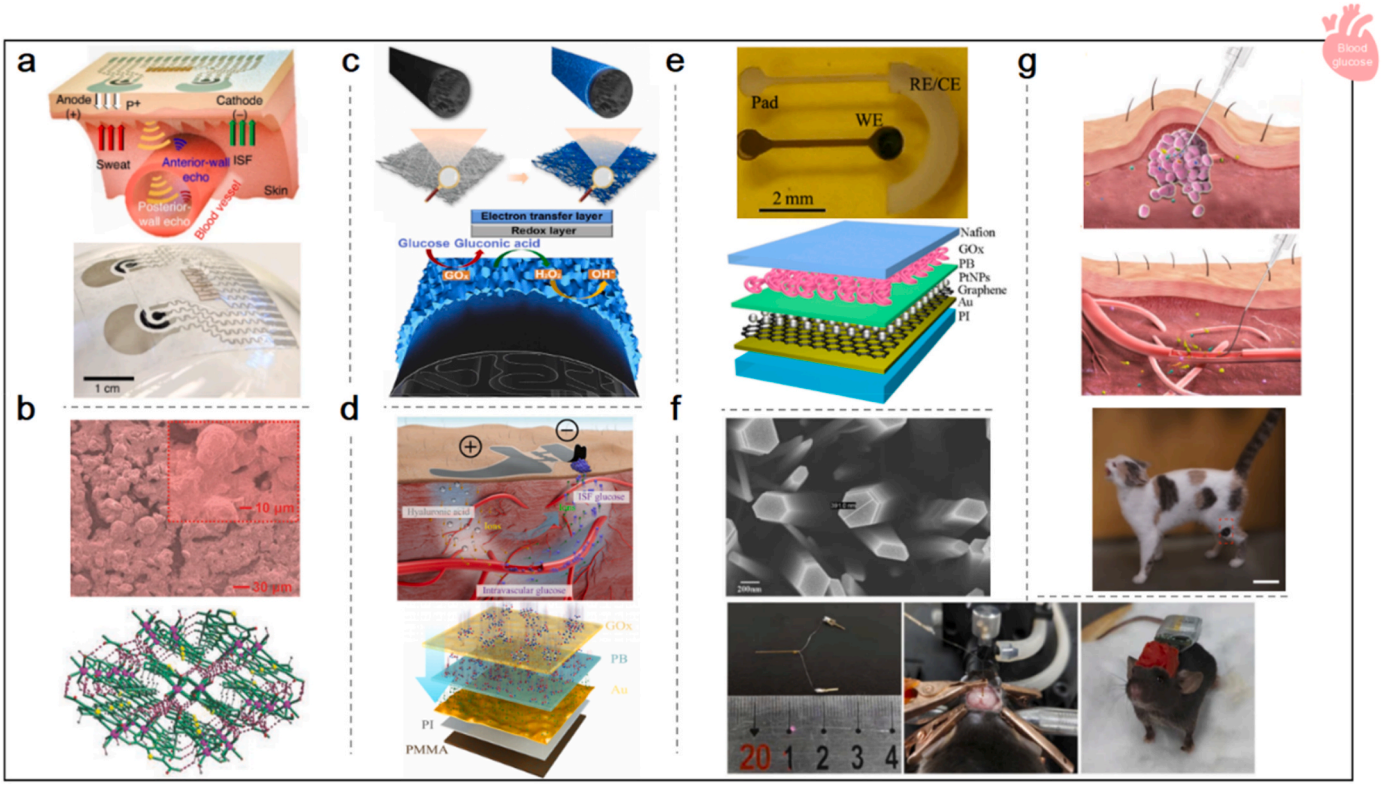

Fig. 13. The applications of flexible sensors in blood glucose. a) Acoustic sensing and IP mechanisms for integrated sensors (top). Photo of the sensor under bending (bottom) [288]. b) SEM micrograph of a Co-MOF modified electrode (top). Co-MOF 3D frameworks formed by hydrogen bonding (bottom) [289]. c) Electrode preparation including electrodeposition of PB on GFF (top). Glucose detection principle (bottom) [290]. d) Schematic diagram of the ETC performing HA osmosis, glucose refiltration and glucose transport outwards (top). Schematic of an ultra-thin skin-like biosensor with multiple layers (bottom) [291]. e) A prototype flexible electrochemical glucose sensor containing working electrode (WE) and counter electrode (CE) also used as reference electrode (RE) (top). The Cross-sectional structure of the WE of the glucose sensor (bottom) [292]. f) Cross-sectional view of a single nanowire (top). Electrode implantation and electrical stimulation experiments (bottom) [293]. g) Injection of fibers into the target tumor (top) and blood vessels (middle). Photograph of a cat wearing a "smart wristband". Scale bar: 6 cm [294]. Reprinted from Refs. [288–290,291,292,293,294] with permission.

transported and transdermally absorbed. It then combines with M choline receptors to stimulate the sweat glands, causing them to release sweat. Chemical sensors are used to analyze the biomolecules contained in the sweat. This approach leverages drug receptors to enable non-invasive extraction of sweat and avoids skin irritation. To avoid mutual interference between ultrasonic sensing and chemical sensing, the device uses a solid-state ultrasonic approach and a sensing hydrogel layer. This integration of rigid ultrasonic sensors and flexible electrochemical sensors enables multifunctional simultaneous monitoring of physiological signals and metabolism. (Fig. 13a) [288]. Flexible electronic devices using novel materials can achieve detecting a variety of biochemical substances. Ling et al. [289] proposed a surface modification design of single or multi-channel implantable flexible sensors using conductive metal-organic frameworks (MOFs) such as copper-MOF and cobalt-MOF. This integration allows highly specific and sensitive electrochemical detection of glucose, L-tryptophan (l-Trp), glycine and ascorbic acid (AA) (Fig. 13b) [289]. Besides, Cai et al. [290] presented a technique for the detection of glucose in ISF with the non-invasive method by RI technology using a textile electrode consisting of a Prussian blue (PB) nanoparticle transducer layer deposited on graphene fiber fabric (GFF). Due to the strong interconnection of the GFFs cross-linked by the wet fusion method, the device has excellent mechanical properties. The graphene fiber fabric-prussian blue -glucose oxidase-chitosan can be used as a dry sensing patch for non-invasive glucose monitoring on the human skin surface (Fig. 13c) [290]. Reverse iontophoresis, the most common method for sampling ISF [375], is prone to cause patient skin irritation due to its prolonged warm-up and high current density [376,377]. Chen et al. [291] proposed a skin-like biosensor system with promising applications for medical-grade CGM and insulin therapy. By integrating an ultra-thin skin-like biosensor with a dual electrochemical channel (ETC) that can drain blood glucose from the subcutaneous vessels to the body's surface, the system is able to monitor intravascular blood glucose and glucose in the interstitial fluid (ISF) without causing trauma. When the paper battery is attached to the skin, it initiates a subcutaneous electrochemical dual-channel (ETC). This innovative technology employs glucose reverse iontophoresis to transport blood glucose to the surface of the skin. ETC enhances the penetration of hyaluronic acid (HA) into the ISF, thereby increasing the osmotic pressure within the ISF. Consequently, an imbalance occurs between the filtration and reabsorption of glucose in the ISF, leading to more intravascular blood glucose being expelled from the blood vessels and move to the surface of the skin. This system opens up the possibility of non-invasive continuous monitoring of blood glucose in the clinical setting (Fig. 13d) [291]. Wearable blood glucose monitoring usually requires continuous perspiration [149,378], and individual differences are prone to affect the amount of ISF extraction. Pu et al. [292] proposed a flexible bio-microfluidic technology based on the epidermis that can overcome the shortcomings of current wearable device measurements and enable continuous blood glucose monitoring. Moreover, this work proposed a thermal activation method that involves locally heating the skin to 37 °C and maintaining that temperature continuously aiming to enhance ISF extraction efficiency and reduce skin irritation by lowering the extraction current density and extraction time, a Na^+ sensor and a correction model to eliminate individual differences, and a structure for eliminating differential forms for passive sweating. Epidermal bio-microfluidic devices were prepared by fabricating nanomaterial modification, flexible electrodes and enzyme immobilization through an inkjet printing method, which can facilitate batches of practical production with ultra-low-cost fabrication protocol. By leveraging the in-situ measurement capability of a skin-mounted electrochemical glucose sensor, significant improvements have been made in the precision of glucose detection. (Fig. 13e) [292]. Traditional treatments and testing methods to maintain blood glucose balance, such as insulin injections and blood analysis, commonly fail to achieve timely and ideal adjustment and real-time monitoring. A new closed-loop brain-computer interface system, which is capable of real-time detection and rapid regulation of blood glucose concentration in a very different way from conventional blood glucose regulation, has been reported recently. It adopts a self-powered method that supplies energy to the system through the movement of the applied individual. The system consists of a glucose sensor constructed from an enzyme/ZnO nanowire array capable of outputting glucose signals through a biosensing-piezoelectric coupling effect, an energy harvester using piezoelectric ceramics to transform the mechanical energy of the application object into electrical energy, a microcontroller and a brain stimulator. The micro-control unit is responsible for the delivery of brain stimulation pulses to the dorsomedial part of the ventral medial hypothalamus in the central system. This strategy of forming a closed loop between the body, the brain and the system allows for the expansion development of brain-computer interfaces in precision medicine (Fig. 13f) [293]. Implantable electronic devices may cause tissue damage over time if they are not compatible with the body's dynamic physiological environment [379]. Thus an implantable electrochemical sensor has been developed trying to provide a potential solution. This sensor twisted CNT into layers and spiral fiber bundles to simulate the layered and spiral assembly of soft tissues, among which the implantable fibers were with great biocompatibility. Different sensing elements were combined to create single-ply sensing fibers (SSFs) capable of detecting specific chemicals, and the SSFs were twisted to create multi-ply sensing fibers (MSFs) to enable signal monitoring of various biological substances. The device is capable of monitoring H_2O_2 inside implanted mouse tumors in a spatially resolved and real-time way and, in addition, integrated with a wireless transmission system on an adhesive skin patch to enable monitoring of calcium and glucose in cat venous snow for up to 28 days (Fig. 13g) [294].

4.1.5. Other applications

As evidenced by the following researchers, flexible sensors have exhibited promising prospects in providing cardiovascular toxicology and drug testing in vitro as clinical diagnosis-assisted tools [257]. A reported multi-well cardiac muscular thin film (MTF) platform containing flexible integrated strain gauges can be used to obtain continuous data on systolic stress and the beat rate of independent cardiac tissues. The design of the open-well platform makes it possible to combine cardiac MTF with endothelial barrier inserts and to study temporal drug transport across the barriers [257]. Another example demonstrated drug testing potential, a flexible sensor developed using the principle of affinity interaction between antibodies and antigens is successfully designed to simultaneously screen cardiac-Troponin-T and cardiac Troponin-I [295].

For patients going through complex reconstructive surgery, monitoring of blood flow circumstances need to be paid great attention and can directly reflect the clinical recovery. Boutry et al. [296] proposed a pressure transducer capable of wireless monitoring arterial blood flow through inductive coupling, which adopted biodegradable materials for the fabricartion. Due to the fact that it does not require disassembly, it reduces the vascular bed surgical risk associated with mounting and dismounting. More importantly, in clinical practice, it is often necessary to use a microscope to connect fractured blood vessels or reconstruct blocked blood vessels. Due to the risks after the surgery, there is a possibility of hematoma or thrombus formation, which can lead to the failure of vascular patency and require timely rescue. At this point, real-time monitoring becomes particularly important. This sensor is capable of real-time monitoring of blood flow, allowing prompt detection of any abnormalities in blood flow. This maximizes the opportunity to save time for intervention. The researchers demonstrated the artificial artery model in vitro, by delivering air inside the artificial blood vessel, causing the blood vessel to expand to simulate the pulsation of the artery. And it was implanted around the rat femoral artery, which is very similar to the arterial pulsation behavior of human children's face, and the LCR meter was used to measure the capacitance change and record the pulse rate. The pulse rate measured one week after implantation was

very close to that of Doppler ultrasound, except that the quality factor of the signal decreased, which may be due to the influence of the humid environment around the femoral artery (Fig. 14a) [296]. As a promising alternative [380], most microphysiological systems still lack properly integrated sensors, and the achievement of the system fabrication typically demands multi-step lithography processes. Lind et al. [297] present a novel microphysiological device instrumented to continuously acquire systolic stress data from multiple laminar cardiac microtissues using multi-material full 3D printing with six functional inks. Each device includes multiple layers of cantilevers, which consist of an embedded strain sensor, tissue-guiding layers, and a base layer. When the anisotropic engineered cardiac tissue is attached to it, the contractions generated will cause deflection in the cantilever base, further stretching the embedded strain sensors, resulting in a change in resistance. Additionally, the device includes two other fundamental components: electrical interconnects for signal readout and eight independent wells. The entire device is manufactured using a fully printable method, with the cover made of PDMS, PLA, or ABS materials to insulate the wires and holes for cell and media loading. The selected and designed functional inks materials exhibit great properties in piezoresistive, biocompatible, flexible and high electrical conductivity, thus the fabricated strain gauge sensors can be integrated into the microarchitecture to aid the self-assembly of physically simulated laminar cardiac tissues (Fig. 14b) [297]. Arterial occlusion has a significant impact on arterial pressure, certain high-risk surgeries may lead to postoperative arterial occlusion. Long-term monitoring of arterial status after surgery is crucial for early disease detection and recurrence prevention. Ruth et al. [298] presented a fringe-field sensor that is used for detecting arterial obstruction to assess PVD, heart attack and stroke. The design of interdigitated electrodes and pyramidal elastic microstructures of the fringe-field sensor is thin and flexible enough to be placed over a wide range of various arterial locations, together with the capability of long monitoring duration time (Fig. 14c) [298]. Currently, devices for monitoring cell culture with impedance sensors still lack wireless [381], versatility [324], and multi-layer array mapping capabilities for large-scale cell culture [382]. Additionally, comprehensive portable equipment for monitoring critical culture conditions such as temperature and pH, radio and thermal stimuli have not yet been developed, while the culture conditions are crucial for cell proliferation and differentiation. According to a recent report, a cell culture platform (LISCCP) with integrated ultra-thin sensor and stimulator arrays has been proposed, it is large and smart enough to facilitate wall-dependent cell culture and implement real-time multi-modal 3D monitoring and local control. It is worth noting that designing the engineering substrate as a five-layer integrated structure with perforations and prominent hemispherical features that increase the surface area is more advantageous for the adhesion of C2C12 cells (Fig. 14d) [299]. Current characterization methods for mechanical assessment of soft

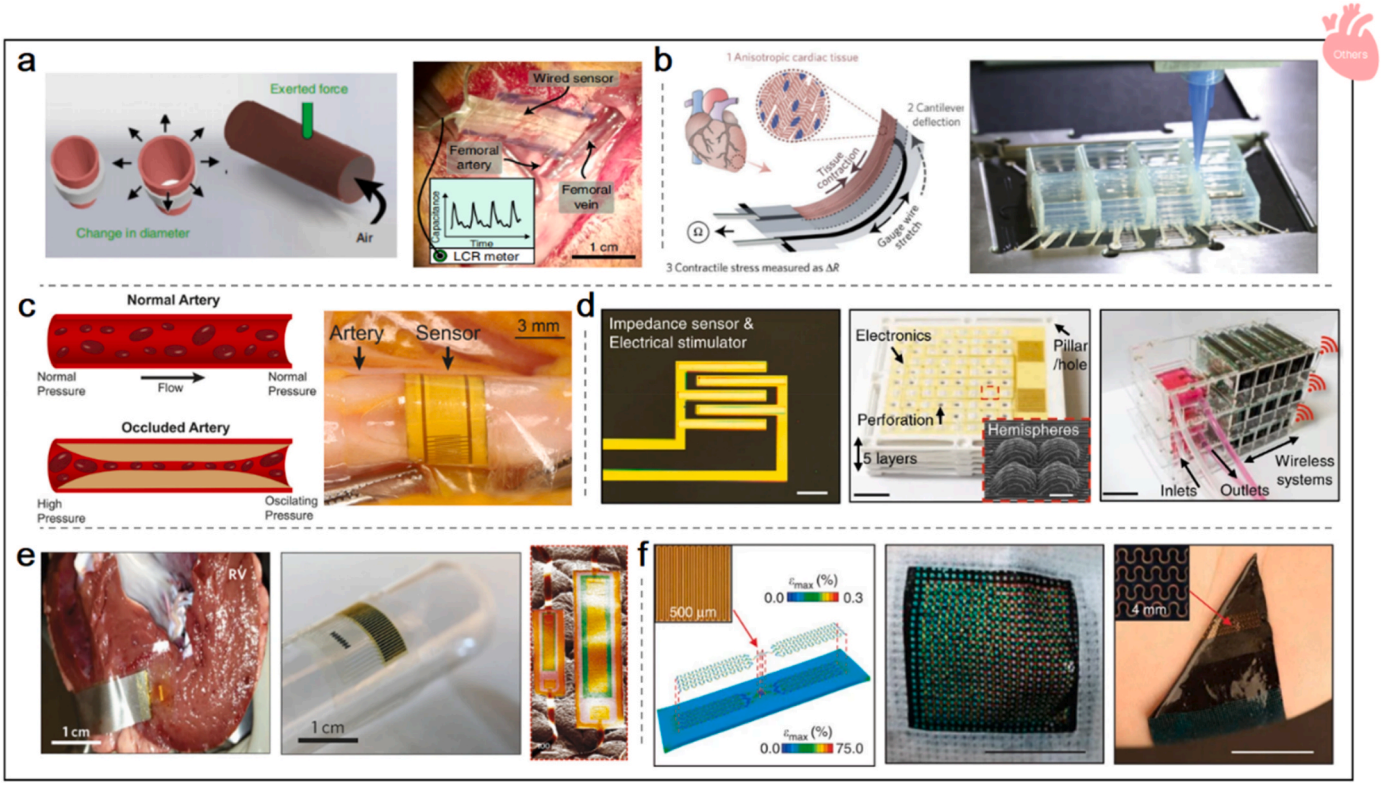

Fig. 14. The other applications of flexible sensors in the heart. a) Characterization of arterial models (left). Image of a wired sensor wrapped around the femoral artery and secured with sutures (right) [296]. b) The schematic illustration of the device principle. The contraction of anisotropic engineered heart tissue deflects the base of the cantilever so as to stretch the soft strain gauges embedded in the cantilever, thereby producing a change in resistance proportional to the contraction stress of the tissue (left). PDMS, PLA or ABS prints a cover for isolating the exposed wires and holes to contain the cells and media (right) [297]. c) Occluded arteries can lead to significant changes in arterial pressure (left). The close-up view image of the implantation site (right) [298]. d) The impedance sensor/electrical stimulator (left). Five-layer stack of 3D printed engineered PLA substrates, scale bar: 1 cm. SEM images of the prominent hemispheres are shown in the inset, scale bar: 500 μm (middle). Photograph of the 3D stack assembly of three LISCCPs. Scale bar: 5 cm (right) [299]. e) The photograph of the device placed in the right ventricle (left). The photo of the device on a cylindrical glass stand (middle). SEM image of the device on an artificial skin sample. The sensor is on the left and the actuator is on the right (right) [300]. f) Schematic illustration of the results of finite element modeling of the device with wireless heaters under tensile strain, the inset shows an enlarged view of the Joule heating element (left). The device runs calibrated colors on skin surfaces. Scale bar: 2 cm (middle). A device containing an RF antenna and a Joule heating element located on its back, inset showing a magnified view of the structure with the serpentine antenna. Scale bar: 2 cm (right) [301]. Reprinted from Refs. [296,297,298,299–301] with permission. (For interpretation of the references to colour in this figure legend, the reader is referred to the Web version of this article.)

organs and tissues in biology, which are invasive, commonly lack microscale spatial resolution, and the applied regions are confined to specific locations under quasi-static conditions. Dagdeviren et al. [300] have proposed piezoelectric conformal devices capable of measuring the viscoelasticity of soft tissues in vivo on the proximal surface area of the epidermis, which is important for the rapid and clinical non-invasive characterization of the mechanical properties of the skin. This particular kind of conformal modulus sensor relies on arrays of mechanical actuators and sensors composed of PZT nanoribbons. The device has a wide range of applications, including the heart. Researchers used cow's heart as experimental subject and directly attached a shape-preserving structure that could couple with the tissue surface through van der Waals forces to the surface of the cow's heart, including the left ventricle, right ventricle, and apex. The experimental results were as expected, with the highest modulus measured at the apex. (Fig. 14e) [300]. Besides, the characterization of temperature and heat transport properties of skin is of great significance in providing fundamental information. By combining a chromatic temperature indicator with a wireless stretchable electronic device and adopting a thermochromic liquid crystal on a thin elastic substrate, Gao et al. [301] have achieved a novel sensor design applied for the assessment of blood flow responsiveness to congestion related to reflecting cardiovascular health, among others. The device integrates radio frequency (RF) components and antennas to capture incident RF energy and provide power to the Joule heating element. By controlling the RF signal, localized heating can be achieved and a temperature map generated (Fig. 14f) [301].

4.2. Cerebral applications

4.2.1. Temperature

Brain temperature, one of the compulsory parameters in brain monitoring under pathological conditions, expresses great value in reflecting the neurometabolic heat production [383], cerebral blood flow (CBF) [384] and incoming arterial blood temperature.[385] Noted that the temperature distribution inside the brain of humans is not uniform, for example, the temperature of the epidural space is slightly lower than the temperature around the center of the brain [386]. In a normal and stable physiological body environment, the range of continuous fluctuations in temperature in the brain is typically 3–4 °C [387]. Due to the thermoregulatory center located in brain tissue, brain temperature tends to be used as an important indicator for diseases like fever [388]. The value of brain temperature exceeding the physiological upper limit may lead to brain hyperthermia, which will affect neurological function and may cause severe damage to brain cells [387]. The rise in brain temperature appears due to a cellular healing response, which is occurred when an injured brain develops an inflammatory response to infection [49]. Therefore, accurate measurement of brain temperature is of great significance during the treatment of injured brains [116]. Owing to the difficulty of direct monitoring, brain temperature is commonly measured through NMR spectroscopy, microwave radiometry, near-infrared spectroscopy, and ultrasonic thermometry. Whereas these monitoring methods are not suitable for real-time monitoring during patients' daily activities [388]. At present, implantable temperature probes and sensors are designed using various principles, such as optical fibers, thermal resistors, thermocouples, thermistors, and other methods [116,389]. Among these RTDs are considered one of the most accurate sensors for temperature measuring. With the advent of microfabrication, thin-film metals can be deposited easily into RTD temperature sensors. Thus thin-film RTD temperature sensor has the characteristics of small size and short response time, which can measure temperature more accurately than traditional thermocouples [110].

Moreover, Wu et al. [116] proposed a temperature sensor with a polysilicon thermistor and showed that the polysilicon thermistor has superior performance compared to RTD. As aforementioned, there were few temperature arrays used to directly measure spatial temperature changes inside the brain owing to technical difficulties. While the flexible sensor reported based on flexible PI, which has the characteristics of high precision, can monitor brain temperature with a high spatial resolution. The proposed ultra-small-sized polycrystalline silicon thermistor has a larger resistance compared to the temperature sensor developed by researchers before, with a reduced level of noise, thereby achieving higher accuracy (Fig. 15a) [116]. Optical sensors are notable for their compatibility with magnetic resonance imaging (MRI), however, traditional implanted optic sensors are usually fabricated with non-absorbable materials, which may cause secondary trauma owing to the necessary surgery for removing the device later. Currently, there are two reported bioresorbable optical sensors implanted with Fabry-Perot interferometers and two-dimensional photonic crystal structures, which achieve accurate and continuous monitoring of intracranial pressure (ICP) and temperature, meanwhile avoiding the risks of surgical removal thanks to their excellent bioabsorbability (Fig. 15b) [302]. Implantable sensor probes are considered standard devices for monitoring various cranial physiological indicators, however, only a few monitoring methods of multimodal cortical physiological indicators through minimally invasive sensors have been reported. Liu et al. [303] developed a flexible polyimide-based multimodal sensor that builds a technical framework for implantable intracranial sensors. It was capable of measuring intracranial temperature, brain tissue oxygen content, cerebral cortical discharge, ICP, sodium and potassium in cerebrospinal fluid (CSF) (Fig. 15c) [303]. Besides, it is worth mentioning that Lee et al. [304] prepared a bioresorbable electronic patch (BEP) by integrating a polymeric drug reservoir with a wireless flexible electronic device made from biodegradable materials. The BEP not only expresses temperature sensing capacity but also facilitates drug delivery to brain tumors through thermal actuation. The oxidized starch (OST) used in the device for dispersing and storing Doxorubicin (DOX) provides strong imine conjugation to both brain tissue and DOX, allowing the patch to have strong adhesion. The wireless heater operates with gentle heat drive, enabling the drug to reach deeper tissues. Both of these features enhance the utilization of the medication. (Fig. 15d) [304].

4.2.2. Intracranial pressure

As a result of the pressure exerted by the intracranial components [390], intracranial pressure (ICP) is vital for the monitoring of traumatic brain injury patients [49]. In a normal scenario, sustained ICP over 20 mmHg is considered pathological, while normal ICP is supposed to fall between 5 and 15 mmHg [391]. According to the Monro-Kellie hypothesis, the volume of brain tissue, CSF and blood in the skull remains constant, any increases in one component will lead to a decrease in other components or an increase in pressure [392]. As a diagnosis-assisted indicator for various diseases such as infection, stroke, tumor, hydrocephalus and epilepsy, etc. [393], ICP can be obtained to avoid secondary brain injury (SBI) such as hematoma, edema, which is the main cause of traumatic brain injury (TBI) [394]. As a consequence, accurate, timely and continuous monitoring of ICP is of great significance for clinical treatment. According to the working principles, currently, there are three main sensing types for ICP monitoring: implantable transducers [395], fluid-based systems [396] and Doppler sonography [397]. Furthermore, fiber-optic pressure sensors (FOPS) are now becoming commonly selected ICP sensors due to their compatibility with MRI for routine clinical applications [49]. These non-implanted methods that perform an indirect measurement exhibit the advantages of non-invasiveness and no risk of infection, while they are inappropriate for long-term accurate clinical monitoring [398]. In contrast, implanted methods have the superiority of accurate ICP measuring, however, the patient's mobility will be limited due to the catheter connecting the sensor to the detection device [390]. Therefore, the wireless method which enables catheter removal provides a potential solution, and either active or passive wireless manners are widely adopted. The passive method has advantages over the active method that involves complex transmitter circuits and power supplies owing to its simple structures,

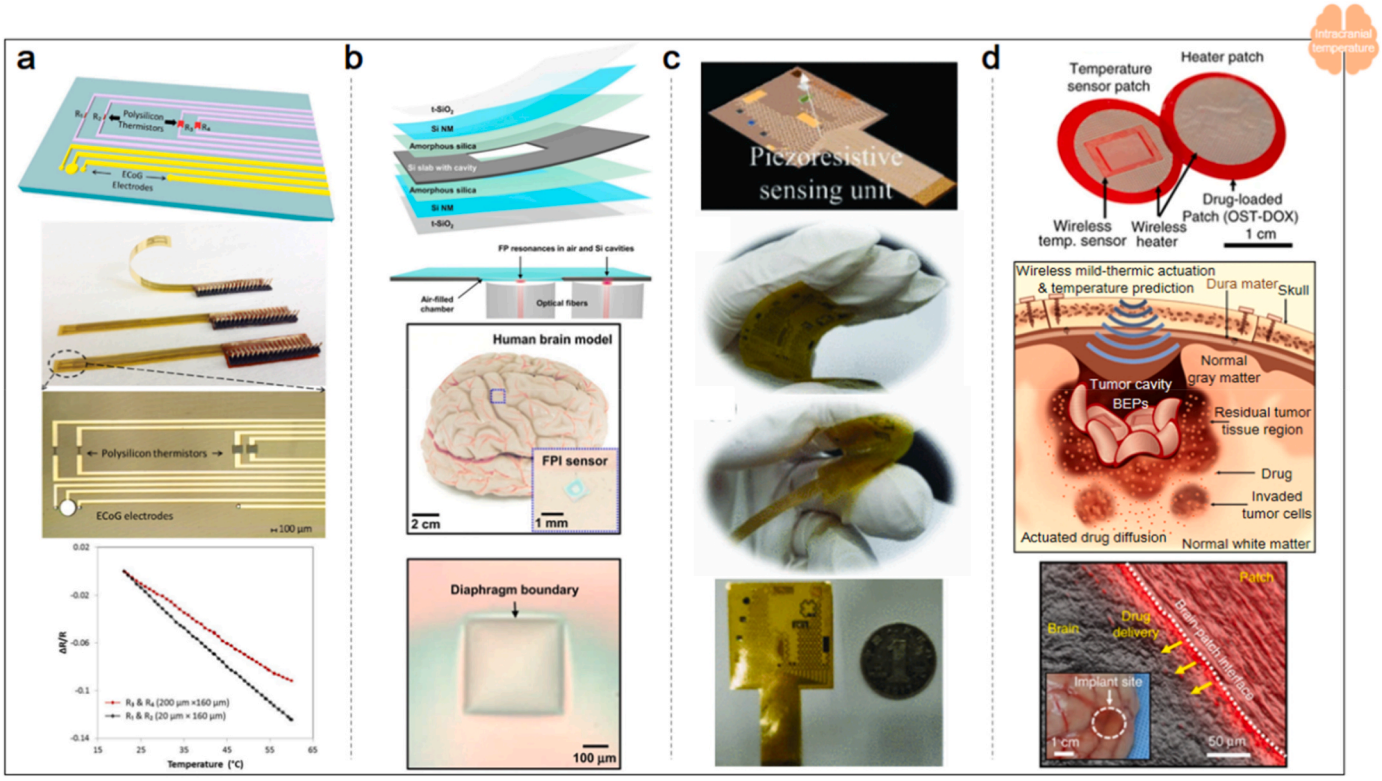

Fig. 15. The applications of flexible sensors in intracranial temperature. a) The polysilicon thermistor array with 4 sensing elements (R 1 and R 2 with dimensions of 20 μ m × 160 μ m, R 3 and R 4 with dimensions of 200 μ m × 160 μ m) (top) and the flexible device with sensor patterning under microscope magnification (middle). Sensitivity tests performed on the sensor, polysilicon thermistors R 1 and R 2 have a sensitivity of −0.0031 °C $^{-1}$, and R 3 and R 4 have a sensitivity of −0.0025 °C $^{-1}$ (bottom) [116]. b) Schematic diagram of the pressure and temperature sensor (top). The device is placed on a brain model with an inset showing a magnified view (middle). The optical micrograph of the top diaphragm (bottom) [302]. c) Fabrication of piezoresistive sensing unit (top 1). The photographs of the multiplex sensor arrays (top 2, bottom 2 and bottom 1) [303]. d) Image of a BEP including a bioabsorbable wireless heater and a temperature sensor , the sensor is on an oxidized starch (OST) patch containing doxorubicin (DOX) (top). Local and penetrating drug delivery to deep GBM tissue via wireless gentle thermally driven BEP (middle). Fluorescence microscopy images (red) at the brain-BEP interface are shown overlaid with light microscopy images (grey). Inset shows a canine brain image after DOX diffusion from BEP (bottom) [304]. Reprinted from Refs. [116,302–304] with permission. (For interpretation of the references to colour in this figure legend, the reader is referred to the Web version of this article.)

non-power supply, and low cost. However, the rigid materials used in passive ICP sensors increase the risk of brain tissue damage [307].

Yang et al. [308] presented a bioresorbable monitoring platform, which is designed for ICP measurement. The device fabrication involved the usage of the flexible encapsulation materials of monocrystalline silicon wafers and natural wax. The optimized architecture design was modeled through finite element analysis and validated with experimental phenomena, thus the sensor response was maintained during the dissolution processes of the encapsulation layer. As a suspended multilayer film structure for pressure-sensitive applications, it includes a lightly boron-doped micromembrane of monocrystalline Si (Si MM), a PLGA layer, a patterned high boron-doped nanomembrane of monocrystalline Si (Si NM) and another PLGA layer. The silicon in the Si MM biofluid barrier acts as a biodegradable barrier to the permeation of biological fluids. Positioned on top of the PLGA layer, it exhibits good flexibility. Additionally, to protect the device's operational performance, natural wax material is used for edge sealing. The fully encapsulated device is immersed in pH 7.4 PBS at 37 °C for observation. Mg film traces are created on the PLGA-coated silicon wafer to measure water permeation. The results indicate that Candelilla wax has lower water permeability compared to beeswax, but its interface performance with silicon is not as good. However, combining both waxes can harmonize and improve the device's performance. Ultimately, the developed experimental device was demonstrated through implantation in a rat model by the researchers (Fig. 16a) [308]. Ideally, an implantable sensor for clinical application should be able to perform real-time quantification and stable monitoring within a specific time frame [399]. The bioresorbable pressure sensing technology presented by Lu et al. [309] can be applied for a variety of medical internal pressure detection. Si_3N_4 membranes are adopted in the sensor and encapsulated with natural wax edge sealing through battery-free operation is achieved with passive LC-resonance mechanisms (Fig. 16b) [309]. In order to further explore non-invasive ICP monitoring methods with high accuracy, low cost and easier operation, Zhang et al. [310] reported a freeze-casting method to encapsulate liquid metal Ga microstructures to fabricate a band-aid-like flexible Ga-based wearable ICP sensor. The liquid metal microstructure is encapsulated in a thin and flexible polymer. When the liquid metal is deformed by inflation, it fills the microchannel and produces a resistance change. By measuring this resistance change, the monitoring of infant ICP is able to be realized (Fig. 16c) [310]. Notably, Wei et al. [307] proposed a passive wireless pressure sensor for monitoring ICP, the pressure-sensitive device was created based on a novel microfabrication method of flexible materials. The pressure-sensitive capacitor has the characteristics of being ultra-thin and flexible, which can adapt to the topographies of the skull and the dura mater. The flexible features and increased sensitivity make the sensor possible for future application in ICP monitoring (Fig. 16d) [307].

As aforementioned, biodegradable implantable devices have the advantage of avoiding re-extraction procedures [400,401], which can reduce the risk of infection and patient suffering. Shin et al. [311] fabricated a degradable and flexible ICP sensor for real-time monitoring using silicon nanomembranes (Si NMs). The pressure sensor is able to

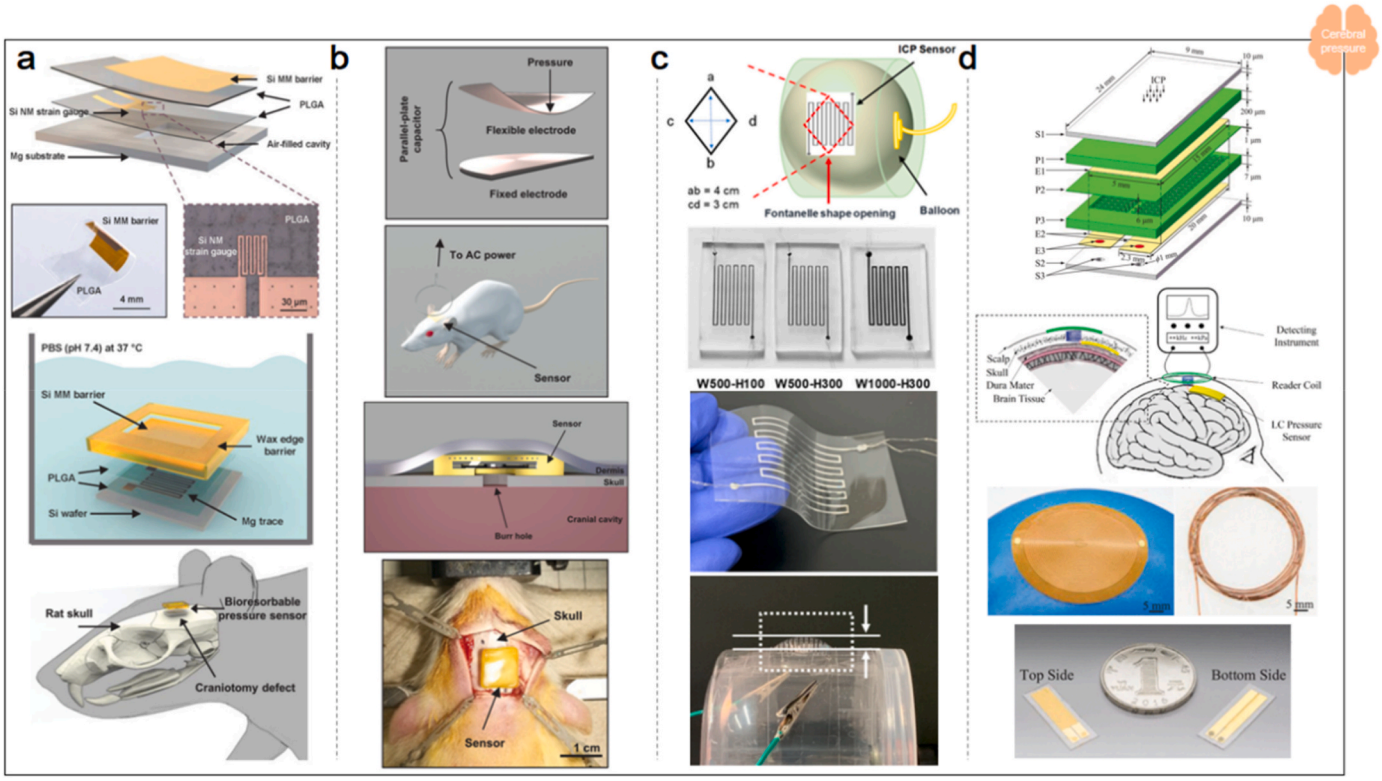

Fig. 16. The applications of flexible sensors in ICP. a) Schematic diagram of a 26.7-μm-thick suspended multilayer film, such as a pressure-sensitive structure, encapsulated on a 2.4 mm × 2 mm × 60 μm gas-filled cavity on a 6 mm × 8 mm × 100 μm magnesium substrate. In this multilayer film, a uniform single crystal lightly doped silicon microfilm acts as the top waterproof layer, a uniform PLGA layer acts as an adhesive interlayer, a single crystal doped silicon patterned nanomembrane acts as the sensing element and another uniform PLGA layer acts as another adhesive interlayer. The inset located at the bottom left shows an optical image of a flexible Si NM biofluidic barrier (4 mm × 4 mm) on a 16.7 μm-thick PLGA substrate. The red right inset shows an optical microscope image of the Si NM serpentine structure forming the strain gauge (top). Diagram representation of the experimental setup for testing the permeation of water through the fully encapsulated structure when immersed in PBS (pH 7.4) at 37 °C (middle). Schematic of the bioabsorbable device on the skull of a rat (bottom) [308]. b) Schematic diagram of the structure of a parallel-plate capacitor with flexible and fixed electrodes that produces pressure-dependent capacitance (top 1). Schematic of wireless sensing of ICP based on an implantable LC resonant sensor coupled to a readout coil (top 2). Schematic cross-section of the sensor placed on a burr hole through the skull to allow the coupling to fluids in the intracranial space (bottom 2). Photograph of the implanted sensor before stitching the surgical site (bottom 1) [309]. c) Model of the balloon fontanelle in the box, inset showing the open area of the fontanelle model (top 1). Photographs of three different designs of solidified Ga structures (Height: 100 μm or 300 μm, W: width) using contact wires in PDMS molds after incubation in a −20 °C refrigerator and removal of sealing tape (top 2). The final ICP sensor (5 cm × 7 cm × 500 μm) (bottom 2). Model of balloon-in-box assembled with ICP sensor (W500–H300) at different inflation heights at different pressure levels [310]. d) Design of flexible varistor capacitors. P: flexible pressure-sensitive layer including deformable layer P1, PDMS adhesive layer P2 and corrugated cavity structure P3; E: electrode layer including upper electrode E1, lower electrode E2 and wire bonding pad E3; S: a flexible substrate layer including an upper substrate S1, a lower substrate S2 and a wire hole S3 (top 1). Schematic diagram of the wireless passive ICP monitoring system (top 2). The reader coil made of flexible printed circuit (FPC) and unoptimized handheld reader coil (bottom 2). Microfabricated flexible varistor capacitors (bottom 1) [307]. Reprinted from Refs. [307,308,309,310] with permission. (For interpretation of the references to colour in this figure legend, the reader is referred to the Web version of this article.)

timely detect the piezoresistive response of deformable Si NMs that reflects changes in external pressure [311]. As stated in the report, Si NMs present high mechanical flexibility, which makes the sensor withstand pressure without mechanical breakage. In addition, the ICP sensor possesses the ability to return to its original shape after the pressure is removed, as discovered [311]. Since sharp thin-film electrodes generally have poor electrical properties, they are prone to cause tissue damage and reduce implant system stability when nerve stimulation is performed over them. To solve this, Manikandan et al. [305] designed a flexible microelectrode array (MEA) made from a cell culture dish in a micro-fabricated method with microelectrodes embedded in the bottom, adopting MEMS technology to fabricate the biocompatible materials. The MEA, which does not penetrate tissue, is capable of sensing stimuli from neurons. As indicated, pressure sensors and temperature sensors are also integrated into the MEA to measure ICP and temperature data for judging neurological disorders [305]. In addition, unlike the case mentioned above, a thin-film flexible wireless pressure sensor that is designed to be applied for wound healing, muscle rehabilitation, and intracranial and extracranial pressure monitoring was reported, while it mainly works for interface pressure detection during compression therapy [312].

4.2.3. *Cerebral blood flow*

Cerebral blood flow (CBF), which refers to the blood flow through a certain cross-sectional area of cerebral blood vessels per unit of time, is strictly regulated to maintain the cerebral metabolism for normal functional activities [314]. Cerebral oxygen supply has an intimate connection with blood oxygen content and CBF, meanwhile CBF is determined by cerebral perfusion pressure and the inversely proportional cerebrovascular resistance [402]. For the measurement of CBF, the whole CBF of normal people in quiet conditions varies with different measurement methods. Insufficient blood flow, or interruption of blood supply, can result in a decrease in oxygen delivery to the brain. This can cause loss of consciousness or fainting [403]. CBF is an important measure of brain health. A CBF value less than 18 mL/100 g/min is generally considered to be an indicator of cerebral ischemia, which is a reduction in blood flow to the brain that can lead to tissue damage and other serious complications. If CBF drops to 10 mL/100 g/min or lower,

it can result in cerebral infarction, which is the death of brain tissue due to lack of oxygen and nutrients [404–406]. The sum of the brain, cerebrospinal fluid (CSF), and intracranial blood volume maintains a certain value within a intact skull, any increase in CBF will cause an increase in intracranial pressure, which can lead to damage of the brain cells. Therefore, it is essential for the brain's blood flow to remain within a healthy range to avoid such complications [407]. Continuous monitoring of CBF can provide important information on the pathogenesis analysis and clinical intervention of various brain diseases. Maintenance of proper CBF is critical for patients with cardiac arrest, cerebral edema, TBI and stroke [314]. Currently, hospitals and outpatient clinics use the Doppler ultrasound imaging technique as a noninvasive method for real-time measurement of cerebral blood flow velocity. This technique is often referred to as transcranial Doppler (TCD) or transcranial color Doppler [408]. By assessing the blood flow velocity in the cerebral vessels, TCD can help diagnose conditions such as arteriovenous malformations [409] and cerebral arteriosclerosis [410]. In addition, other non-invasive methods for monitoring CBF include laser speckle contrast imaging (LSCI) based on optical techniques of dynamic light scattering [411] and diffuse reflectance correlation spectroscopy [412]. Other current clinical devices for CBF measurement through invasive methods include TDF [413], LDF [414], among which LDF is mainly used for monitoring CBF during surgery.

Nowadays, only a few non-invasive tools are available for serial assessment of rodents, which is one commonly adopted animal model in research. The insufficient tissue penetration depth of LDF and LSCI restricts their further application on animals with thicker skulls. Deep brain tissue measurement using DSC requires the use of rigid fiber-coupled light sources and detectors, which can limit the motion of the object being measured. This is because any movement may cause the fibers to dislodge or detach from the tissue, leading to inaccurate results [314]. To address this, one wearable, fiber-free, flexible, and compact diffuse speckle contrast flowmeter (DSCF) sensor developed by Huang et al. [314] possesses a penetration depth sufficient for transcranial detection of CBF in rodent and neonatal cortex through the intact scalp and skull. DSCF enables rapid quantification of spatial fluctuations in laser speckles caused by moving red blood cells using a NIR laser diode as a point source and a lensless bare CCD chip as a 2D detector array. Furthermore, the device not only stabilizes the output light intensity, but also realizes the potential of wearable or wireless probes through the connection between the probe and the control unit (circuit and laptop) by flexible cables, which can thus ensure the free movement of the monitored objects [314]. Aerosol jet printing (AJP), a technology that can be digitally designed, optimized and directly printed compared with traditional processing technology, has rarely been realized in the application of stretchable and wireless electronic devices. Herbert et al. [34] created a wireless, fully printed, implantable and stretchable biosystem for real-time monitoring of cerebral aneurysm hemodynamics

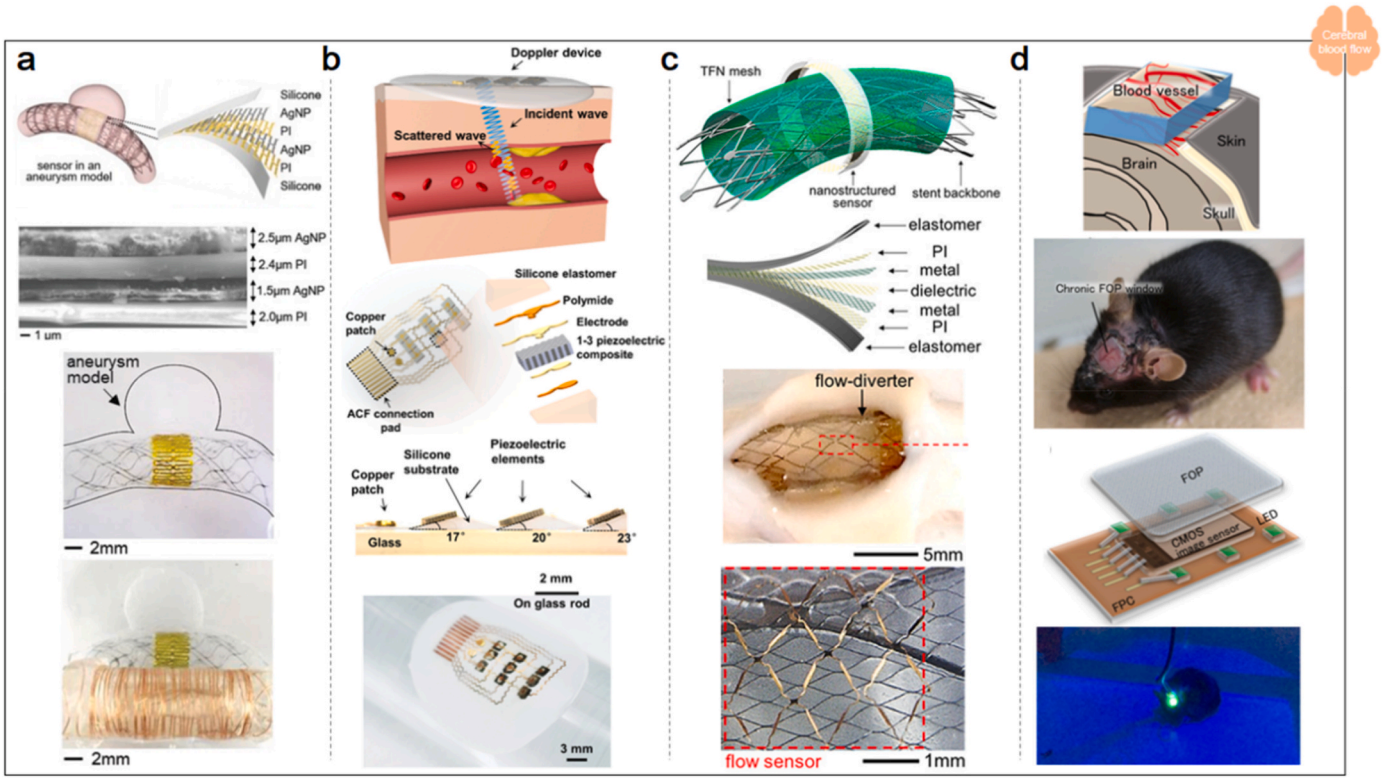

Fig. 17. The applications of flexible sensors applied in CBF. a) Fabrication of implantable flow sensors using AJP on aneurysm models. The inset exhibits the schematic representation of the multilayer structure of the sensor package (top 1). Cross-sectional view of SEM image of the multilayer sensor structure (top 2). Photo of a medical stent with integrated sensors in an aneurysm model (bottom 2). The sensor is connected to copper coil for wireless monitoring of hemodynamics in biomimetic models (bottom 1) [34]. b) Schematic of a Doppler ultrasound device that continuously emits ultrasound and receives echoes from moving scatterers such as red blood cells (top 1). A block diagram of the device (left) and an exploded illustration view of the components (right). ACF, Anisotropic conductive film (top 2). Image of a cross-section view of a semi-finished device without top electrode bonding. The mentioned device with the transducer array, bottom electrode and substrate is placed on a glass plate (bottom 2). The photo of the curved device (bottom 1) [315]. c) The diagram of the integrated flow diverter with a nanostructured sensor on scaffold backbone, which is wrapped in a TFN mesh (top 1) and the multilayer capacitive flow sensor (top 2). The device is centered on the neck of the aneurysm (bottom 2). Image of flow sensor under a microscope (bottom 1) [316]. d) The schematic of the chronic fiber-optic plate (FOP) window (top 1). The mouse is attached by a chronic FOP window on the head (top 2). Schematic illustration of the structure of the device consisting of a CMOS image sensor, six green LEDs, and FOP on an FPC (bottom 2). A photograph of a mouse behavioral experiment showing the device's green LED light source being illuminated (bottom 1) [317]. Reprinted from Refs. [34,315,316,317] with permission. (For interpretation of the references to colour in this figure legend, the reader is referred to the Web version of this article.)

using an aerosol jet 3D printing fabrication method. The stretchable wireless electronic device was fabricated through high-throughput, large-scale and aerosol-jet 3D printing methods to achieve a highly flexible and stretchable sensor with conformal insertion into a blood vessel through seamless integration with an implantable stent and stretchable mechanical modeling. Biocompatible silver nanoparticles and direct microstructured patterning of PI are crucial parts of the core printing process. The flexible and highly stretchable sensor can be deployed through the catheter and inserted into the blood vessel with a very low profile. By optimization of a transient, the wireless inductive coupling method achieves wireless detection of the hemodynamics of biomimetic cerebral aneurysms with a readable distance of up to 6 cm across the meat (Fig. 17a) [34]. Techniques based on thermal analysis or photoplethysmography, which only detect relative changes in flow, are not deep enough for blood vessel monitoring. Wang et al. [315] have proposed a flexible, lightweight ultrasound device based on the Doppler Effect. This device was successfully used to measure the blood flow spectrum of the carotid artery by attaching it to the surface of the human body near the artery. Researchers evaluated the accuracy of the newly developed device by comparing its measurements of carotid artery blood flow velocity with those obtained using commercial devices. The common carotid artery is the main arterial trunk of the head and neck, and its branched internal carotid artery ascends and its terminal branches include the anterior cerebral artery and the middle cerebral artery, which are important arteries supplying the brain [415]. Therefore, the information obtained from carotid artery measurements has a positive correlation with cerebral blood flow (Fig. 17b) [315]. Apart from this, monitoring hemodynamics is important for the evaluation of sac occlusion after cerebral aneurysm treatment. Howe et al. [316] proposed a stretchable, nanostructured implantable flow sensor system that can quantify intra-aneurysmal hemodynamics. The stent is constructed using a superelastic nickel-titanium Nitinol (TFN) membrane to wrap around the stent mesh, with a capacitive ring-type flow sensor sandwiched by PI and positioned on the periphery, which aims to create a functional stent that can monitor and treat the hemodynamics of arterial aneurysms at the same time. The device has up to 500% radial stretchability and 180° bendability with a curvature radius of 0.75 mm as evidenced, besides, it has shown less platelet deposition than existing implantable materials (Fig. 17c) [316]. Unlike the aforementioned case, a reported study has developed a device consisting of a complementary metal-oxide semiconductor (CMOS) image sensor and a chronic fiber-optic plate window to achieve chronic CBF imaging in mice. The device is used to measure changes in the blood flow of target subjects with behavioral experiments. In general, chronic CBF imaging equipment should be helpful for the clinical diagnosis of the etiology and treatment of cerebrovascular disease (Fig. 17d) [317].

4.2.4. Brain tissue oxygenation

Partial oxygen pressure ($PbtO_2$), an indicator of local brain tissue oxygenation content, which is measured at the bedside can also be used as an alternative index for cerebral blood flow (CBF) [416]. $PbtO_2$ arises as a result of the interplay between cerebral blood flow (CBF) and arteriovenous tension of O_2, signifying that both sufficient oxygen perfusion, oxygenation, extraction and diffusion are crucial for maintaining cerebral oxygenation [417]. The normal range for $PbtO_2$ is recorded as 20–35 mmHg for Licox invasive probes, whereas $PbtO_2$ less than 15 mmHg is usually caused by hypoxia and ischemia [418,419]. $PbtO_2$ is believed to reflect the equilibrium between regional oxygen supply and cellular oxygen consumption in patients with severe TBI. This relationship is influenced by the interplay between plasma oxygen partial pressure and CBF, which can be mathematically expressed as the equation: $PbtO_2 = CBF \times AVTO_2$ [420]. As observed in studies, the monitoring of brain O_2 and $PbtO_2$-targeted therapeutic approaches can greatly enhance patient recovery.[421,422] For patients with severe acute encephalopathy (eg. TBI), aneurysmal subarachnoid hemorrhage (aSAH), and in certain neurosurgery procedures [423–425], timely monitoring of local brain tissue oxygenation content is well-accepted and increasingly being adopted to ensure normal O_2 levels in neurological intensive care units.[408]Thus, $PbtO_2$ is treated as a reliable marker of CBF and cerebral ischemia under certain conditions. The current clinical methods used to monitor $PbtO_2$ include invasive techniques such as Clark electrode-based electrochemical sensing and fluorescence quenching-based optical sensing [49], also the non-invasive techniques like NIRS [426,427]. The basic device of an electrochemical PO_2 sensor designed for medicine was first proposed by Leland Clark in 1956 [106]. For intracranial fiber optic oxygen sensors, the sensors based on the effect of fluorescence quenching are mainly adopted [49]. NIRS indirectly detects O_2 by measuring hemoglobin saturation within a specific tissue volume [82].

NIRS-based devices designed for adults [428] are certainly not suitable for application in children due to their large size and rigid structure, which can easily cause potential damage to the delicate skin of children [429]. By combining a multi-photodiode array with a pair of light-emitting diodes, a small and flexible wireless device capable of conducting simultaneous whole-body and cerebral hemodynamic monitoring was fabricated by Rwei et al. [318] The indicators measured include peripheral oxygenation, HR, cerebral oxygenation, and potentially cerebral pulse pressure. The overall structure of the device includes a flexible printed circuit board with two units. One unit consists of a bluetooth low-energy system on a chip module with wireless communication and power regulation capabilities. The other unit is an optical sensor that monitors blood flow dynamics. As demonstrated experimentally, the platform significantly improves the effect of care for pediatric patients, which greatly benefits patients suffering from cerebral and neurodevelopmental disorders (Fig. 18a) [318]. Besides, the aforementioned sensors can also be used to monitor brain tissue oxygen levels [303]. Human-machine interaction has attracted more and more attention from various fields, such as the study of automatic classification with different sorts of human mental states [430]. Gurel et al. [319] achieved differentiation between mental arithmetic, rest, and N-back memory tasks by fusing sensing modalities for monitoring of human prefrontal cortex (PFC) oxygenation and cardiovascular physiology. The designed flexible NIRS-PPG headband enables measurements of quantified PFC oxygenation and peripheral cardiovascular signals including ECG, PPG and SCG (Fig. 18b) [319]. Notably, Si et al. [320] presented a portable modular cerebral tissue oximeter (BRS-1) that can be applied for local oxygen saturation measurement in targeted areas of the body such as the finger and brain, and also is available for wireless brain-brain oxygenation monitoring. The device is expected to be broadly adopted clinically thanks to its compact and lightweight design (Fig. 18c) [320]. In terms of monitoring cerebral oxygen saturation, a more accurate sensor system can provide better treatment guidance for newborns. Petersen et al. [321] proposed a sensor to detect oxygen saturation in brain tissue for the treatment of preterm infants using a near-infrared spectroscopic approach. The silicon photodetectors that make up the sensor are fully integrated into a flexible array. To achieve higher flexibility, silicon is combined with polydimethyloxane while polyimide manufactured from standard ICs is adopted as well. The electrical interconnections on the sensor enable it to be well-placed on the head of the newborn owing to its great capacity for bending deformations (Fig. 18d) [321].

4.2.5. Cerebral metabolism

Metabolic disturbances caused by ischemia or hypoxia can be assessed by monitoring ions, glucose, lactate, pyruvate, glycerol, etc., as cerebral metabolism is highly correlated with whether cerebral blood flow (CBF) provides sufficient oxygen and energy substrates [49]. In the setting of hypoperfusion, decreased blood glucose levels can also indicate ischemia and long-term low pH situation is thought to be significantly associated with mortality [431]. Furthermore, since the pH of the tumor extracellular microenvironment is considered to have a reduction, the pH value can also be taken as one index for brain cancer

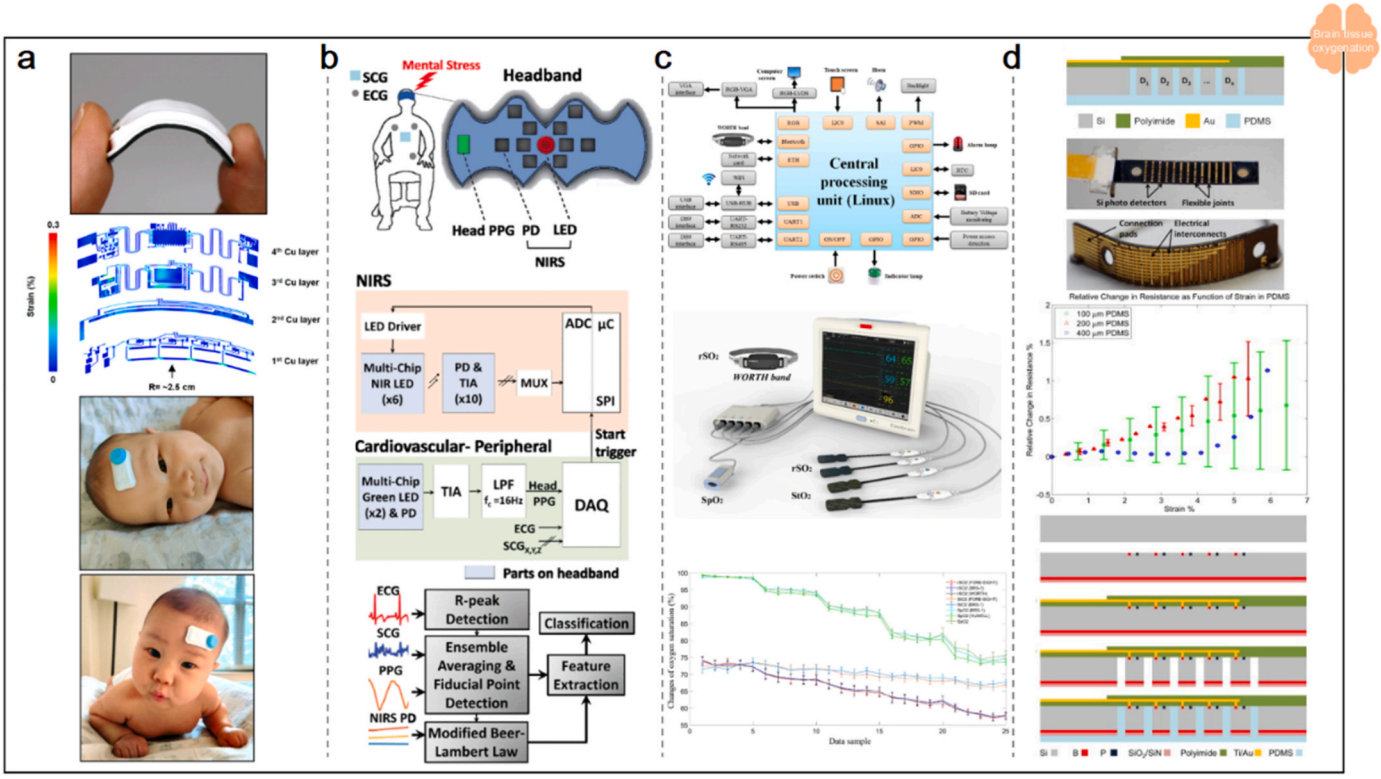

Fig. 18. The applications of flexible sensors applied in brain tissue oxygenation. a) The soft wireless device under mechanical stress in bending (top 1). The calculated strain distribution of the device copper layer with a bending radius of 2.5 cm (top 2). The photographs of the rest and prone position of a 9-week-old infant with the device on the forehead (bottom 2 and bottom 1) [318]. b) Schematic diagrams of the headband collecting PPG, SCG, ECG, NIRS signals (top) and the sensing method (middle). The signal processing and feature extraction block diagram (bottom) [319]. c) The schematic diagram of the brain oximeter (BRS-1) (top). The photography of the BRS-1 oximeter. The equipment includes two regional cerebral oxygen saturation (rSO_2) brain sensor probes, two tissue oxygen saturation (StO_2) sensor probes, and a peripheral arterial saturation (SpO_2) sensor probe. WORTH band can achieve wireless monitoring rSO_2 (when connected to the oximeter via Bluetooth) (middle). Group-averaged results of varying oxygen saturation values in validation experiments (bottom) [320]. d) A cross-sectional view schematic of the design of a flexible sensor array which is composed of a single silicon photodetector (D1 – Dn), gold conductors, polyimide, and PDMS (top 1). Pictures of the front and back of the sensor (top 2). The plot of tensile test results for sensors with 100 µm, 200 µm, and 400 µm wide flexible joints. Error bars: sensor-to-sensor standard deviation (bottom 2). The process flow diagram (bottom 1) [321]. Reprinted from Refs. [318,319–321] with permission. (For interpretation of the references to colour in this figure legend, the reader is referred to the Web version of this article.)

diagnosis [393]. In addition, the detection of specific chemical elements also helps to diagnose a variety of diseases related to the nervous system [393]. To be specific, the concentration of dopamine (DA) in healthy individuals is typically 0.01 µM–10 µM for instance. Brain diseases such as Parkinson's disease (PD) and Alzheimer's disease (AD) commonly can be diagnosed by detecting dopamine [258]. Detecting specific chemical elements provides an important reference for the diagnosing of AD, PD, epilepsy and other brain diseases that are highly correlated with neurotransmitter concentrations [393].

For the monitoring of cerebral metabolism, the commonly adopted methods are electrochemical analysis based on Clark electrode and optical analyzer with fluorescence sensing [49]. Asif et al. [33] proposed a new method for fabricating highly active Cu–Fe hybrid electrodes via SRB-assisted corrosion engineering, which enabled the value-added conversion of iron substrates with low fabricating cost to high-efficiency Cu–$Fe(OH)_2$–FeS/PCF electrode. Note that the fabricated electrodes can be used for real-time tracking of H_2O_2 discharged from different normal and human brain cancer cell lines in vitro or in situ (Fig. 19a) [33]. Adrenaline, one kind of hormone and neurotransmitter, is a catecholamine and adrenal cortical hormone released by the renal glands [432]. Normal concentrations of adrenaline in human body fluids are usually in the range of 0.015 µM–40 µM [433]. Adrenaline can increase myocardial contractility and is a commonly used first-aid appliance in clinical practice. In addition, as a physiological indicator of stress, the dramatic increment of adrenaline can lead to behaviors such as instinctive flight or fight responses [434,435], thus the detection of which aids in the clinical diagnosis of depression, post-traumatic stress disorder (PTSD) and anxiety [433]. Yu et al. [322] developed a capacitive sensor by means of layer-by-layer (LbL) assembly with the function of detecting adrenaline. The fabricating method of the sensor contains simple drop-casting, with PDMS substrate and carbon nanotube-cellulose nanocrystals (CNC/CNT) nanofilm as the first layer, the adrenaline imprinted poly (aniline/phenylboronic acid) (pANI/PBA) moieties as the second layer to construct the LbL assembly. The chemical sensor with the ability of capacitive detection of adrenaline exhibits excellent properties of flexibility, highly sensitive, highly selective, and disposable. As stated, the proposed sensor, which was validated to screen adrenaline rapidly in zebrafish brain samples, is expected to be further applied in the detection of adrenaline in medicine (Fig. 19b) [322]. Another great work reported by Liu et al. [306] has fabricated flexible conformal sensor devices which is capable of simultaneously sensing pH, DA, serotonin, and temperature. To explain further, these sensors are made by fabricating In_2O_3 nanoribbon field-effect transistors (FETs) arrays on thin (1.4 µm) PET and enable selective detection of neurotransmitters. This was achieved by surface functionalization of In_2O_3 with aptamers capable of binding target molecules, including dopamine and serotonin. When serotonin binds to the aptamer, a part of the negatively charged main chain of the aptamer will be far away from the semiconductor channel, the electrostatic repulsion between the negatively charged aptamer and the electrons in the semiconductor channel will decrease, and the transconductance of the n-type semiconductor will increase. When dopamine binds to the aptamer,

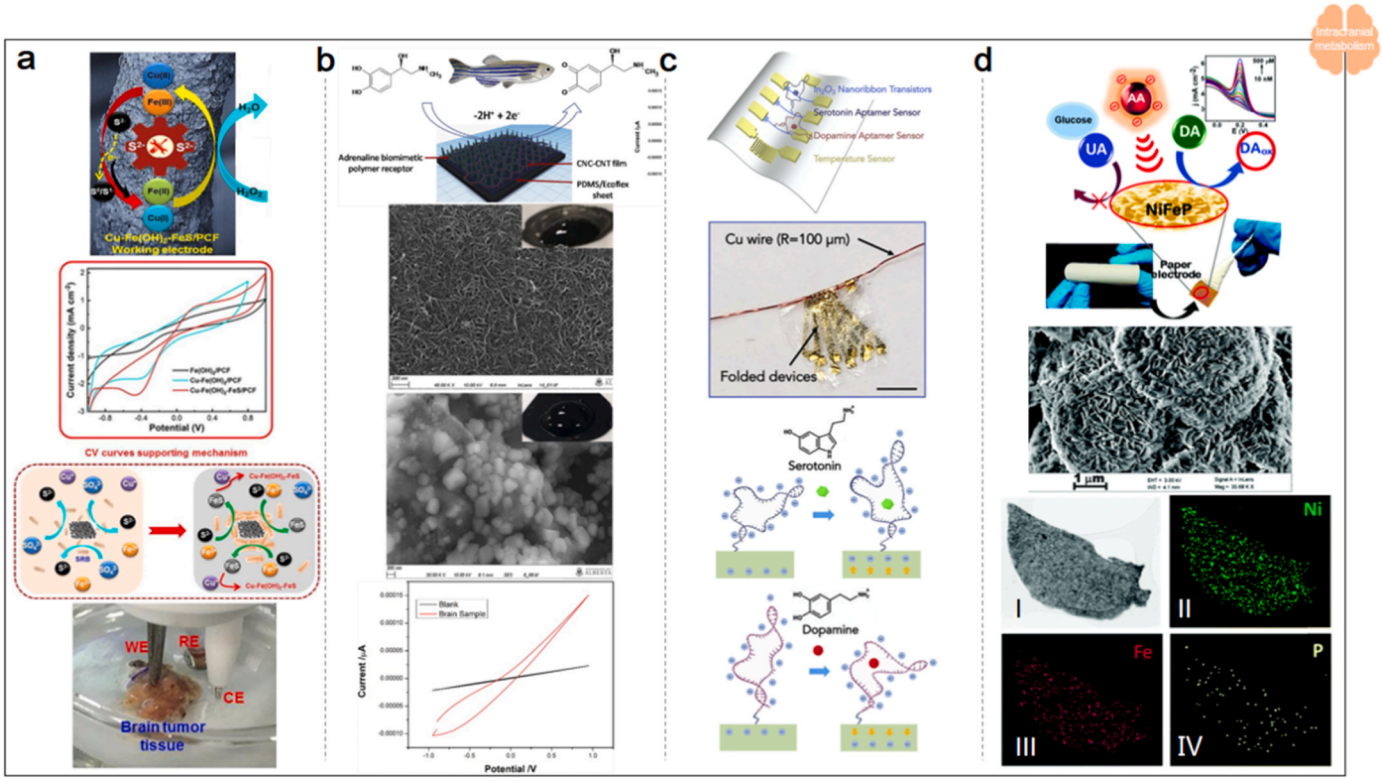

Fig. 19. The applications of flexible sensors applied in cerebral metabolism. a) Schematic illustration of the mechanism of S2- cocatalysis in Cu–$Fe(OH)_2$–FeS/PCF electrodes (top 1). The related CV curve in the presence of 0.5 mM H_2O_2 in 0.1 M PBS (top 2). Schematic illustration of the fabrication of Cu–$Fe(OH)_2$–FeS/PCF electrodes by SRB-assisted corrosion engineering strategy (bottom 2). Photo of a three-electrode system for tissue measurement (bottom 1) [33]. b) The illustration of the detection principle of adrenaline on the sensor (top 1). The scanning electron micrographs of PDMS/CNC-CNT (top 2) and the micrograph of PDMS/CNC-CNT/PBA-pANI (bottom 2). The cyclic voltammograms of the sensor for blank and after the addition of neat brain sample (bottom 1) [322]. c). The schematic diagram of the biosensor film (top 1). Image of a flexible thin-film PET In_2O_3 sensor array with a thickness of 1.4 μm wound on a copper wire with a radius of 100 μm, scale bar: 5 mm (top 2). Schematic illustration of redirecting a portion of the backbone of an aptamer for serotonin recognition away from the semiconductor channel upon target binding to increase the transconductance of the n-type semiconductor (bottom 2). The schematic diagram of redirection of a portion of the negatively charged oligonucleotide backbone of the dopamine aptamer to a position closer to the field-effect transistor upon target recognition to electrostatically depletes the channel (bottom 1) [306]. d) The schematic diagram of DA detection (top). The FE-SEM images (middle). The STEM photo of the NiFeP catalyst, corresponding EDS elemental dot plots of Ni, Fe and P (bottom) [258]. Reprinted from Refs. [33,258,322,306] with permission.

redirecting it's negatively charged backbone closer to the semiconductor channel produces the opposite result. In addition, the device exhibits excellent flexibility and long-term stability in high ionic strength solutions such as artificial cerebrospinal fluid and undiluted physiological buffered saline (PBS) (Fig. 19c) [306]. Ascorbic acid (AA) concentrations are much higher than DA, which interferes with the precise determination of DA. To solve this, Thakur et al. [258] chose nickel iron phosphide/phosphate (NiFeP) as an effective catalyst for the detection of DA with selectivity and sensitivity, and successfully achieved an electrochemical sensor based on NiFeP to detect DA. The NiFeP catalyst on the paper electrode can oxidize DA to dopamino quinone, and this chemical sensor possesses ultrasensitive properties. The sensor that has been developed demonstrates total immunity to interference caused by AA and other substances such as glucose and UA. (Fig. 19d) [258]. Besides, a study also developed modulated single-walled carbon nanotube (SWCNT) network to generate transparent and flexible sensors for dopamine detection [323].

4.2.6. Other applications

Besides the above representative applications, some recent studies have reported other applications of flexible sensors applied in the brain and cerebrovascular system with relatively unique working principles. A study utilizing microwave sensors to monitor neurodegenerative diseases has been evaluated by simulating brain atrophy and lateral ventricle enlargement [259]. To be specific, Saied et al. [259] fabricated six planar monopole antenna sensors and developed a wearable system by integrating the flexible hybrid silicone-textile sensors with a switching circuit. Due to the flexible materials adopted through the manufacturing process, the sensors and switching circuits conform better to the patient's head, which provides great potential for diagnostic-assisting in the medical field [259]. Moreover, there is a study of brain edema monitoring through MIPS sensing as well [120]. Inside the cranium, a pressure sensor providing timely intracranial pressure (ICP) monitoring [307] can help to reveal force feedback with more intuition for surgeons controlling the flexible neurosurgical tools [325]. Similarly, the pressure sensor is broadly adopted during surgery to avoid surgery-induced brain damage [326]. Furthermore, implantable electrocorticography (ECoG) recording systems are often used to localize epilepsy lesions and diagnose brain disorders. Xu et al. [313] fabricated flexible bioabsorbable ECoG devices using the bioresorbable material poly (L-lactide) and polycaprolactone (PLLA/PCL) (PLLA:PCL = 80:20) and the transitional metal molybdenum (Mo), with an ICP sensor integrated to monitor the dynamic changes of brain signals in different epilepsy stages and ICP [313]. Notably, Yang et al. [327] proposed a flexible multifunctional electrode (FME) capable of recording ECoG and extracellular ions of K^+, Ca^{2+}, and Na^+ on the surface region of the cerebral cortex, based on the high specific surface area and ion-electron transfer of the conductive carbon nanotube arrays (CNTA). As stated in the study, CNTA electrodes have low impedance, high specific capacitance and charge storage capacity compared to conventional gold electrodes (Fig. 20a) [327].

Graphene-active sensors also exhibit great potential in detecting

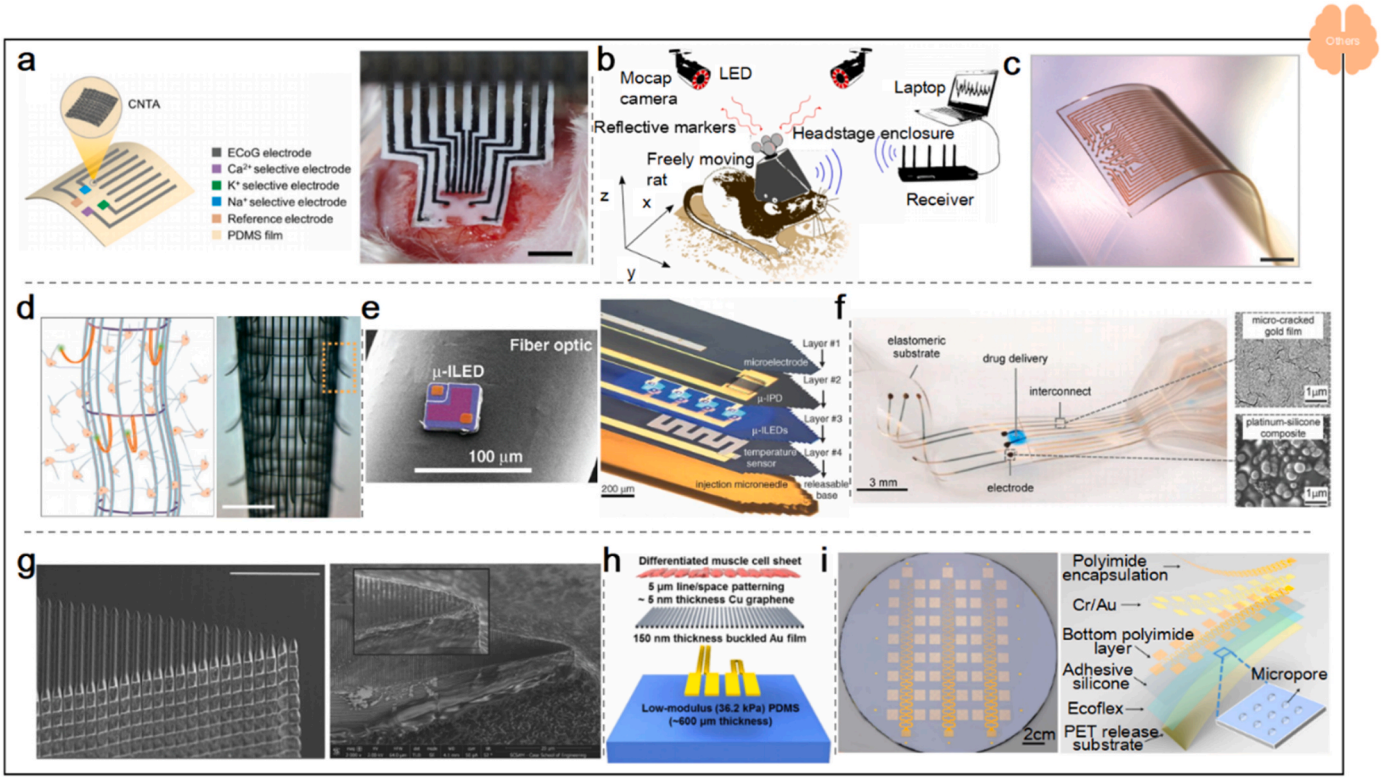

Fig. 20. The other applications of flexible sensors in the brain. a) Schematic diagram of FME. CNTA shown as a plane-parallel orientation structure is shown in an enlarged section (left). Photograph showing the FME attached to the cerebral cortex. Scale bar: 4 mm (right) [327]. b) Schematic showing a rat implanted with an unrestricted recording system [328]. c) Electrode grid containing 32 electrodes with 200 μm spacing made from Au–TiO_2 NW conductors embedded in PDMS [329]. d) The microscopic schematic showing the interface between macroporous nanoelectronic brain probes and neural circuits. The probe consists of polymer-encapsulated metal interconnects, arms (orange) that support and connect the sensor (green) and support elements (pink, violet, and light blue) (left). The sensor element is indicated by the dashed box. The scale bar measures 50 μm (right) [330]. e). Color SEM pictures showing μ-ILEDs mounted on 200-μm fiber optic implants (left). Tilt exploded view layout of a multifunctional, implantable optoelectronic device. The system consists of an electrophysiological measurement layer composed of a Pt contact pad and microelectrodes, an optical measurement layer composed of silicon μ-IPD, a photostimulation layer composed of the μ-ILED array, and a temperature sensing layer composed of snake Pt resistor (right) [331]. f) Images of implants, and scanning electron micrographs of gold films and platinum-silicon composites [332]. g) Nanopatterned electrode tip at 10 000× magnification, scale bar: 4 μm (left). SEM images of the nanopatterned laterally explanted probes show that the etched nanopatterns are visible. Scale bar of the inset: 4 μm (right) [333]. h) The expanded view of elements of a cell culture platform [324]. i) The photography of epidermal electrodes fabricated on 8-inch silicon wafers (left). Schematic diagram of functional layers of a flexible stretchable device (right) [334]. Reprinted from Refs. [324,327–334] with permission. (For interpretation of the references to colour in this figure legend, the reader is referred to the Web version of this article.)

brain electrophysiological signals. Garcia-Cortadella et al. [328] fabricated a sensing system capable of long-term and broadband recording of freely moving animals using a wireless headstage which consists of a flexible 64-channel g-SGFET array with robustness, high sensitivity, and biocompatibility properties (Fig. 20b) [328]. Flexible electronics suitable for neural interfaces require the combination properties of long-term stability, high performance, and high electrode density of soft electrode meshes, while current materials and related fabrication processes have not achieved the target level yet. Tybrandt et al. [329] developed a stretchable, high-density flexible mesh capable of resolving high spatiotemporal neural signals from the murine cortical surface of freely moving rats. The electrode grid is fabricated with an inert composite material with high performance, including gold-coated titania nanowires embedded in a silicone matrix. By exploiting the flexibility and stretchability of the electrodes, a reduction in the size of the required craniotomy is achieved (Fig. 20c) [329]. As another notable case, Xie et al. [330] proposed an ultra-flexible electronic probe capable of being cryo-implanted and used in rodent brains, which overcame the limitations of 3D macroporous nanoelectronic brain probes by combining subcellular feature size and ultra-flexibility. The probe is also capable of recording multiple local field potentials and single-unit action potentials from the somatosensory cortex (Fig. 20d) [330]. Commonly in optogenetics, in order to achieve relatively comprehensive functions, various components, including sensors, light sources and detectors, have to be implanted into specific parts of the brain tissue. Kim et al. [331] demonstrated a class of cell-scale optoelectronics of the injectable type, which has multiple functions such as sensing, driving and stimulating. Researchers exemplified unparalleled modes of operation in optogenetics including complex behavioral target control of fully wireless and programmed freely moving animals. The extremely small size of the μ-ILED device offers significant advantages when it comes to implantation in living bodies. Its small dimensions effectively minimize tissue damage and reduce inflammatory reactions, making it suitable for long-term implantation scenarios. Furthermore, the efficient thermal management and the spatially accurate, cell-scale photon transport capability of the μ-ILED device are also due to its extremely small dimension. Notably, the temperature sensor integrated into the device serves a dual purpose. Firstly, it functions as a sensing component to determine the heating temperature, providing crucial feedback for controlling the device's operation. Secondly, it can act as a heater itself. (Fig. 20e) [331]. For neural prostheses, an ideal range of mechanical stiffness is required to avoid degradation from being too soft and tissue damage from being too stiff. Minev et al. [332] designed soft nerve implants capable of extracting cortical states in freely behaving animals as brain-computer interface, and triggered electro-chemical spinal nerve modulation to promote motor recovery after spinal cord injury paralysis.

As evidenced in the study, the shape of these implants is quite suitable for the geometry of the dura mater (Fig. 20f) [332]. The surface structure with smooth features of intracortical microelectrodes, which is implanted within nanoscale structures of brain tissue, is considered to be associated with foreign body responses. To explore it, Ereifej et al. [333] used focused ion beam lithography to etch the silicon shank of a nonfunctional intracortical microelectrode probe and investigated the neuroinflammatory response of nanopatterned surface grooves on the microelectrodes (Fig. 20g) [333]. Until now, there is no developed soft integrated system capable of in vitro physiological monitoring of aligned cells prior to in vivo application for tissue regeneration. Kim et al. [324] proposed a multifunctional platform equipped with stretchable ultrathin gold nanomembrane sensors and graphene-nanoribbon cell aligners for soft cell culture and in situ monitoring of cellular physiology. Furthermore, a transfer printing mechanism of scaffold-free cell sheets for delivering localized cell therapy in an in vivo setting is also proposed (Fig. 20h) [324]. In addition, Tian et al. [334] proposed a device for electrophysiological recording that can cover the entire scalp and the whole circumference of the forearm. At the same time, the usage of EEG and long-term EEG functional magnetic resonance imaging for large-area interfaces is realized (Fig. 20i) [334].

5. Summary and outlook

As the most crucial and complex system of the human body, cardiocerebral vascular system together with heart-brain network attracts researchers inputting profuse and indefatigable efforts on an exploration of proper methods for these timely vital signal monitoring and obtaining. Flexible electronics and wearable sensors functioned to reflect the real-time body signals of cardiocerebral vascular system, not only for patients with chronic and acute diseases, but also can serve the general public as much as possible. Traditional sensors involving rigid materials normally cannot perfectly conform to the morphological changes of the body contact surface, especially in the continuously moving situation, and thus will inevitably affect the data accuracy and precision. Furthermore, the utilization of rigid sensors can potentially lead to a range of physiological adversities, particularly when employed in implantable contexts. Addressing these aforementioned concerns has been a focal point of rigorous research endeavors. The intrinsic attributes of wearability, comfort, implantability, biocompatibility, sustained monitoring and treatment, real-time assessment, heightened sensitivity, and precision exhibited by flexible electronic devices, when integrated into the cardiocerebral vascular system, equip them to surmount many challenges ingrained within the realm of conventional rigid devices. The intrinsic thinness and lightweight nature of flexible electronic devices facilitate a seamless adaptation to the intricate contours of biological tissues, a feat that often eludes larger, bulkier rigid counterparts, thereby imbuing convenience into their utilization. Notably, the application of biocompatible materials within flexible electronics precludes irritation and mitigates the potential for inflammatory responses, an attribute particularly salient when contemplating implantable applications. Conversely, implantable rigid devices may not only incite inflammatory reactions but also compromise their overall functionality, rendering them less conducive to sustained real-time monitoring of cardiocerebral vascular ailments. Consequently, the inherent flexibility of electronics renders them notably more apt for prolonged, real-time monitoring. Ultimately, owing to their unparalleled capacity to seamlessly conform, flexible electronics possess the capability to discern even the most nuanced physiological signals. This review mainly summarizes recent breakthroughs in flexible electronics specifically applied to the cardiocerebral vascular system and heart-brain network, aiming to provide a relatively thorough reference.

In terms of the cardiovascular system, the reported flexible sensors are mainly developed to detect heart rate (HR), blood oxygen saturation, blood pressure (BP), blood glucose and other indicators. The measurement methods of HR include ECG signals obtained through the bioelectric method to measure changes in biopotential and PPG signals acquisition based on the optoelectric method to detect light absorption variance. HR can also be acquired from SCG, radial pulse, and BCG signals utilizing the mechanoelectrical principle to detect strain, pressure, and acceleration, which reflect the pulse wave signals to reveal changes in arterial diameter. For blood oxygen saturation, it can adopt optoelectric-based methods to obtain PPG signals determining changes in light absorption, and the measurement can help diagnose diseases such as hypoxia and ischemia. For BP estimation based on signals from bioelectric, optoelectric, and mechanoelectrical sensors, it works typically including algorithms according to PTT (pulse transient time), PAT (pulse arrival time), and ML (machine learning). With obtaining PPG, BCG, ECG, SCG, and mechanical pulse wave signals, they are easily transferred to BP-related parameters such as PTT and PAT. Blood glucose is commonly obtained with the electrochemical method, while the current or voltage signals changing in saliva, tears, sweat and ISF can sensitively reflect the glucose concentration. In terms of brain tissue and cerebrovascular system, flexible sensors can be broadly adopted to measure brain temperature, intracranial pressure (ICP), cerebral blood flow (CBF), brain tissue oxygen, cerebral metabolism and other indicators. Brain temperature plays a crucial role in reflecting the balance of neurometabolic heat production, CBF and arterial blood entering temperature, thus can be clinically used to help diagnose fever-sensitive diseases. RTDs are considered to be one of the most accurate sensors for measuring temperature. The monitoring of ICP is very necessary for patients with brain injury, inflammatory infection, stroke, tumor, hydrocephalus, and epilepsy, etc., of which the working principle currently mainly includes fluid-based systems, Doppler sonography and implantable transducers. CBF is associated with diseases such as cerebral arteriosclerosis, and current invasive methods for CBF measurement normally include TDF and LDF, while only a few non-invasive tools are available for serial assessment in rodents. Brain tissue oxygen concentration is directly related to cerebral hypoxia. Invasive techniques for monitoring $PbtO_2$ currently contain electrochemical sensing based on Clark electrodes and optical sensing based on fluorescence quenching, and the non-invasive techniques include NIRS. Similarly, for brain ischemia or hypoxia, commonly chosen monitoring principles of cerebral metabolism include optical analyzers based on fluorescence sensing and electrochemical analysis based on Clark electrodes. In addition, flexible sensors can monitor neurodegenerative diseases and inside the cranium, and pressure sensors providing timely intracranial pressure (ICP) monitoring can help to reveal more intuitive force feedback for surgeons controlling the flexible neurosurgical tools.

Anticipating the road ahead, several trends are poised to shape the evolution of flexible electronics within the cardiovascular domain. These trends encompass enhanced sensing technology, intelligent data analysis, wireless real-time data transmission, and therapeutic applications. As manufacturing techniques evolve and flexible materials continue to progress, the sensing capabilities of flexible electronics are set to be refined, yielding heightened accuracy and sensitivity. In the foreseeable future, the landscape of flexible electronics integrated into the cardiocerebral vascular system will increasingly gravitate toward wireless communication, thereby streamlining remote monitoring and diagnostics. With ongoing refinements in structural design and technological prowess, the domain of therapeutic flexible electronics is poised for gradual expansion. Furthermore, propelled by the rapid strides of artificial intelligence, the development of advanced algorithms will persist, culminating in the emergence of intelligent data analysis algorithms.

Although flexible sensors have exhibited extraordinary advantages with numerous successful trial cases, a difficult road still lies ahead to further fulfill the clinical and marketing demands in the future. First of all, wearable and implantable flexible sensors will inevitably cause damage to the body, not only due to the insufficient development of fabrication processes, and mismatching of large-scale sensor surfaces versus exquisite various tissues, but also owing to the deficiency of ideal

materials with excellent biocompatibility and degradation. These factors of uncertainty will greatly increase the risk of infection, especially for implanted components such as intracranial sensors, which may damage nerves and cause severe sequelae. In addition, most of the current sensors and devices are short of product normalization and integration, which directly reveals the complexity and difficulties of device miniaturization, proper components integration, connection optimization and power supply with portable form. Moreover, most sensors can only present basic signals or parameters for the monitored information, while are lack of intuitive professional interpretation of obtained data, thus resulting in the inconvenience of product prevailing to the market. Overall, the excellent merits of flexible and soft sensors have brought immeasurable application potential in medicine and other related fields. Subsequently developed methods regarding the outstanding issues with relevant improvements and upgradation are expected to achieve more breakthroughs within the medical field and healthcare treatment.

Declaration of competing interest

The authors declare that they have no known competing financial interests or personal relationships that could have appeared to influence the work reported in this paper.

Data availability

No data was used for the research described in the article.

Acknowledgments

The authors appreciate the support of **The Science and Technology Development Fund, Macau SAR** (0021/2022/A1, 006/2022/ALC, 0007/2021/AKP), and Research Grant (MYRG2022-00088-IAPME, SRG2021-00003-IAPME) from the Research & Development Administration Office at the University of Macau.

References

[1] V.L. Bautch, Vascular development and organogenesis: depots of diversity among conduits of connectivity define the vasculome, in: The Vasculome, Elsevier, 2022, pp. 241–249.
[2] J. Burrin, C. Price, Measurement of blood glucose, Ann. Clin. Biochem. 22 (4) (1985) 327–342.
[3] L.C. Boyette, B. Burns, Physiology, Pulmonary Circulation, 2018.
[4] Z. Filip, K. Jan, S. Vendula, K.Z. Jana, M. Kamil, K. Kamil, Albumin and α1-acid glycoprotein: old acquaintances, Expet Opin. Drug Metabol. Toxicol. 9 (8) (2013) 943–954.
[5] E. Pasini, R. Aquilani, F.S. Dioguardi, Amino acids: chemistry and metabolism in normal and hypercatabolic states, Am. J. Cardiol. 93 (8) (2004) 3–5.
[6] J. Badimon, V. Fuster, J. Chesebro, L. Badimon, Coronary atherosclerosis. A multifactorial disease, Circulation 87 (3 Suppl) (1993) II3–16.
[7] F.H. Messerli, B. Williams, E. Ritz, Essential hypertension, Lancet 370 (9587) (2007) 591–603.
[8] L. Kopin, C.J. Lowenstein, Dyslipidemia, Ann. Intern. Med. 167 (11) (2017) ITC81–ITC96.
[9] C.D. Kemp, J.V. Conte, The pathophysiology of heart failure, Cardiovasc. Pathol. 21 (5) (2012) 365–371.
[10] S.W. Chen, J.M. Qi, S.C. Fan, Z. Qiao, J.C. Yeo, C.T. Lim, Flexible wearable sensors for cardiovascular health monitoring, Adv. Healthcare Mater. 10 (17) (2021), e2100116.
[11] S. Yomo, M. Hayashi, Fatal tumoral hemorrhage after stereotactic radiosurgery for metastatic brain tumors: report of three cases and review of literature, Acta Neurochir. 154 (9) (2012) 1685–1690.
[12] Z. Li, W. Ran, Y. Yan, L. Li, Z. Lou, G. Shen, High-performance optical noncontact controlling system based on broadband PtTex/Si heterojunction photodetectors for human–machine interaction, InfoMat 4 (1) (2022), e12261.
[13] B. Zhong, K. Jiang, L. Wang, G. Shen, Wearable sweat loss measuring devices: from the role of sweat loss to advanced mechanisms and designs, Adv. Sci. 9 (1) (2022), 2103257.
[14] Y. Zheng, Y. Wang, Z. Li, Z. Yuan, S. Guo, Z. Lou, W. Han, G. Shen, L. Wang, MXene quantum dots/perovskite heterostructure enabling highly specific ultraviolet detection for skin prevention, Matter 6 (2) (2023) 506–520.
[15] H.C. Koydemir, Ozcan, A. J. A. R. o. A. C., Wearable and implantable sensors for biomedical applications 11 (2018) 127–146.
[16] S.H. Sunwoo, K.H. Ha, S. Lee, N. Lu, D.H. Kim, Wearable and implantable soft bioelectronics: device designs and material strategies, in: M.F. Doherty, R. A. Segalman (Eds.), Annual Review of Chemical and Biomolecular Engineering, Vol 12, vol. 12, 2021, pp. 359–391, 2021.
[17] L. Wang, X. Fu, J. He, X. Shi, T. Chen, P. Chen, B. Wang, H. Peng, Application challenges in fiber and textile electronics, Adv. Mater. 32 (5) (2020), 1901971.
[18] C. Legner, U. Kalwa, V. Patel, A. Chesmore, S. Pandey, Sweat sensing in the smart wearables era: towards integrative, multifunctional and body-compliant perspiration analysis, Sensor Actuator Phys. 296 (2019) 200–221.
[19] C. Drees, M.B. Makic, K. Case, M.P. Mancuso, A. Hill, P. Walczak, S. Limon, K. Biesecker, L. Frey, Skin irritation during video-EEG monitoring, Neurodiagn. J. 56 (3) (2016) 139–150.
[20] A. Lau-Zhu, M.P. Lau, G. McLoughlin, Mobile EEG in research on neurodevelopmental disorders: opportunities and challenges, Dev. Cognit. Neurosci. 36 (2019), 100635.
[21] M.R. Abidian, D.C. Martin, Experimental and theoretical characterization of implantable neural microelectrodes modified with conducting polymer nanotubes, Biomaterials 29 (9) (2008) 1273–1283.
[22] S.M. Wellman, T.D. Kozai, Understanding the inflammatory tissue reaction to brain implants to improve neurochemical sensing performance, ACS Publ., ACS chem. Neurosci. 8 (2017) 2578–2582.
[23] S.M. Lee, J.H. Kim, C. Park, J.-Y. Hwang, J.S. Hong, K.H. Lee, S.H. Lee, Self-adhesive and capacitive carbon nanotube-based electrode to record electroencephalograph signals from the hairy scalp, Ieee T. Bio-Med. Eng. 63 (1) (2015) 138–147.
[24] Y. Zou, O. Dehzangi, V. Nathan, R. Jafari, Automatic removal of EEG artifacts using electrode-scalp impedance, in: IEEE International Conference on Acoustics, Speech and Signal Processing (ICASSP), IEEE, 2014, pp. 2054–2058, 2014.
[25] S.R. Bhattarai, N. Bhattarai, P. Viswanathamurthi, H.K. Yi, P.H. Hwang, H.Y. Kim, Hydrophilic nanofibrous structure of polylactide; fabrication and cell affinity, J. Biomed. Mater. Res. Part A: An Official Journal of The Society for Biomaterials, The Japanese Society for Biomaterials, and The Australian Society for Biomaterials and the Korean Society for Biomaterials 78 (2) (2006) 247–257.
[26] R.J. Soto, J.R. Hall, M.D. Brown, J.B. Taylor, M.H. Schoenfisch, In vivo chemical sensors: role of biocompatibility on performance and utility, Anal. Chem. 89 (1) (2017) 276–299.
[27] Z. Lv, Y. Li, Wearable sensors for vital signs measurement: a survey, J. Sens. Actuator Netw. 11 (1) (2022) 19.
[28] Y.J. Hong, H. Jeong, K.W. Cho, N. Lu, D.H. Kim, Wearable and implantable devices for cardiovascular healthcare: from monitoring to therapy based on flexible and stretchable electronics, Adv. Funct. Mater. 29 (19) (2019), 1808247.
[29] O. Bettucci, G.M. Matrone, F. Santoro, Conductive polymer-based bioelectronic platforms toward sustainable and biointegrated devices: a journey from skin to brain across human body interfaces, Adv. Mater. Technol. 7 (2) (2022), 2100293.
[30] X. Xia, Q. Liu, Y. Zhu, Y. Zi, Recent advances of triboelectric nanogenerator based applications in biomedical systems, EcoMat. 2 (4) (2020), e12049.
[31] R.F. Li, H. Qi, Y. Ma, Y.P. Deng, S.N. Liu, Y.S. Jie, J.Z. Jing, J.L. He, X. Zhang, L. Wheatley, C.X. Huang, X. Sheng, M.L. Zhang, L. Yin, A flexible and physically transient electrochemical sensor for real-time wireless nitric oxide monitoring, Nat. Commun. 11 (1) (2020) 3207.
[32] H. Xu, J. Liu, J. Zhang, G. Zhou, N. Luo, N. Zhao, Flexible organic/inorganic hybrid near-infrared photoplethysmogram sensor for cardiovascular monitoring, Adv. Mater. 29 (31) (2017), 1700975.
[33] M. Asif, A. Aziz, G. Ashraf, T. Iftikhar, Y. Sun, F. Xiao, H. Liu, Unveiling microbiologically influenced corrosion engineering to transfigure damages into benefits: a textile sensor for H2O2 detection in clinical cancer tissues, Chem. Eng. J. 427 (2022), 131398.
[34] R. Herbert, S. Mishra, H.R. Lim, H. Yoo, W.H. Yeo, Fully printed, wireless, stretchable implantable biosystem toward batteryless, real-time monitoring of cerebral aneurysm hemodynamics, Adv. Sci. 6 (18) (2019).
[35] Y. Liu, M. Pharr, G.A. Salvatore, Lab-on-skin: a review of flexible and stretchable electronics for wearable health monitoring, ACS Nano 11 (10) (2017) 9614–9635.
[36] A. Servati, L. Zou, Z.J. Wang, F. Ko, P. Servati, Novel flexible wearable sensor materials and signal processing for vital sign and human activity monitoring, Sensors 17 (7) (2017).
[37] Y. Wu, G. Alici, J.D. Madden, G.M. Spinks, G.G. Wallace, Soft mechanical sensors through reverse actuation in polypyrrole, Adv. Funct. Mater. 17 (16) (2007) 3216–3222.
[38] S. Wang, J.Y. Oh, J. Xu, H. Tran, Z. Bao, Skin-inspired electronics: an emerging paradigm, Acc. Chem. Res. 51 (5) (2018) 1033–1045.
[39] W. Gao, H. Ota, D. Kiriya, K. Takei, A. Javey, Flexible electronics toward wearable sensing, Acc. Chem. Res. 52 (3) (2019) 523–533.
[40] Y. Khan, A.E. Ostfeld, C.M. Lochner, A. Pierre, A.C. Arias, Monitoring of vital signs with flexible and wearable medical devices, Adv. Mater. 28 (22) (2016) 4373–4395.
[41] M. Teodorescu, H.-N. Teodorescu, In *Capacitive Interdigital Sensors for Flexible Enclosures and Wearables*, 2020 International Conference on Applied Electronics (AE), IEEE, 2020, pp. 1–6.
[42] Y. Liu, H. Wang, W. Zhao, M. Zhang, H.B. Qin, Y.Q. Xie, Flexible, stretchable sensors for wearable health monitoring: sensing mechanisms, materials, fabrication strategies and features, Sensors 18 (2) (2018).
[43] Q. Yan, L. Gao, J. Tang, H. Liu, Flexible and stretchable photodetectors and gas sensors for wearable healthcare based on solution-processable metal chalcogenides, J. Semiconduct. 40 (11) (2019), 111604.
[44] W. Jin-Fen, T. Hui-Hui, F. Ying, Implantable and flexible electronics for in vivo brain activity recordings, Chin. J. Anal. Chem. 47 (10) (2019) 1549–1558.
[45] H. Li, J. Wang, Y. Fang, Bioinspired flexible electronics for seamless neural interfacing and chronic recording, Nanoscale Adv. 2 (8) (2020) 3095–3102.

[46] Q. Zheng, Q.Z. Tang, Z.L. Wang, Z. Li, Self-powered cardiovascular electronic devices and systems, Nat. Rev. Cardiol. 18 (1) (2021) 7–21.
[47] Y. Cho, S. Park, J. Lee, K.J. Yu, Emerging materials and technologies with applications in flexible neural implants: a comprehensive review of current issues with neural devices, Adv. Mater. 33 (47) (2021), 2005786.
[48] S. Gupta, A. Sharma, R.S. Verma, Polymers in biosensor devices for cardiovascular applications, Curr. Opini. Biomed. Eng. 13 (2020) 69–75.
[49] N. Jiang, S. Flyax, W. Kurz, M. Jakobi, S. Tasoglu, A.W. Koch, A.K. Yetisen, Intracranial sensors for continuous monitoring of Neurophysiology, Adv. Mater. Technol. 6 (12) (2021).
[50] V. Quaresima, M. Ferrari, In A Mini-Review on Functional Near-Infrared Spectroscopy (fNIRS): where Do We Stand, and where Should We Go? Photonics, MDPI, 2019, p. 87.
[51] Wang, J. J. E. A. I. J. D. t. F., P.A.o. Electroanalysis, Glucose Biosens.: 40 years of advances and challenges 13 (12) (2001) 983–988.
[52] A. Yan, L. Lin, C. Liu, J. Shi, S. Na, L.V. Wang, Microwave-induced thermoacoustic tomography through an adult human skull, Med. Phys. 46 (4) (2019) 1793–1797.
[53] Y. Fu, J. Zhao, Y. Dong, X. Wang, Dry electrodes for human bioelectrical signal monitoring, Sensors 20 (13) (2020) 3651.
[54] X. Liu, H. Wang, Z. Li, L.J.K.-B.S. Qin, Deep learning in ECG diagnosis: A review 227 (2021), 107187.
[55] A. Stojanova, S. Koceski, N. Koceska, Continuous blood pressure monitoring as a basis for ambient assisted living (AAL) - review of methodologies and devices, J. Med. Syst. 43 (2) (2019).
[56] Klabunde, R. E. J. A. i. p. e., Cardiac electrophysiology: normal and ischemic ionic currents and the ECG 41 (1) (2017) 29–37.
[57] S. Ramasamy, A. Balan, Wearable sensors for ECG measurement: a review, Sens. Rev. 38 (4) (2018) 412–419.
[58] S.K. Padala, J.A. Cabrera, K.A.J.P. Ellenbogen, C. Electrophysiology, Anatomy of the cardiac conduction system 44 (1) (2021) 15–25.
[59] K.J.H.E.J. Khunti, Accurate interpretation of the 12-lead ECG electrode placement, A Syst. Rev. 73 (5) (2014) 610–623.
[60] M. Zulqarnain, S. Stanzione, G. Rathinavel, S. Smout, M. Willegems, K. Myny, E. Cantatore, A flexible ECG patch compatible with NFC RF communication, npj Flexible Electronics 4 (1) (2020) 1–8.
[61] M. Merone, P. Soda, M. Sansone, Sansone, C. J. E. S. w. A., ECG databases for biometric systems, A Syst. Rev. 67 (2017) 189–202.
[62] R. Oostenveld, P. Praamstra, The five percent electrode system for high-resolution EEG and ERP measurements, Clin. Neurophysiol. 112 (4) (2001) 713–719.
[63] T. Tamura, Y. Maeda, M. Sekine, M.J.E. Yoshida, Wearable photoplethysmographic sensors—past and present 3 (2) (2014) 282–302.
[64] G.S. Ryu, J. You, V. Kostianovskii, E.B. Lee, Y. Kim, C. Park, Y.Y. Noh, Flexible and printed PPG sensors for estimation of drowsiness, IEEE Trans. Electron. Dev. 65 (7) (2018) 2997–3004.
[65] T. Thompson, T. Steffert, T. Ros, J. Leach, J.J.M. Gruzelier, EEG applications for sport and performance 45 (4) (2008) 279–288.
[66] U.R. Acharya, S.V. Sree, G. Swapna, R.J. Martis, Suri, J. S. J. K.-B. S., Automated EEG analysis of epilepsy: Review 45 (2013) 147–165.
[67] M. Seeck, L. Koessler, T. Bast, F. Leijten, C. Michel, C. Baumgartner, B. He, S.J. C. n. Beniczky, The standardized EEG electrode array of the IFCN 128 (10) (2017) 2070–2077.
[68] J.N. Acharya, A. Hani, J. Cheek, P. Thirumala, T.N. Tsuchida, American clinical Neurophysiology society guideline 2: guidelines for standard electrode position nomenclature, J. Clin. Neurophysiol. 33 (4) (2016) 308–311.
[69] M. Abo-Zahhad, S.M. Ahmed, S.N. Abbas, State-of-the-art methods and future perspectives for personal recognition based on electroencephalogram signals, IET Biom. 4 (3) (2015) 179–190.
[70] J.h. Li, J.h. Chen, F. Xu, Sensitive and wearable optical microfiber sensor for human health monitoring, Adv. Mater. Technol. 3 (12) (2018), 1800296.
[71] P.D. Mannheimer, The light–tissue interaction of pulse oximetry, Anesth. Analg. 105 (6) (2007) S10–S17.
[72] T. Tamura, Current progress of photoplethysmography and SPO2 for health monitoring, Biomed. Eng. Lett. 9 (1) (2019) 21–36.
[73] P.C.Y. Chow, T. Someya, Organic photodetectors for next-generation wearable electronics, Adv. Mater. 32 (15) (2020).
[74] G. Turri, V. Sudesh, M. Richardson, M. Bass, A. Toncelli, Tonelli, M. J. J. o. A. P., Temperature-dependent spectroscopic properties of Tm 3+ in germanate, silica, and phosphate glasses, A comparative study 103 (9) (2008), 093104.
[75] J. Brubach, J.P. Feist, A. Dreizler, Characterization of manganese-activated magnesium fluorogermanate with regards to thermographic phosphor thermometry, Meas. Sci. Technol. 19 (2) (2008).
[76] Y. Zhao, X.-g. Hu, S. Hu, Y. Peng, Applications of fiber-optic biochemical sensor in microfluidic chips: a review, Biosens. Bioelectron. 166 (2020), 112447.
[77] B.-y. Wang, L. Cai, Y. Zhao, An optical fiber sensor for the simultaneous measurement of pressure and position based on a pair of fiber Bragg gratings, Opt. Fiber Technol. 67 (2021), 102742.
[78] L. Carlson, Fluorescence Detector, and a Device for Supporting a Replacable Sample Cuvette in a Fluorescence Detector, Google Patents, 1997.
[79] T. Myllylä, A. Popov, V. Korhonen, A. Bykov, M. Kinnunen, In *Optical Sensing of a Pulsating Liquid in a Brain-Mimicking Phantom*, European Conference on Biomedical Optics, Optica Publishing Group, 2013, p. 87990X.
[80] R.B. Chavan, N. Bhargavi, A. Lodagekar, Shastri, N. R. J. D. D. T., Near infra red spectroscopy, A tool for solid state characterization 22 (12) (2017) 1835–1843.
[81] P.M. Arenth, J.H. Ricker, M.T. Schultheis, Applications of Functional Near-Infrared Spectroscopy (fNIRS) to neurorehabilitation of cognitive disabilities, Clin. Neuropsychol. 21 (1) (2007) 38–57.
[82] J.M. Murkin, M. Arango, Near-infrared spectroscopy as an index of brain and tissue oxygenation, Br. J. Anaesth. 103 (suppl_1) (2009) i3–i13.
[83] W.-L. Chen, J. Wagner, N. Heugel, J. Sugar, Y.-W. Lee, L. Conant, M. Malloy, J. Heffernan, B. Quirk, A.J. F.i. n. Zinos, Functional near-infrared spectroscopy and its clinical application in the field of neuroscience: advances and future directions 14 (2020) 724.
[84] M. Amjadi, K.U. Kyung, I. Park, M. Sitti, Stretchable, skin-mountable, and wearable strain sensors and their potential applications: a review, Adv. Funct. Mater. 26 (11) (2016) 1678–1698.
[85] W.R. Chen, Y.X. Zhang, W.G. Zhang, Q. Chen, Y.X. Zhang, M.X. Li, W. Zhao, Y. S. Zhang, T.Y. Yan, High-sensitive tilt sensor based on macro-bending loss of single mode fiber, Opt. Fiber Technol. 50 (2019) 1–7.
[86] A. Taebi, B.E. Solar, A.J. Bomar, R.H. Sandler, H.A. Mansy, Recent advances in seismocardiography, Vibrations 2 (1) (2019) 64–86.
[87] E. Vogt, D. MacQuarrie, J.P. Neary, Using ballistocardiography to measure cardiac performance: a brief review of its history and future significance, Clin. Physiol. Funct. Imag. 32 (6) (2012) 415–420.
[88] X.W. Wang, Z. Liu, T. Zhang, Flexible sensing electronics for wearable/attachable health monitoring, Small 13 (25) (2017).
[89] W.Z. Wu, X.N. Wen, Z.L. Wang, Taxel-addressable matrix of vertical-nanowire piezotronic transistors for active and adaptive tactile imaging, Science 340 (6135) (2013) 952–957.
[90] C. Pang, G.Y. Lee, T.I. Kim, S.M. Kim, H.N. Kim, S.H. Ahn, K.Y. Suh, A flexible and highly sensitive strain-gauge sensor using reversible interlocking of nanofibres, Nat. Mater. 11 (9) (2012) 795–801.
[91] S. Gong, W. Schwalb, Y. Wang, Y. Chen, Y. Tang, J. Si, B. Shirinzadeh, W. Cheng, A wearable and highly sensitive pressure sensor with ultrathin gold nanowires, Nat. Commun. 5 (1) (2014) 1–8.
[92] Z.L. Wang, On Maxwell's displacement current for energy and sensors: the origin of nanogenerators, Mater. Today 20 (2) (2017) 74–82.
[93] X.J. Pu, S.S. An, Q. Tang, H.Y. Guo, C.G. Hu, Wearable triboelectric sensors for biomedical monitoring and human-machine interface, iScience 24 (1) (2021), 102027.
[94] A. Fiorillo, C. Critello, S.J.S. Pullano, A.A. Physical, Theory, technology and applications of piezoresistive sensors, A review 281 (2018) 156–175.
[95] Y. Zhao, Y. Liu, Y. Li, Q.J.S. Hao, Development and application of resistance strain force sensors 20 (20) (2020) 5826.
[96] J.B. Chossat, Y.L. Park, R.J. Wood, V. Duchaine, A soft strain sensor based on ionic and metal liquids, Ieee Sens. J. 13 (9) (2013) 3405–3414.
[97] D.C. Kim, H.J. Shim, W. Lee, J.H. Koo, D.H. Kim, Material-based approaches for the fabrication of stretchable electronics, Adv. Mater. 32 (15) (2020), 1902743.
[98] B. Bera, Literature review on triboelectric nanogenerator, Imp. J. Interdiscip. Res. 2 (10) (2016) 1263–1271.
[99] Z.L. Wang, Triboelectric nanogenerators as new energy technology for self-powered systems and as active mechanical and chemical sensors, ACS Nano 7 (11) (2013) 9533–9557.
[100] M. Ramuz, B.C.K. Tee, J.B.H. Tok, Z. Bao, Transparent, optical, pressure-sensitive artificial skin for large-area stretchable electronics, Adv. Mater. 24 (24) (2012) 3223–3227.
[101] Z.L. Wang, Triboelectric nanogenerator (TENG)-Sparking an energy and sensor revolution, Adv. Energy Mater. 10 (17) (2020).
[102] Y. Yang, H.L. Zhang, Z.H. Lin, Y.S. Zhou, Q.S. Jing, Y.J. Su, J. Yang, J. Chen, C. G. Hu, Z.L. Wang, Human skin based triboelectric nanogenerators for harvesting biomechanical energy and as self-powered active tactile sensor system, ACS Nano 7 (10) (2013) 9213–9222.
[103] X. Wang, X. Chen, Novel Nanomaterials for Biomedical, Environmental and Energy Applications, Elsevier, 2018.
[104] Y. Picó, Chemical Analysis of Food: Techniques and Applications, Academic Press, 2012.
[105] J.P. Hart, S.A. Wring, Screen-printed voltammetric and amperometric electrochemical sensors for decentralized testing, Electroanalysis 6 (8) (1994) 617–624.
[106] L. Qlark Jr., Monitor and control of blood and tissue oxygen tensions, Am. Soc. Artif. Intern. Organs J. 2 (1) (1956) 41–48.
[107] L.C. Clark Jr., Lyons, C. J. A. o. t. N. Y. A. o. s., Electrode systems for continuous monitoring in cardiovascular surgery 102 (1) (1962) 29–45.
[108] L. Tang, S.J. Chang, C.J. Chen, J.T. Liu, Non-invasive blood glucose monitoring technology: a review, Sensors 20 (23) (2020).
[109] H. Lee, Y.J. Hong, S. Baik, T. Hyeon, D.H. Kim, Enzyme-based glucose sensor: from invasive to wearable device, Adv. Healthcare Mater. 7 (8) (2018).
[110] C.Y. Li, P.M. Wu, Z.Z. Wu, C.H. Ahn, D. LeDoux, L.A. Shutter, J.A. Hartings, R. K. Narayan, Brain temperature measurement: a study of in vitro accuracy and stability of smart catheter temperature sensors, Biomed. Microdevices 14 (1) (2012) 109–118.
[111] S. Schwab, M. Spranger, A. Aschoff, T. Steiner, W. Hacke, Brain temperature monitoring and modulation in patients with severe MCA infarction, Neurology 48 (3) (1997) 762–767.
[112] I. Marshall, B. Karaszewski, J.M. Wardlaw, V. Cvoro, K. Wartolowska, P. A. Armitage, T. Carpenter, M.E. Bastin, A. Farrall, K. Haga, Measurement of regional brain temperature using proton spectroscopic imaging: validation and application to acute ischemic stroke, Magn. Reson. Imaging 24 (6) (2006) 699–706.

[113] C. Krafft, M. Kirsch, C. Beleites, G. Schackert, R. Salzer, Methodology for fiber-optic Raman mapping and FTIR imaging of metastases in mouse brains, Anal. Bioanal. Chem. 389 (4) (2007) 1133–1142.
[114] C. Stewart, I. Haitsma, Z. Zador, J.C. Hemphill, D. Morabito, G. Manley, G. Rosenthal, The new licox combined brain tissue oxygen and brain temperature monitor: assessment OF IN vitro accuracy and clinical experience in severe traumatic brain injury, Neurosurgery 63 (6) (2008) 1159–1164.
[115] M. Hrovat, D. Belavič, J. Kita, J. Holc, S. Drnovšek, J. Cilenšek, L. Golonka, A. Dziedzic, Thick-film strain and temperature sensors on LTCC substrates, Microelectron. Int. 23 (3) (2006) 33–41.
[116] Z.Z. Wu, C.Y. Li, J. Hartings, S. Ghosh, R. Narayan, C. Ahn, Polysilicon-based flexible temperature sensor for brain monitoring with high spatial resolution, J. Micromech. Microeng. 27 (2) (2017).
[117] C.-C. Huang, Z.-K. Kao, Y.-C. Liao, Flexible miniaturized nickel oxide thermistor arrays via inkjet printing technology, ACS Appl. Mater. Interfaces 5 (24) (2013) 12954–12959.
[118] T.W. Cheung, T. Liu, M.Y. Yao, Y. Tao, H. Lin, L.J.T.R.J. Li, Structural development of a flexible textile-based thermocouple temperature sensor 92 (9–10) (2022) 1682–1693.
[119] Q.N. Xue, Z.Y. Li, Q.K. Wang, W.W. Pan, Y. Chang, X.X. Duan, Nanostrip flexible microwave enzymatic biosensor for noninvasive epidermal glucose sensing, Nanoscale Horiz 5 (6) (2020) 934–943.
[120] J.B. Chen, G. Li, M.S. Chen, G. Jin, S.L. Zhao, Z.L. Bai, J. Yang, H.Y. Liang, J. Xu, J. Sun, M.X. Qin, A noninvasive flexible conformal sensor for accurate real-time monitoring of local cerebral edema based on electromagnetic induction, PeerJ 8 (2020), e10079.
[121] Carter, L. P. J. N. c. o. N. A., Thermal diffusion flowmetry 7 (4) (1996) 749–754.
[122] A.W. Vanherwaarden, P.M. Sarro, Thermal sensors based on the seebeck effect, Sensor. Actuator. 10 (3–4) (1986) 321–346.
[123] Q. Zhou, S. Lau, D. Wu, Shung, K. K. J. P. i. m. s., Piezoelectric films for high frequency ultrasonic transducers in biomedical applications 56 (2) (2011) 139–174.
[124] W. Lee, Y.J. B.e. l. Roh, Ultrasonic transducers for medical diagnostic imaging 7 (2) (2017) 91–97.
[125] C.H. Wang, X.S. Li, H.J. Hu, L. Zhang, Z.L. Huang, M.Y. Lin, Z.R. Zhang, Z.N. Yin, B. Huang, H. Gong, S. Bhaskaran, Y. Gu, M. Makihata, Y.X. Guo, Y.S. Lei, Y. M. Chen, C.F. Wang, Y. Li, T.J. Zhang, Z.Y. Chen, A.P. Pisano, L.F. Zhang, Q. F. Zhou, S. Xu, Monitoring of the central blood pressure waveform via a conformal ultrasonic device, Nat. Biomed. Eng. 2 (9) (2018) 687–695.
[126] Jensen, J. A. J. P. i. b., m. biology, Med. Ultrasound Imag. 93 (1–3) (2007) 153–165.
[127] P.M. Nabeel, J. Joseph, S. Karthik, M. Sivaprakasam, M. Chenniappan, Bi-modal arterial compliance probe for calibration-free cuffless blood pressure estimation, Ieee T. Bio-Med. Eng. 65 (11) (2018) 2392–2404.
[128] A. Bhalla, M. Gray, N. Fosko, G. Atlas, In Ultrasonic Sensor to Quantify Brain Pulsatility, IEEE MIT Undergraduate Research Technology Conference (URTC), IEEE, 2017, pp. 1–4, 2017.
[129] A.B.E. Attia, G. Balasundaram, M. Moothanchery, U. Dinish, R. Bi, V. Ntziachristos, M.J.P. Olivo, A review of clinical photoacoustic imaging, Current and future trends 16 (2019), 100144.
[130] F. Cao, Z. Qiu, H. Li, P.J.A.S. Lai, Photoacoustic imaging in oxygen detection 7 (12) (2017) 1262.
[131] C. Li, Wang, L. V. J. P. i. M., Biology, Photoacoustic tomography and sensing in biomedicine 54 (19) (2009) R59.
[132] R. Chandra, H. Zhou, I. Balasingham, R.M. Narayanan, On the opportunities and challenges in microwave medical sensing and imaging 62 (7) (2015) 1667–1682.
[133] A.T. Mobashsher, A.M. Abbosh, Y.F. Wang, Microwave system to detect traumatic brain injuries using compact unidirectional antenna and wideband transceiver with verification on realistic head phantom, Ieee T. Microw. Theory. 62 (9) (2014) 1826–1836.
[134] L. Yao, G. Guo, H.J. M.p. Jiang, Quantitative microwave-induced thermoacoustic tomography 37 (7Part1) (2010) 3752–3759.
[135] J. Gao, Z. Jiang, S. Zhang, Z. Mao, Y. Shen, Z. Chu, In Review of Magnetoelectric Sensors, Actuators, MDPI, 2021, p. 109.
[136] C. Trigona, V. Sinatra, B. Ando, S. Baglio, A.R. Bulsara, G. Mostile, A. Nicoletti, M. Zappia, Measurements of iron compound content in the brain using a flexible core fluxgate magnetometer at room temperature, Ieee T. Instrum. Meas. 67 (4) (2018) 971–980.
[137] V.N. Popov, Carbon nanotubes: properties and application, Mater. Sci. Eng. R Rep. 43 (3) (2004) 61–102.
[138] J.E. Park, H.S. Kang, M. Koo, C. Park, Autonomous surface reconciliation of a liquid-metal conductor micropatterned on a deformable hydrogel, Adv. Mater. 32 (37) (2020), e2002178.
[139] L.J. Chen, G.N. Chen, L.L. Bi, Z.L. Yang, Z. Wu, M.C. Huang, J.S. Bao, W.W. Wang, C. Ye, J. Pan, Y.W. Peng, C.H. Ye, A highly sensitive strain sensor with a sandwich structure composed of two silver nanoparticles layers and one silver nanowires layer for human motion detection, Nanotechnology 32 (37) (2021).
[140] J.C. Wang, R.S. Karmakar, Y.J. Lu, S.H. Chan, M.C. Wu, K.J. Lin, C.K. Chen, K. C. Wei, Y.H. Hsu, Miniaturized flexible piezoresistive pressure sensors: poly(3,4-ethylenedioxythiophene):poly(styrenesulfonate) copolymers blended with graphene oxide for biomedical applications, ACS Appl. Mater. Interfaces 11 (37) (2019) 34305–34315.
[141] J. Yang, Q. Liu, Z. Deng, M. Gong, F. Lei, J. Zhang, X. Zhang, Q. Wang, Y. Liu, Z. Wu, Ionic liquid–activated wearable electronics, Materials Today Physics 8 (2019) 78–85.
[142] S.T. Han, H.Y. Peng, Q.J. Sun, S. Venkatesh, K.S. Chung, S.C. Lau, Y. Zhou, V.A. L. Roy, An overview of the development of flexible sensors, Adv. Mater. 29 (33) (2017).
[143] R.Z. Zhang, A. Palumbo, G. Hader, K. Yan, J. Chang, H.J. Wang, E.H. Yang, A flexible pressure sensor with sandwiched carpets of vertically aligned carbon nanotubes partially embedded in polydimethylsiloxane substrates, Ieee Sens. J. 20 (20) (2020) 12146–12153.
[144] X. Zhou, Y.N. Zhang, J. Yang, J.L. Li, S. Luo, D.P. Wei, Flexible and highly sensitive pressure sensors based on microstructured carbon nanowalls electrodes, Nanomaterials 9 (4) (2019).
[145] M.A. Jamlos, A.H. Ismail, Ieee in *graphene-based magnetite polydimethylsiloxane (PDMS) Sensor for human brain microwave imaging*, in: IEEE International RF and Microwave Conference (RFM), Kuching, MALAYSIA, Kuching, MALAYSIA, 2015, pp. 248–251. Dec 14-16.
[146] H. Ouyang, J. Tian, G. Sun, Y. Zou, Z. Liu, H. Li, L. Zhao, B. Shi, Y. Fan, Y.J.A. M. Fan, Self-powered pulse sensor for antidiastole of cardiovascular disease 29 (40) (2017), 1703456.
[147] A. Koh, D. Kang, Y. Xue, S. Lee, R.M. Pielak, J. Kim, T. Hwang, S. Min, A. Banks, P. Bastien, A soft, wearable microfluidic device for the capture, storage, and colorimetric sensing of sweat, Sci. Transl. Med. 8 (366) (2016), 366ra165-366ra165.
[148] S. Palit, K. Singh, B.S. Lou, J.L. Her, S.T. Pang, T.M. Pan, Ultrasensitive dopamine detection of indium-zinc oxide on PET flexible based extended-gate field-effect transistor, Sensor. Actuator. B Chem. (2020) 310.
[149] W. Gao, S. Emaminejad, H.Y.Y. Nyein, S. Challa, K.V. Chen, A. Peck, H.M. Fahad, H. Ota, H. Shiraki, D. Kiriya, D.H. Lien, G.A. Brooks, R.W. Davis, A. Javey, Fully integrated wearable sensor arrays for multiplexed in situ perspiration analysis, Nature 529 (7587) (2016) 509–+.
[150] Y.H. Kwak, W. Kim, K.B. Park, K. Kim, S. Seo, Flexible heartbeat sensor for wearable device, Biosens. Bioelectron. 94 (2017) 250–255.
[151] M.W. Billard, H.A. Basantani, M.W. Horn, B.J. Gluckman, A flexible vanadium oxide thermistor array for localized temperature field measurements in brain, Ieee Sens. J. 16 (8) (2016) 2211–2212.
[152] P. Gutruf, R.T. Yin, K.B. Lee, J. Ausra, J.A. Brennan, Y. Qiao, Z. Xie, R. Peralta, O. Talarico, A. Murillo, Wireless, battery-free, fully implantable multimodal and multisite pacemakers for applications in small animal models, Nat. Commun. 10 (1) (2019) 1–10.
[153] G. Schwartz, B.C.-K. Tee, J. Mei, A.L. Appleton, D.H. Kim, H. Wang, Z.J. N.c. Bao, Flexible polymer transistors with high pressure sensitivity for application in electronic skin and health monitoring 4 (1) (2013) 1–8.
[154] D. Lo Presti, C. Romano, C. Massaroni, J. D'Abbraccio, L. Massari, M.A. Caponero, C.M. Oddo, D. Formica, E. Schena, Cardio-respiratory monitoring in archery using a smart textile based on flexible fiber Bragg grating sensors, Sensors 19 (16) (2019).
[155] L. Gao, C.X. Zhu, L. Li, C.W. Zhang, J.H. Liu, H.D. Yu, W. Huang, All paper-based flexible and wearable piezoresistive pressure sensor, ACS Appl. Mater. Interfaces 11 (28) (2019) 25034–25042.
[156] P.S. Das, S.H. Park, K.Y. Baik, J.W. Lee, J.Y. Park, Thermally reduced graphene oxide-nylon membrane based epidermal sensor using vacuum filtration for wearable electrophysiological signals and human motion monitoring, Carbon 158 (2020) 386–393.
[157] Y.N. Zhao, L. Liu, Z. Li, F.F. Wang, X.X. Chen, J.K. Liu, C.H. Song, J.M. Yao, Facile fabrication of highly sensitive and durable cotton fabric-based pressure sensors for motion and pulse monitoring, J. Mater. Chem. C 9 (37) (2021) 12605–12614.
[158] C. Peng, M.Y. Chen, H.K. Sim, Y. Zhu, X.N. Jiang, Ieee in *A flexible piezo-composite ultrasound blood pressure Sensor with silver nanowire-based stretchable electrodes*, in: IEEE 15th International Conference on Nano/Micro Engineered and Molecular System (NEMS), Electr Network, 2020, pp. 143–146. Electr Network, Sepp. 27–30.
[159] M. Ion, S. Dinulescu, B. Firtat, M. Savin, O.N. Ionescu, C. Moldovan, Design and fabrication of a new wearable pressure sensor for blood pressure monitoring, Sensors 21 (6) (2021).
[160] F. Criscuolo, F. Cantu, I. Taurino, S. Carrara, G. De Micheli, Ieee in *Flexible Sweat Sensors for Non-invasive Optimization of Lithium Dose in Psychiatric Disorders*, 18th IEEE Sensors Conference, CANADA, Montreal, CANADA, Oct 27-30.
[161] Q. Wu, Y.C. Qiao, R. Guo, S. Naveed, T. Hirtz, X.S. Li, Y.X. Fu, Y.H. Wei, G. Deng, Y. Yang, X.M. Wu, T.L. Ren, Triode-mimicking graphene pressure sensor with positive resistance variation for physiology and motion monitoring, ACS Nano 14 (8) (2020) 10104–10114.
[162] H. Lee, T.K. Choi, Y.B. Lee, H.R. Cho, R. Ghaffari, L. Wang, H.J. Choi, T.D. Chung, N. Lu, T. Hyeon, A graphene-based electrochemical device with thermoresponsive microneedles for diabetes monitoring and therapy, Nat. Nanotechnol. 11 (6) (2016) 566–572.
[163] P.F. Zhao, R.M. Zhang, Y.H. Tong, X.L. Zhao, Q.X. Tang, Y.C. Liu, All-paper, all-organic, cuttable, and foldable pressure sensor with tuneable conductivity polypyrrole, Adv. Electron. Mater. 6 (8) (2020).
[164] S.H. Ko, S.W. Kim, Y.J. Lee, Flexible sensor with electrophoretic polymerized graphene oxide/PEDOT:PSS composite for voltammetric determination of dopamine concentration, Sci. Rep. 11 (1) (2021).
[165] L.-W. Lo, J. Zhao, H. Wan, Y. Wang, S. Chakrabartty, C. Wang, An inkjet-printed PEDOT: PSS-based stretchable conductor for wearable health monitoring device applications, ACS Appl. Mater. Interfaces 13 (18) (2021) 21693–21702.
[166] L. Zhou, H.F. Hou, H. Wei, L.N. Yao, L. Sun, P. Yu, B. Su, L.Q. Mao, In vivo monitoring of oxygen in rat brain by carbon fiber microelectrode modified with antifouling nanoporous membrane, Anal. Chem. 91 (5) (2019) 3645–3651.

[167] W.Z. He, R.T. Liu, P. Zhou, Q.Y. Liu, T.H. Cui, Flexible micro-sensors with self-assembled graphene on a polyolefin substrate for dopamine detection, Biosens. Bioelectron. 167 (2020), 112473.
[168] I.A.D. Andreotti, L.O. Orzari, J.R. Camargo, R.C. Faria, L.H. Marcolino, M. F. Bergarnini, A. Gatti, B.C. Janegitz, Disposable and flexible electrochemical sensor made by recyclable material and low cost conductive ink, J. Electroanal. Chem. 840 (2019) 109–116.
[169] D. Sangamithirai, S. Munusamy, V. Narayanan, A. Stephen, Fabrication of neurotransmitter dopamine electrochemical sensor based on poly(o-anisidine)/CNTs nanocomposite, Surface. Interfac. 4 (2016) 27–34.
[170] W. Dou, M. Malhi, T. Cui, M. Wang, T. Wang, G. Shan, J. Law, Z. Gong, J. Plakhotnik, T. Filleter, A carbon-based biosensing platform for simultaneously measuring the contraction and electrophysiology of iPSC-cardiomyocyte monolayers, ACS Nano 16 (7) (2022) 11278–11290.
[171] Y.J. Hong, H. Lee, J. Kim, M. Lee, H.J. Choi, T. Hyeon, D.H. Kim, Multifunctional wearable system that integrates sweat-based sensing and vital-sign monitoring to estimate pre-/post-exercise glucose levels, Adv. Funct. Mater. 28 (47) (2018), 1805754.
[172] S.Y. Hong, J.H. Oh, H. Park, J.Y. Yun, S.W. Jin, L. Sun, G. Zi, J.S. Ha, Polyurethane foam coated with a multi-walled carbon nanotube/polyaniline nanocomposite for a skin-like stretchable array of multi-functional sensors, NPG Asia Mater. 9 (2017).
[173] W. Li, J. Guo, D. Fan, 3D graphite–polymer flexible strain sensors with Ultrasensitivity and durability for real-time human vital sign monitoring and musical instrument education, Adv. Mater. Technol. 2 (6) (2017), 1700070.
[174] H. Lee, E. Kim, Y. Lee, H. Kim, J. Lee, M. Kim, H.-J. Yoo, S. Yoo, Toward all-day wearable health monitoring: an ultralow-power, reflective organic pulse oximetry sensing patch, Sci. Adv. 4 (11) (2018) eaas9530.
[175] K.H. Ha, W. Zhang, H. Jang, S. Kang, L. Wang, P. Tan, H. Hwang, N. Lu, Highly sensitive capacitive pressure sensors over a wide pressure range enabled by the hybrid responses of a highly porous nanocomposite, Adv. Mater. 33 (48) (2021), 2103320.
[176] F. Zhang, K. Yang, Z. Pei, Y.G. Wu, S.B. Sang, Q. Zhang, H.M. Jiao, A highly accurate flexible sensor system for human blood pressure and heart rate monitoring based on graphene/sponge, RSC Adv. 12 (4) (2022) 2391–2398.
[177] J.H. Oh, J.Y. Woo, S. Jo, C.S. Han, Pressure-conductive rubber sensor based on liquid-metal-PDMS composite, Sensor Actuator Phys. 299 (2019).
[178] M.H. Cao, M.Q. Wang, L. Li, H.W. Qiu, M.A. Padhiar, Z. Yang, Wearable rGO-Ag NW@cotton fiber piezoresistive sensor based on the fast charge transport channel provided by Ag nanowire, Nano Energy 50 (2018) 528–535.
[179] S. Choi, S.I. Han, D. Jung, H.J. Hwang, C. Lim, S. Bae, O.K. Park, C. M. Tschabrunn, M. Lee, S.Y. Bae, Highly conductive, stretchable and biocompatible Ag–Au core–sheath nanowire composite for wearable and implantable bioelectronics, Nat. Nanotechnol. 13 (11) (2018) 1048–1056.
[180] Y. Khan, M. Garg, Q. Gui, M. Schadt, A. Gaikwad, D. Han, N.A. Yamamoto, P. Hart, R. Welte, W. Wilson, Flexible hybrid electronics: direct interfacing of soft and hard electronics for wearable health monitoring, Adv. Funct. Mater. 26 (47) (2016) 8764–8775.
[181] K. Dong, Z. Wu, J. Deng, A.C. Wang, H. Zou, C. Chen, D. Hu, B. Gu, B. Sun, Z. L. Wang, A stretchable yarn embedded triboelectric nanogenerator as electronic skin for biomechanical energy harvesting and multifunctional pressure sensing, Adv. Mater. 30 (43) (2018), 1804944.
[182] A. Fallahi, S. Mandla, T. Kerr-Phillip, J. Seo, R.O. Rodrigues, Y.A. Jodat, R. Samanipour, M.A. Hussain, C.K. Lee, H. Bae, A. Khademhosseini, J. Trayas-Sejdic, S.R. Shin, Flexible and stretchable PEDOT-embedded hybrid substrates for bioengineering and sensory applications, Chemnanomat 5 (6) (2019) 729–737.
[183] M. Ganji, A.T. Elthakeb, A. Tanaka, V. Gilja, E. Halgren, S.A. Dayeh, Scaling effects on the electrochemical performance of poly (3, 4-ethylenedioxythiophene (PEDOT), Au, and Pt for electrocorticography recording, Adv. Funct. Mater. 27 (42) (2017), 1703018.
[184] K.Y. Shin, J.S. Lee, J. Jang, Highly sensitive, wearable and wireless pressure sensor using free-standing ZnO nanoneedle/PVDF hybrid thin film for heart rate monitoring, Nano Energy 22 (2016) 95–104.
[185] K. Takashima, K. Ota, M. Yamamoto, M. Takenaka, S. Horie, K. Ishida, Development of catheter-type tactile sensor composed of polyvinylidene fluoride (PVDF) film, ROBOMECH Journal 6 (1) (2019) 1–11.
[186] A. Economou, C. Kokkinos, M. Prodromidis, Flexible plastic, paper and textile lab-on-a chip platforms for electrochemical biosensing, Lab Chip 18 (13) (2018) 1812–1830.
[187] Y. Qin, M.M. Howlader, M.J. Deen, Y.M. Haddara, P.R. Selvaganapathy, Polymer integration for packaging of implantable sensors, Sensor. Actuator. B Chem. 202 (2014) 758–778.
[188] Y. Cao, K.E. Uhrich, Biodegradable and biocompatible polymers for electronic applications: a review, J. Bioact. Compat Polym. 34 (1) (2019) 3–15.
[189] I. Jeerapan, S. Poorahong, Flexible and stretchable electrochemical sensing systems: materials, energy sources, and integrations, J. Electrochem. Soc. 167 (3) (2020), 037573.
[190] A. Kausar, Corrosion prevention prospects of polymeric nanocomposites: a review, J. Plastic Film Sheeting 35 (2) (2019) 181–202.
[191] K.F. Lei, K.-F. Lee, M.-Y.J.M.E. Lee, Development of a flexible PDMS capacitive pressure sensor for plantar pressure measurement 99 (2012) 1–5.
[192] J.C. McDonald, Whitesides, G. M. J. A. o. c. r., Poly (dimethylsiloxane) as a material for fabricating microfluidic devices 35 (7) (2002) 491–499.
[193] I. Miranda, A. Souza, P. Sousa, J. Ribeiro, E.M. Castanheira, R. Lima, Minas, G. J. J. o. F. B., Properties and applications of PDMS for biomedical engineering, A review 13 (1) (2021) 2.
[194] R.J.P.T. Nisticò, Polyethylene terephthalate (PET) in the packaging industry 90 (2020), 106707.
[195] Y. Wang, X. Wang, W. Lu, Q. Yuan, Y. Zheng, B.J.T. Yao, A thin film polyethylene terephthalate (PET) electrochemical sensor for detection of glucose in sweat 198 (2019) 86–92.
[196] A. Sezer Hicyilmaz, A.J.S.A.S. Celik Bedeloglu, Applications of polyimide coatings: A review 3 (2021) 1–22.
[197] J. Eom, R. Jaisutti, H. Lee, W. Lee, J.S. Heo, J.Y. Lee, S.K. Park, Y.H. Kim, Highly sensitive textile strain sensors and wireless user-interface devices using all-polymeric conducting fibers, ACS Appl. Mater. Interfaces 9 (11) (2017) 10190–10197.
[198] T.B. Jele, P. Lekha, B.J.C. Sithole, Role of cellulose nanofibrils in improving the strength properties of paper, A review (2021) 1–27.
[199] A.K. Das, M.N. Islam, M. Ashaduzzaman, , Nazhad, M. M. J. J. o. P. T., Nanocellulose Research, its applications, consequences and challenges in papermaking 4 (2020) 253–260.
[200] G.N. Islam, A. Ali, S.J.C. Collie, Textile sensors for wearable applications, A comprehensive review 27 (2020) 6103–6131.
[201] C.M. Choi, S.-N. Kwon, Na, S.-I. J. J. o. I., Chemistry, E., Conductive PEDOT: PSS-coated poly-paraphenylene terephthalamide thread for highly durable electronic textiles 50 (2017) 155–161.
[202] Y.J. Gao, L.T. Yu, J.C. Yeo, C.T. Lim, Flexible hybrid sensors for health monitoring: materials and mechanisms to render wearability, Adv. Mater. 32 (15) (2020), e1902133.
[203] M. Gerard, A. Chaubey, B.D. Malhotra, Application of conducting polymers to biosensors, Biosens. Bioelectron. 17 (5) (2002) 345–359.
[204] Y. Wang, A. Liu, Y. Han, T.J.P.I. Li, Sensors based on conductive polymers and their composites, Review 69 (1) (2020) 7–17.
[205] G.B. Tseghai, D.A. Mengistie, B. Malengier, K.A. Fante, L. Van Langenhove, PEDOT:PSS-Based conductive textiles and their applications, Sensors 20 (7) (2020).
[206] F. Xu, Y. Zhu, Highly conductive and stretchable silver nanowire conductors, Adv. Mater. 24 (37) (2012) 5117–5122.
[207] R. Dingle, The electrical conductivity of thin wires, Proc. Roy. Soc. Lond. Math. Phys. Sci. 201 (1067) (1950) 545–560.
[208] G. Pike, C. Seager, Percolation and conductivity: a computer study. I, Phys. Rev. B 10 (4) (1974) 1421.
[209] J. Ouyang, Secondary doping" methods to significantly enhance the conductivity of PEDOT: PSS for its application as transparent electrode of optoelectronic devices, Displays 34 (5) (2013) 423–436.
[210] A. Nag, N. Afasrimanesh, S.L. Feng, S.C. Mukhopadhyay, Strain induced graphite/PDMS sensors for biomedical applications, Sensor Actuator Phys. 271 (2018) 257–269.
[211] S.W. Watts, S.F. Morrison, R.P. Davis, S.M. Barman, Serotonin and blood pressure regulation, Pharmacol. Rev. 64 (2) (2012) 359–388.
[212] K. Hara, Y. Hirowatari, Y. Shimura, H. Takahashi, Serotonin levels in platelet-poor plasma and whole blood in people with type 2 diabetes with chronic kidney disease, Diabetes Res. Clin. Pract. 94 (2) (2011) 167–171.
[213] A. Kereveur, J. Callebert, M. Humbert, P. Herve, G. Simonneau, J.-M. Launay, L. Drouet, High plasma serotonin levels in primary pulmonary hypertension: effect of long-term epoprostenol (prostacyclin) therapy, Arterioscler. Thromb. Vasc. Biol. 20 (10) (2000) 2233–2239.
[214] M.D. Dickey, Stretchable and soft electronics using liquid metals, Adv. Mater. 29 (27) (2017).
[215] D.Y. Park, D.J. Joe, D.H. Kim, H. Park, J.H. Han, C.K. Jeong, H. Park, J.G. Park, B. Joung, K.J. Lee, Self-powered real-time arterial pulse monitoring using ultrathin epidermal piezoelectric sensors, Adv. Mater. 29 (37) (2017), 1702308.
[216] S.F. Zhao, W.H. Ran, D.P. Wang, R.Y. Yin, Y.X. Yan, K. Jiang, Z. Lou, G.Z. Shen, 3D dielectric layer enabled highly sensitive capacitive pressure sensors for wearable electronics, ACS Appl. Mater. Interfaces 12 (28) (2020) 32023–32030.
[217] J.B. Yu, X.J. Hou, J. He, M. Cui, C. Wang, W.P. Geng, J.L. Mu, B. Han, X.J. Chou, Ultra-flexible and high-sensitive triboelectric nanogenerator as electronic skin for self-powered human physiological signal monitoring, Nano Energy 69 (2020).
[218] N. Sinha, J. Ma, , Yeow, J. T. J. J. o. n., nanotechnology, Carbon nanotube-based sensors 6 (3) (2006) 573–590.
[219] M.N. Norizan, M.H. Moklis, S.Z.N. Demon, N.A. Halim, A. Samsuri, I.S. Mohamad, V.F. Knight, N.J. R.a. Abdullah, Carbon nanotubes: Functionalisation and their application in chemical sensors 10 (71) (2020) 43704–43732.
[220] T.P. Huynh, H. Haick, Autonomous flexible sensors for health monitoring, Adv. Mater. 30 (50) (2018).
[221] A.K. Geim, Graphene: status and prospects, Science 324 (5934) (2009) 1530–1534.
[222] Y. Hancock, The 2010 Nobel Prize in physics-ground-breaking experiments on graphene, J. Phys. D Appl. Phys. 44 (47) (2011).
[223] R.S. Edwards, K.S. Coleman, Graphene synthesis: relationship to applications, Nanoscale 5 (1) (2013) 38–51.
[224] J. Lin, Z.W. Peng, Y.Y. Liu, F. Ruiz-Zepeda, R.Q. Ye, E.L.G. Samuel, M.J. Yacaman, B.I. Yakobson, J.M. Tour, Laser-induced porous graphene films from commercial polymers, Nat. Commun. 5 (2014) 5714.
[225] A. Kaidaorva, M. Marengo, G. Marinaro, N. Geraldi, R. Wilson, C.M. Duarte, J. Kosel, Flexible, four-electrode conductivity cell for biologging applications, Results in Materials 1 (2019), 100009.
[226] A. Kaidarova, N. Alsharif, B.N.M. Oliveira, M. Marengo, N.R. Geraldi, C. M. Duarte, J. Kosel, Laser-printed, flexible graphene pressure sensors, Glob. Chall. 4 (4) (2020), 2000001.

[227] S. Yao, P. Swetha, Y.J. A.h. m. Zhu, Nanomaterial-enabled wearable sensors for healthcare 7 (1) (2018), 1700889.
[228] M. Baharfar, K. Kalantar-Zadeh, Emerging role of liquid metals in sensing, ACS Sens. 7 (2) (2022) 386–408.
[229] W. Zhang, Z. Su, X. Zhang, W. Wang, Z.J.V. Li, Recent progress on PEDOT-based wearable bioelectronics 3 (5) (2022), 20220030.
[230] Y. Yang, H.L. Zhang, G. Zhu, S. Lee, Z.H. Lin, Z.L. Wang, Flexible hybrid energy cell for simultaneously harvesting thermal, mechanical, and solar energies, ACS Nano 7 (1) (2013) 785–790.
[231] W.J. Hu, D.M. Juo, L. You, J.L. Wang, Y.C. Chen, Y.H. Chu, T. Wu, Universal ferroelectric switching dynamics of vinylidene fluoride-trifluoroethylene copolymer films, Sci. Rep. 4 (2014) 4772.
[232] X. Zhang, J. Hillenbrand, G.M. Sessler, Ferroelectrets with improved thermal stability made from fused fluorocarbon layers, J. Phys. D Appl. Phys. 101 (5) (2007).
[233] C. Baur, J.R. DiMaio, E. McAllister, R. Hossini, E. Wagener, J. Ballato, S. Priya, A. Ballato, D.W. Smith, Enhanced piezoelectric performance from carbon fluoropolymer nanocomposites, J. Phys. D Appl. Phys. 112 (12) (2012).
[234] L.J. Pan, A. Chortos, G.H. Yu, Y.Q. Wang, S. Isaacson, R. Allen, Y. Shi, R. Dauskardt, Z.N. Bao, An ultra-sensitive resistive pressure sensor based on hollow-sphere microstructure induced elasticity in conducting polymer film, Nat. Commun. 5 (2014) 3002.
[235] D.M. Correia, L.C. Fernandes, M.M. Fernandes, B. Hermenegildo, R.M. Meira, C. Ribeiro, S. Ribeiro, J. Reguera, S. Lanceros-Méndez, Ionic liquid-based materials for biomedical applications, Nanomaterials 11 (9) (2021) 2401.
[236] S.G. Yoon, H.J. Koo, S.T. Chang, Highly stretchable and transparent microfluidic strain sensors for monitoring human body motions, ACS Appl. Mater. Interfaces 7 (49) (2015) 27562–27570.
[237] H. Li, Y. Ma, Y. Huang, Material innovation and mechanics design for substrates and encapsulation of flexible electronics: a review, Mater. Horiz. 8 (2) (2021) 383–400.
[238] D. Yu, Y.-Q. Yang, Z. Chen, Y. Tao, Y.-F. Liu, Recent progress on thin-film encapsulation technologies for organic electronic devices, Opt Commun. 362 (2016) 43–49.
[239] C.-Y. Hong, Y.-F. Zhang, M.-X. Zhang, L.M.G. Leung, L.-Q. Liu, Application of FBG sensors for geotechnical health monitoring, a review of sensor design, implementation methods and packaging techniques, Sensor Actuator Phys. 244 (2016) 184–197.
[240] D.-H. Kim, J.-H. Ahn, W.M. Choi, H.-S. Kim, T.-H. Kim, J. Song, Y.Y. Huang, Z. Liu, C. Lu, J.A. Rogers, Stretchable and foldable silicon integrated circuits, Science 320 (5875) (2008) 507–511.
[241] Z. You, L. Wei, M. Zhang, F. Yang, X. Wang, Hermetic and bioresorbable packaging materials for MEMS implantable pressure sensors: a review, Ieee Sens. J. 22 (24) (2022) 23633–23648.
[242] W. Wu, L. Wang, G. Shen, Flexible photoplethysmographic sensing devices for intelligent medical treatment, J. Mater. Chem. C 11 (1) (2023) 97–112.
[243] M. Sang, K. Kim, J. Shin, K.J. Yu, Ultra-thin flexible encapsulating materials for soft bio-integrated electronics, Adv. Sci. 9 (30) (2022), 2202980.
[244] J.A. Chiong, H. Tran, Y. Lin, Y. Zheng, Z. Bao, Integrating emerging polymer chemistries for the advancement of recyclable, biodegradable, and biocompatible electronics, Adv. Sci. 8 (14) (2021), 2101233.
[245] J. Ouyang, Application of intrinsically conducting polymers in flexible electronics, SmartMat 2 (3) (2021) 263–285.
[246] Y. Wei, X. Shi, Z. Yao, J. Zhi, L. Hu, R. Yan, C. Shi, H.-D. Yu, W. Huang, Fully paper-integrated hydrophobic and air permeable piezoresistive sensors for high-humidity and underwater wearable motion monitoring, npj Flexible Electronics 7 (1) (2023) 13.
[247] G.S. Upadhyaya, Materials science of cemented carbides—an overview, Mater. Des. 22 (6) (2001) 483–489.
[248] J. Yi, Y. Xianyu, Gold nanomaterials-implemented wearable sensors for healthcare applications, Adv. Funct. Mater. 32 (19) (2022), 2113012.
[249] A. Miranda, N. Barekar, B. McKay, MWCNTs and their use in Al-MMCs for ultra-high thermal conductivity applications: a review, J. Alloys Compd. 774 (2019) 820–840.
[250] S. Abdalla, F. Al-Marzouki, A.A. Al-Ghamdi, A. Abdel-Daiem, Different technical applications of carbon nanotubes, Nanoscale Res. Lett. 10 (2015) 1–10.
[251] L. Guo, K. Wan, B. Liu, Y. Wang, G. Wei, Recent advance in the fabrication of carbon nanofiber-based composite materials for wearable devices, Nanotechnology 32 (44) (2021), 442001.
[252] C.W. Tan, K.H. Tan, Y.T. Ong, A.R. Mohamed, S.H.S. Zein, S.H. Tan, Energy and environmental applications of carbon nanotubes, Environ. Chem. Lett. 10 (2012) 265–273.
[253] M. Paradise, T. Goswami, Carbon nanotubes–production and industrial applications, Mater. Des. 28 (5) (2007) 1477–1489.
[254] G. Xiong, C. Meng, R.G. Reifenberger, P.P. Irazoqui, T.S. Fisher, A review of graphene-based electrochemical microsupercapacitors, Electroanalysis 26 (1) (2014) 30–51.
[255] X. Wang, J. Liu, Recent advancements in liquid metal flexible printed electronics: properties, technologies, and applications, Micromachines 7 (12) (2016) 206.
[256] P. Kubisa, Ionic liquids as solvents for polymerization processes—progress and challenges, Prog. Polym. Sci. 34 (12) (2009) 1333–1347.
[257] J.U. Lind, M. Yadid, I. Perkins, B.B. O'Connor, F. Eweje, C.O. Chantre, M. A. Hemphill, H.Y. Yuan, P.H. Campbell, J.J. Vlassak, K.K. Parker, Cardiac microphysiological devices with flexible thin-film sensors for higher-throughput drug screening, Lab Chip 17 (21) (2017) 3692–3703.
[258] N. Thakur, A. Chaturvedi, D. Mandal, T.C. Nagaiah, Ultrasensitive and highly selective detection of dopamine by a NiFeP based flexible electrochemical sensor, Chem. Commun. 56 (60) (2020) 8448–8451.
[259] I.M. Saied, S. Chandran, T. Arslan, Integrated flexible hybrid silicone-textile dual-resonant sensors and switching circuit for wearable neurodegeneration monitoring systems, Ieee T. Biomed. Circ. S. 13 (6) (2019) 1304–1312.
[260] H.Y. Chen, S.J. Bao, C.M. Lu, L.S. Wang, J.H. Ma, P. Wang, H.B. Lu, F. Shu, S. B. Oetomo, W. Chen, Design of an integrated wearable multi-sensor platform based on flexible materials for neonatal monitoring, IEEE Access 8 (2020) 23732–23747.
[261] R.K. Pandey, E.F. Pribadi, P.C.P. Chao, Ieee in *A New Adaptive Readout System for a New OLED OPD Flexible Patch PPG Sensor*, 18th IEEE Sensors Conference, CANADA, Montreal, 2019. Montreal, CANADA, Oct 27-30.
[262] C.C. Zhou, H.W. Wang, Y.M. Zhang, X.S. Ye, Study of a ring-type surgical Pleth index monitoring system based on flexible PPG sensor, Ieee Sens. J. 21 (13) (2021) 14360–14368.
[263] S.C. Fan, L. Dan, L.J. Meng, W. Zheng, A. Elias, X.H. Wang, Improved response time of flexible microelectromechanical sensors employing eco-friendly nanomaterials, Nanoscale 9 (43) (2017) 16915–16921.
[264] T. Jin, Y. Pan, G.J. Jeon, H.I. Yeom, S.Y. Zhang, K.W. Paik, S.H.K. Park, Ultrathin nanofibrous membranes containing insulating microbeads for highly sensitive flexible pressure sensors, ACS Appl. Mater. Interfaces 12 (11) (2020) 13348–13359.
[265] X. Tang, C.Y. Wu, L. Gan, T. Zhang, T.T. Zhou, J. Huang, H. Wang, C.S. Xie, D. W. Zeng, Multilevel microstructured flexible pressure sensors with ultrahigh sensitivity and ultrawide pressure range for versatile electronic skins, Small 15 (10) (2019).
[266] J.B. Park, M.S. Song, R. Ghosh, R.K. Saroj, Y. Hwang, Y. Tchoe, H. Oh, H. Baek, Y. Lim, B. Kim, S.W. Kim, G.C. Yi, Highly sensitive and flexible pressure sensors using position- and dimension-controlled ZnO nanotube arrays grown on graphene films, NPG Asia Mater. 13 (1) (2021).
[267] J. Hughes, F. Iida, Multi-functional soft strain sensors for wearable physiological monitoring, Sensors 18 (11) (2018).
[268] A. Huang, M. Yoshida, Y. Ono, S. Rajan, Ieee in *Continuous Measurement of Arterial Diameter Using Wearable and Flexible Ultrasonic Sensor*, IEEE International Ultrasonics Symposium (IUS), Washington, DC, 2017. Washington, DC, Sepp. 06–09.
[269] G.M. Wang, S.M. Zhang, S.R. Dong, D. Lou, L. Ma, X.C. Pei, H.S. Xu, U. Farooq, W. Guo, J.K. Luo, Stretchable optical sensing patch system integrated heart rate, pulse oxygen saturation, and sweat pH detection, Ieee T. Bio-Med. Eng. 66 (4) (2019) 1000–1005.
[270] H.C. Li, Z.H. Wang, Z. Qu, Z.W. Liang, Y. Chen, Y.J. Ma, X. Feng, Flexible hybrid electronics for monitoring hypoxia, Ieee T. Biomed. Circ. S. 15 (3) (2021) 559–567.
[271] Y. Khan, D. Han, A. Pierre, J. Ting, X.C. Wang, C.M. Lochner, G. Bovo, N. Yaacobi-Gross, C. Newsome, R. Wilson, A.C. Arias, A flexible organic reflectance oximeter array, P. Natl. Acad. Sci. Usa. 115 (47) (2018), E11015-E11024.
[272] W.B. Bai, H.J. Yang, Y.J. Ma, H. Chen, J. Shin, Y.H. Liu, Q.S. Yang, I. Kandela, Z. H. Liu, S.K. Kang, C. Wei, C.R. Haney, A. Brikha, X.C. Ge, X. Feng, P.V. Braun, Y. G. Huang, W.D. Zhou, J.A. Rogers, Flexible transient optical waveguides and surface-wave biosensors constructed from monocrystalline silicon, Adv. Mater. 30 (32) (2018), e1801584.
[273] D. Han, Y. Khan, J. Ting, S.M. King, N. Yaacobi-Gross, M.J. Humphries, C. J. Newsome, A.C. Arias, Flexible blade-coated multicolor polymer light-emitting diodes for optoelectronic sensors, Adv. Mater. 29 (22) (2017), 1606206.
[274] T. Yokota, P. Zalar, M. Kaltenbrunner, H. Jinno, N. Matsuhisa, H. Kitanosako, Y. Tachibana, W. Yukita, M. Koizumi, T. Someya, Ultraflexible organic photonic skin, Sci. Adv. 2 (4) (2016), e1501856.
[275] C.M. Lochner, Y. Khan, A. Pierre, A.C. Arias, All-organic optoelectronic sensor for pulse oximetry, Nat. Commun. 5 (1) (2014) 1–7.
[276] J. Kim, P. Gutruf, A.M. Chiarelli, S.Y. Heo, K. Cho, Z. Xie, A. Banks, S. Han, K. I. Jang, J.W. Lee, Miniaturized battery-free wireless systems for wearable pulse oximetry, Adv. Funct. Mater. 27 (1) (2017), 1604373.
[277] Bijender, A. Kumar, Flexible and wearable capacitive pressure sensor for blood pressure monitoring, Sensing and Bio-Sensing Research (2021) 33.
[278] C. Peng, M.Y. Chen, H.K. Sim, Y. Zhu, X.N. Jiang, Noninvasive and nonocclusive blood pressure monitoring via a flexible piezo-composite ultrasonic sensor, Ieee Sens. J. 21 (3) (2021) 2642–2650.
[279] W.J. Luo, V. Sharma, D.J. Young, A paper-based flexible tactile sensor array for low-cost wearable human health monitoring, J. Microelectromech. Syst. 29 (5) (2020) 825–831.
[280] Y.X. Peng, J.Z. Zhou, X. Song, K. Pang, A. Samy, Z.M. Hao, J. Wang, A flexible pressure sensor with ink printed porous graphene for continuous cardiovascular status monitoring, Sensors 21 (2) (2021).
[281] Z. Yi, Z. Liu, W. Li, T. Ruan, X. Chen, J. Liu, B. Yang, W. Zhang, Piezoelectric dynamics of arterial pulse for wearable continuous blood pressure monitoring, Adv. Mater. 34 (16) (2022), 2110291.
[282] Z. Zhu, R. Li, T. Pan, Imperceptible epidermal–iontronic interface for wearable sensing, Adv. Mater. 30 (6) (2018), 1705122.
[283] A. Petritz, E. Karner-Petritz, T. Uemura, P. Schäffner, T. Araki, B. Stadlober, T. Sekitani, Imperceptible energy harvesting device and biomedical sensor based on ultraflexible ferroelectric transducers and organic diodes, Nat. Commun. 12 (1) (2021) 1–14.
[284] K.Y. Chun, S. Seo, C.S. Han, A wearable all-gel multimodal cutaneous sensor enabling simultaneous single-site monitoring of cardiac-related biophysical signals, Adv. Mater. 34 (16) (2022), 2110082.

[285] U. Hassan, M.H. Zulfiqar, M.M.U. Rahman, K. Riaz, In *Low Cost and Flexible Sensor System for Non-invasive Glucose In-Situ Measurement*, 17th International Bhurban Conference on Applied Sciences and Technology (IBCAST), Natl Ctr Phys, Islamabad, PAKISTAN, Jan 14-18, Natl Ctr Phys, Islamabad, PAKISTAN, 2020, pp. 187–190.
[286] Y. Yao, J.Y. Chen, Y.H. Guo, T. Lv, Z.L. Chen, N. Li, S.K. Cao, B.D. Chen, T. Chen, Integration of interstitial fluid extraction and glucose detection in one device for wearable non-invasive blood glucose sensors, Biosens. Bioelectron. (2021) 179.
[287] S.Y. Lin, W.D. Feng, X.F. Miao, X.X. Zhang, S.J. Chen, Y.Q. Chen, W. Wang, Y. N. Zhang, A flexible and highly sensitive nonenzymatic glucose sensor based on DVD-laser scribed graphene substrate, Biosens. Bioelectron. 110 (2018) 89–96.
[288] J.R. Sempionatto, M. Lin, L. Yin, K. Pei, T. Sonsa-ard, A.N. de Loyola Silva, A. A. Khorshed, F. Zhang, N. Tostado, S. Xu, An epidermal patch for the simultaneous monitoring of haemodynamic and metabolic biomarkers, Nat. Biomed. Eng. 5 (7) (2021) 737–748.
[289] W. Ling, G. Liew, Y. Li, Y. Hao, H. Pan, H. Wang, B. Ning, H. Xu, X. Huang, Materials and techniques for implantable nutrient sensing using flexible sensors integrated with metal–organic frameworks, Adv. Mater. 30 (23) (2018), 1800917.
[290] S. Cai, C. Xu, D. Jiang, M. Yuan, Q. Zhang, Z. Li, Y. Wang, Air-permeable electrode for highly sensitive and noninvasive glucose monitoring enabled by graphene fiber fabrics, Nano Energy 93 (2022), 106904.
[291] Y. Chen, S. Lu, S. Zhang, Y. Li, Z. Qu, Y. Chen, B. Lu, X. Wang, X. Feng, Skin-like biosensor system via electrochemical channels for noninvasive blood glucose monitoring, Sci. Adv. 3 (12) (2017), e1701629.
[292] Z. Pu, X. Zhang, H. Yu, J. Tu, H. Chen, Y. Liu, X. Su, R. Wang, L. Zhang, D. Li, A thermal activated and differential self-calibrated flexible epidermal biomicrofluidic device for wearable accurate blood glucose monitoring, Sci. Adv. 7 (5) (2021), eabd0199.
[293] G. Yang, Y. Tang, T. Lin, T. Zhong, Y. Fan, Y. Zhang, L. Xing, X. Xue, Y. Zhan, A self-powered closed-loop brain-machine-interface system for real-time detecting and rapidly adjusting blood glucose concentration, Nano Energy 93 (2022), 106817.
[294] L. Wang, S. Xie, Z. Wang, F. Liu, Y. Yang, C. Tang, X. Wu, P. Liu, Y. Li, H. Saiyin, Functionalized helical fibre bundles of carbon nanotubes as electrochemical sensors for long-term in vivo monitoring of multiple disease biomarkers, Nat. Biomed. Eng. 4 (2) (2020) 159–171.
[295] N.R. Shanmugam, S. Muthukumar, S. Chaudhry, J. Anguiano, S. Prasad, Ultrasensitive nanostructure sensor arrays on flexible substrates for multiplexed and simultaneous electrochemical detection of a panel of cardiac biomarkers, Biosens. Bioelectron. 89 (2017) 764–772.
[296] C.M. Boutry, L. Beker, Y. Kaizawa, C. Vassos, H. Tran, A.C. Hinckley, R. Pfattner, S. Niu, J. Li, J. Claverie, Biodegradable and flexible arterial-pulse sensor for the wireless monitoring of blood flow, Nat. Biomed. Eng. 3 (1) (2019) 47–57.
[297] J.U. Lind, T.A. Busbee, A.D. Valentine, F.S. Pasqualini, H. Yuan, M. Yadid, S.-J. Park, A. Kotikian, A.P. Nesmith, P.H. Campbell, Instrumented cardiac microphysiological devices via multimaterial three-dimensional printing, Nat. Mater. 16 (3) (2017) 303–308.
[298] S.R. Ruth, M.-g. Kim, H. Oda, Z. Wang, Y. Khan, J. Chang, P.M. Fox, Z. Bao, Post-surgical wireless monitoring of arterial health progression, iScience 24 (9) (2021), 103079.
[299] K.W. Cho, S.J. Kim, J. Kim, S.Y. Song, W.H. Lee, L. Wang, M. Soh, N. Lu, T. Hyeon, B.-S. Kim, Large scale and integrated platform for digital mass culture of anchorage dependent cells, Nat. Commun. 10 (1) (2019) 1–13.
[300] C. Dagdeviren, Y. Shi, P. Joe, R. Ghaffari, G. Balooch, K. Usgaonkar, O. Gur, P. L. Tran, J.R. Crosby, M. Meyer, Conformal piezoelectric systems for clinical and experimental characterization of soft tissue biomechanics, Nat. Mater. 14 (7) (2015) 728–736.
[301] L. Gao, Y. Zhang, V. Malyarchuk, L. Jia, K.-I. Jang, R. Chad Webb, H. Fu, Y. Shi, G. Zhou, L. Shi, Epidermal photonic devices for quantitative imaging of temperature and thermal transport characteristics of the skin, Nat. Commun. 5 (1) (2014) 1–10.
[302] J. Shin, Z.H. Liu, W.B. Bai, Y.H. Liu, Y. Yan, Y.G. Xue, I. Kandela, M. Pezhouh, M. R. MacEwan, Y.G. Huang, W.Z. Ray, W.D. Zhou, J.A. Rogers, Bioresorbable optical sensor systems for monitoring of intracranial pressure and temperature, Sci. Adv. 5 (7) (2019), eaaw1899.
[303] T.Z. Liu, P. Yao, Z. Li, H.Q. Feng, C.Y. Zhuang, X. Sun, C.X. Liu, N. Xue, Implantable sufficiently integrated multimodal flexible Sensor for intracranial monitoring, 20th IEEE sensors conference, Electron. Netw. (2021). Oct 31-Nov 04; Electr Network.
[304] J. Lee, H.R. Cho, G.D. Cha, H. Seo, S. Lee, C.-K. Park, J.W. Kim, S. Qiao, L. Wang, D.J. N.c. Kang, Flexible, sticky, and biodegradable wireless device for drug delivery to brain tumors 10 (1) (2019) 1–9.
[305] N. Manikandan, S. Muruganand, M. Divagar, C. Viswanathan, Design and fabrication of MEMS based intracranial pressure sensor for neurons study, Vacuum 163 (2019) 204–209.
[306] Q.Z. Liu, C.Z. Zhao, M.R. Chen, Y.H. Liu, Z.Y. Zhao, F.Q. Wu, Z. Li, P.S. Weiss, A. M. Andrews, C.W. Zhou, Flexible multiplexed In2O3 nanoribbon aptamer-field-effect transistors for biosensing, iScience 23 (9) (2020).
[307] Q.X. Wei, C.C. He, J. Chen, D.Y. Chen, J.B. Wang, Wireless passive intracranial pressure sensor based on a microfabricated flexible capacitor, IEEE Trans. Electron. Dev. 65 (6) (2018) 2592–2600.
[308] Q. Yang, S. Lee, Y. Xue, Y. Yan, T.L. Liu, S.K. Kang, Y.J. Lee, S.H. Lee, M.H. Seo, D. Lu, Materials, mechanics designs, and bioresorbable multisensor platforms for pressure monitoring in the intracranial space, Adv. Funct. Mater. 30 (17) (2020), 1910718.
[309] D. Lu, Y. Yan, Y. Deng, Q. Yang, J. Zhao, M.H. Seo, W. Bai, M.R. MacEwan, Y. Huang, W.Z. Ray, Bioresorbable wireless sensors as temporary implants for in vivo measurements of pressure, Adv. Funct. Mater. 30 (40) (2020), 2003754.
[310] B.Y. Zhang, Z.Y. Huang, H.X. Song, H.S. Kim, J. Park, Wearable intracranial pressure monitoring sensor for infants, Biosens. Bioelectron. 11 (7) (2021).
[311] J.H. Shin, Y. Yan, W.B. Bai, Y.G. Xue, P. Gamble, L.M. Tian, I. Kandela, C. R. Haney, W. Spees, Y. Lee, M. Choi, J. Ko, H. Ryu, J.K. Chang, M. Pezhouh, S. K. Kang, S.M. Won, K.J. Yu, J.N. Zhao, Y.K. Lee, M.R. MacEwan, S.K. Song, Y. G. Huang, W.Z. Ray, J.A. Rogers, Bioresorbable pressure sensors protected with thermally grown silicon dioxide for the monitoring of chronic diseases and healing processes, Nat. Biomed. Eng. 3 (1) (2019) 37–46.
[312] M. Farooq, T. Iqbal, P. Vazquez, N. Farid, S. Thampi, W. Wijns, A. Shahzad, Thin-film flexible wireless pressure sensor for continuous pressure monitoring in medical applications, Sensors 20 (22) (2020).
[313] K.D. Xu, S.J. Li, S.R. Dong, S.M. Zhang, G. Pan, G.M. Wang, L. Shi, W. Guo, C. N. Yu, J.K. Luo, Bioresorbable electrode array for electrophysiological and pressure signal recording in the brain, Adv. Healthcare Mater. 8 (15) (2019), e1801649.
[314] C. Huang, Y.T. Gu, J. Chen, A.A. Bahrani, E.G. Abu Jawdeh, H.S. Bada, K. Saatman, G.Q. Yu, L. Chen, A wearable fiberless optical sensor for continuous monitoring of cerebral blood flow in mice, Ieee J. Sel. Top. Quant. 25 (1) (2019).
[315] F. Wang, P. Jin, Y. Feng, J. Fu, P. Wang, X. Liu, Y. Zhang, Y. Ma, Y. Yang, A. Yang, Flexible Doppler ultrasound device for the monitoring of blood flow velocity, Sci. Adv. 7 (44) (2021), eabi9283.
[316] C. Howe, S. Mishra, Y.S. Kim, Y.F. Chen, S.H. Ye, W.R. Wagner, J.W. Jeong, H. S. Byun, J.H. Kim, Y. Chun, W.H. Yeo, Stretchable, implantable, nanostructured flow-diverter system for quantification of intra-aneurysmal hemodynamics, ACS Nano 12 (8) (2018) 8706–8716.
[317] M. Haruta, Y. Kurauchi, M. Ohsawa, C. Inami, R. Tanaka, K. Sugie, A. Kimura, Y. Ohta, T. Noda, K. Sasagawa, T. Tokuda, H. Katsuki, J. Ohta, Chronic brain blood-flow imaging device for a behavioral experiment using mice, Biomed. Opt Express 10 (4) (2019) 1557–1566.
[318] A.Y. Rwei, W. Lu, C.S. Wu, K. Human, E. Suen, D. Franklin, M. Fabiani, G. Gratton, Z.Q. Xie, Y.J. Deng, S.S. Kwak, L.Z. Li, C. Gu, A. Liu, C.M. Rand, T. M. Stewart, Y.G. Huang, D.E. Weese-Mayer, J.A. Rogers, A wireless, skin-interfaced biosensor for cerebral hemodynamic monitoring in pediatric care, P. Natl. Acad. Sci. Usa. 117 (50) (2020) 31674–31684.
[319] N.Z. Gurel, H.W. Jung, S. Hersek, O.T. Inan, Fusing near-infrared spectroscopy with wearable hemodynamic measurements improves classification of mental stress, Ieee Sens. J. 19 (19) (2019) 8522–8531.
[320] J. Si, M. Li, X. Zhang, R. Han, X. Ji, T. Jiang, Cerebral tissue oximeter suitable for real-time regional oxygen saturation monitoring in multiple clinical settings, Cognitive Neurodynamics (2022) 1–12.
[321] S.D. Petersen, A. Thyssen, M. Engholm, E.V. Thomsen, A flexible infrared sensor for tissue oximetry, Microelectron. Eng. 111 (2013) 130–136.
[322] Dhanjai, N. Yu, S.M. Mugo, A flexible-imprinted capacitive sensor for rapid detection of adrenaline, Talanta 204 (2019) 602–606.
[323] J.W. Oh, J. Heo, T.H. Kim, An electrochemically modulated single-walled carbon nanotube network for the development of a transparent flexible sensor for dopamine, Sensor. Actuator. B Chem. 267 (2018) 438–447.
[324] S.J. Kim, H.R. Cho, K.W. Cho, S. Qiao, J.S. Rhim, M. Soh, T. Kim, M.K. Choi, C. Choi, I. Park, Multifunctional cell-culture platform for aligned cell sheet monitoring, transfer printing, and therapy, ACS Nano 9 (3) (2015) 2677–2688.
[325] T.H. Chen, Z. Saadatnia, J. Kim, T. Looi, J. Drake, E. Diller, H.E. Naguib, Novel, flexible, and ultrathin pressure feedback sensor for miniaturized intraventricular neurosurgery robotic tools, Ieee T. Ind. Electron. 68 (5) (2021) 4415–4425.
[326] R.S. Karmakar, J.C. Wang, Y.T. Huang, K.J. Lin, K.C. Wei, Y.H. Hsu, Y.C. Huang, Y.J. Lu, Real-time intraoperative pressure monitoring to avoid surgically induced localized brain injury using a miniaturized piezoresistive pressure sensor, ACS Omega 5 (45) (2020) 29342–29350.
[327] H. Yang, Z. Qian, J. Wang, J. Feng, C. Tang, L. Wang, Y. Guo, Z. Liu, Y. Yang, K. Zhang, Carbon nanotube array-based flexible multifunctional electrodes to record electrophysiology and ions on the cerebral cortex in real time, Adv. Funct. Mater. 32 (38) (2022), 2204794.
[328] R. Garcia-Cortadella, G. Schwesig, C. Jeschke, X. Illa, A.L. Gray, S. Savage, E. Stamatidou, I. Schiessl, E. Masvidal-Codina, K. Kostarelos, Graphene active sensor arrays for long-term and wireless mapping of wide frequency band epicortical brain activity, Nat. Commun. 12 (1) (2021) 1–17.
[329] K. Tybrandt, D. Khodagholy, B. Dielacher, F. Stauffer, A.F. Renz, G. Buzsáki, J. Vörös, High-density stretchable electrode grids for chronic neural recording, Adv. Mater. 30 (15) (2018), 1706520.
[330] C. Xie, J. Liu, T.-M. Fu, X. Dai, W. Zhou, C.M. Lieber, Three-dimensional macroporous nanoelectronic networks as minimally invasive brain probes, Nat. Mater. 14 (12) (2015) 1286–1292.
[331] T.-i. Kim, J.G. McCall, Y.H. Jung, X. Huang, E.R. Siuda, Y. Li, J. Song, Y.M. Song, H.A. Pao, R.-H. Kim, Injectable, cellular-scale optoelectronics with applications for wireless optogenetics, Science 340 (6129) (2013) 211–216.
[332] I.R. Minev, P. Musienko, A. Hirsch, Q. Barraud, N. Wenger, E.M. Moraud, J. Gandar, M. Capogrosso, T. Milekovic, L. Asboth, Electronic dura mater for long-term multimodal neural interfaces, Science 347 (6218) (2015) 159–163.
[333] E.S. Ereifej, C.S. Smith, S.M. Meade, K. Chen, H. Feng, J.R. Capadona, The neuroinflammatory response to nanopatterning parallel grooves into the surface structure of intracortical microelectrodes, Adv. Funct. Mater. 28 (12) (2018), 1704420.
[334] L. Tian, B. Zimmerman, A. Akhtar, K.J. Yu, M. Moore, J. Wu, R.J. Larsen, J. W. Lee, J. Li, Y. Liu, Large-area MRI-compatible epidermal electronic interfaces

for prosthetic control and cognitive monitoring, Nat. Biomed. Eng. 3 (3) (2019) 194–205.
[335] S. Goodacre, R. Irons, Atrial arrhythmias, BMJ 324 (7337) (2002) 594–597.
[336] A.J. Starling, In Diagnosis and Management of Headache in Older Adults, Mayo Clinic Proceedings, Elsevier, 2018, pp. 252–262.
[337] H. Heidbuchel, The athlete's heart is a proarrhythmic heart, and what that means for clinical decision making, EP Europace 20 (9) (2018) 1401–1411.
[338] K.M. McLane, K. Bookout, S. McCord, J. McCain, L.S. Jefferson, The 2003 national pediatric pressure ulcer and skin breakdown prevalence survey: a multisite study, J. Wound, Ostomy Cont. Nurs. 31 (4) (2004) 168–178.
[339] H.U. Chung, B.H. Kim, J.Y. Lee, J. Lee, Z. Xie, E.M. Ibler, K. Lee, A. Banks, J. Y. Jeong, J. Kim, Binodal, wireless epidermal electronic systems with in-sensor analytics for neonatal intensive care, Science 363 (6430) (2019), eaau0780.
[340] Y. Wang, L. Yin, Y. Bai, S. Liu, L. Wang, Y. Zhou, C. Hou, Z. Yang, H. Wu, J. Ma, Electrically compensated, tattoo-like electrodes for epidermal electrophysiology at scale, Sci. Adv. 6 (43) (2020), eabd0996.
[341] J. Kim, D. Son, M. Lee, C. Song, J.-K. Song, J.H. Koo, D.J. Lee, H.J. Shim, J. H. Kim, M. Lee, A wearable multiplexed silicon nonvolatile memory array using nanocrystal charge confinement, Sci. Adv. 2 (1) (2016), e1501101.
[342] J.H. Koo, S. Jeong, H.J. Shim, D. Son, J. Kim, D.C. Kim, S. Choi, J.-I. Hong, D.-H. Kim, Wearable electrocardiogram monitor using carbon nanotube electronics and color-tunable organic light-emitting diodes, ACS Nano 11 (10) (2017) 10032–10041.
[343] H. Yuan, S.D. Silberstein, Vagus nerve and vagus nerve stimulation, a comprehensive review: part I, Headache J. Head Face Pain 56 (1) (2016) 71–78.
[344] H.N. Sabbah, I. Ilsar, A. Zaretsky, S. Rastogi, M. Wang, R.C. Gupta, Vagus nerve stimulation in experimental heart failure, Heart Fail. Rev. 16 (2011) 171–178.
[345] Y. Zhang, N. Zheng, Y. Cao, F. Wang, P. Wang, Y. Ma, B. Lu, G. Hou, Z. Fang, Z. Liang, Climbing-inspired twining electrodes using shape memory for peripheral nerve stimulation and recording, Sci. Adv. 5 (4) (2019), eaaw1066.
[346] T.-H. Kim, C.-S. Lee, S. Kim, J. Hur, S. Lee, K.W. Shin, Y.-Z. Yoon, M.K. Choi, J. Yang, D.-H. Kim, Fully stretchable optoelectronic sensors based on colloidal quantum dots for sensing photoplethysmographic signals, ACS Nano 11 (6) (2017) 5992–6003.
[347] Y. Gao, H. Ota, E.W. Schaler, K. Chen, A. Zhao, W. Gao, H.M. Fahad, Y. Leng, A. Zheng, F. Xiong, Wearable microfluidic diaphragm pressure sensor for health and tactile touch monitoring, Adv. Mater. 29 (39) (2017), 1701985.
[348] B. Ji, Q. Zhou, M. Lei, S. Ding, Q. Song, Y. Gao, S. Li, Y. Xu, Y. Zhou, B. Zhou, Gradient architecture-enabled capacitive tactile sensor with high sensitivity and ultrabroad linearity range, Small 17 (43) (2021), 2103312.
[349] H. Fang, K.J. Yu, C. Gloschat, Z. Yang, E. Song, C.-H. Chiang, J. Zhao, S.M. Won, S. Xu, M. Trumpis, Capacitively coupled arrays of multiplexed flexible silicon transistors for long-term cardiac electrophysiology, Nat. Biomed. Eng. 1 (3) (2017) 1–12.
[350] Y. Cheng, S. Da Ling, Y. Geng, Y. Wang, J. Xu, Microfluidic synthesis of quantum dots and their applications in bio-sensing and bio-imaging, Nanoscale Adv. 3 (8) (2021) 2180–2195.
[351] T. Ha, J. Tran, S. Liu, H. Jang, H. Jeong, R. Mitbander, H. Huh, Y. Qiu, J. Duong, R.L. Wang, A chest-laminated ultrathin and stretchable E-Tattoo for the measurement of electrocardiogram, seismocardiogram, and cardiac time intervals, Adv. Sci. 6 (14) (2019), 1900290.
[352] N. Wilson-Baig, T. McDonnell, A. Bentley, Discrepancy between SpO2 and SaO2 in patients with COVID-19, Anaesthesia 76 (Suppl 3) (2021) 6.
[353] M. Chushkin, L. Popova, E. Shergina, E. Krasnikova, O. Gordeeva, N. Karpina, Comparative Analysis of the Arterial Oxygen Saturation (SaO2) and Pulse Oximetry Measurements (SpO2) in Patients with Pulmonary Tuberculosis, Eur Respiratory Soc, 2020.
[354] P. Seguin, A. Le Rouzo, M. Tanguy, Y.M. Guillou, A. Feuillu, Y. Mallédant, Evidence for the need of bedside accuracy of pulse oximetry in an intensive care unit, Crit. Care Med. 28 (3) (2000) 703–706.
[355] E. Bruno, G. Maira, A. Biondi, M.P. Richardson, R.-C. Consortium, Ictal hypoxemia: a systematic review and meta-analysis, Seizure 63 (2018) 7–13.
[356] A. Sharma, J.F. Arambula, S. Koo, R. Kumar, H. Singh, J.L. Sessler, J.S. Kim, Hypoxia-targeted drug delivery, Chem. Soc. Rev. 48 (3) (2019) 771–813.
[357] R. Deepa, C. Shanthirani, R. Pradeepa, V. Mohan, Is the 'rule of halves' in hypertension still valid? Evidence from the Chennai Urban Population Study, J. Assoc. Phys. India 51 (2) (2003) 153–157.
[358] A. Banker, C. Bell, M. Gupta-Malhotra, J. Samuels, Blood pressure percentile charts to identify high or low blood pressure in children, BMC Pediatr. 16 (1) (2016) 1–7.
[359] J. Mayet, A. Hughes, Cardiac and vascular pathophysiology in hypertension, Heart 89 (9) (2003) 1104–1109.
[360] W. Van Moer, L. Lauwers, D. Schoors, K. Barbe, Linearizing oscillometric blood-pressure measurements: (Non)Sense? Ieee T. Instrum. Meas. 60 (4) (2011) 1267–1275.
[361] J.C. Yang, J. Mun, S.Y. Kwon, S. Park, Z. Bao, S. Park, Electronic skin: recent progress and future prospects for skin-attachable devices for health monitoring, robotics, and prosthetics, Adv. Mater. 31 (48) (2019), 1904765.
[362] Y. Ma, Y. Zhang, S. Cai, Z. Han, X. Liu, F. Wang, Y. Cao, Z. Wang, H. Li, Y. Chen, Flexible hybrid electronics for digital healthcare, Adv. Mater. 32 (15) (2020), 1902062.
[363] M.K. Choi, O.K. Park, C. Choi, S. Qiao, R. Ghaffari, J. Kim, D.J. Lee, M. Kim, W. Hyun, S.J. Kim, Epidermal electronics: cephalopod-inspired miniaturized suction cups for smart medical skin (adv. Healthcare mater. 1/2016), Adv. Healthcare Mater. 5 (1) (2016), 186-186.
[364] D.M. Drotlef, M. Amjadi, M. Yunusa, M. Sitti, Bioinspired composite microfibers for skin adhesion and signal amplification of wearable sensors, Adv. Mater. 29 (28) (2017), 1701353.
[365] J.F. Santiago, F.F. Carvalho, S.R. Perosa, M.R. Siliano, J.W. Cruz, M.J. S. Fernandes, E.A. Cavalheiro, D. Amado, M.d.G. Naffah-Mazzacoratti, Effect of glycemic state in rats submitted to status epilepticus during development, Arquivos de neuro-psiquiatria 64 (2006) 233–239.
[366] S. La Fleur, Daily rhythms in glucose metabolism: suprachiasmatic nucleus output to peripheral tissue, J. Neuroendocrinol. 15 (3) (2003) 315–322.
[367] G. Raue, V. Keim, Secondary diabetes in chronic pancreatitis, Zeitschrift fur Gastroenterologie (1999) 4–9.
[368] N. Waugh, E. Cummins, P. Royle, C. Clar, M. Marien, B. Richter, S. Philip, Newer agents for blood glucose control in type 2 diabetes: systematic review and economic evaluation, Health Technol. Assess. 14 (36) (2010) 1–248.
[369] P. Mitrou, S.A. Raptis, G. Dimitriadis, Insulin action in hyperthyroidism: a focus on muscle and adipose tissue, Endocr. Rev. 31 (5) (2010) 663–679.
[370] A. Ceriello, Acute hyperglycaemia: a 'new'risk factor during myocardial infarction, Eur. Heart J. 26 (4) (2005) 328–331.
[371] C.M. Helgason, Blood glucose and stroke, Stroke 19 (8) (1988) 1049–1053.
[372] D.O. Ferris, G.D. Molnar, N. Schnelle, J.D. Jones, E.A. Moffitt, Recent advances in management of functioning islet cell tumor, Arch. Surg. 104 (4) (1972) 443–446.
[373] E. Webb, M. Dattani, Understanding hypopituitarism, Paediatr. Child Health 25 (7) (2015) 295–301.
[374] N. Gao, W. Zhang, Y.-z. Zhang, Q. Yang, S.-h. Chen, Carotid intima-media thickness in patients with subclinical hypothyroidism: a meta-analysis, Atherosclerosis 227 (1) (2013) 18–25.
[375] A.J. Bandodkar, W. Jia, C. Yardımcı, X. Wang, J. Ramirez, J. Wang, Tattoo-based noninvasive glucose monitoring: a proof-of-concept study, Anal. Chem. 87 (1) (2015) 394–398.
[376] G. Rao, R. Guy, P. Glikfeld, W. LaCourse, L. Leung, J. Tamada, R. Potts, N. Azimi, Reverse iontophoresis: noninvasive glucose monitoring in vivo in humans, Pharmaceut. Res. 12 (12) (1995) 1869–1873.
[377] T.S. Ching, P. Connolly, Simultaneous transdermal extraction of glucose and lactate from human subjects by reverse iontophoresis, Int. J. Nanomed. 3 (2) (2008) 211.
[378] A.J. Bandodkar, P. Gutruf, J. Choi, K. Lee, Y. Sekine, J.T. Reeder, W.J. Jeang, A. J. Aranyosi, S.P. Lee, J.B. Model, Battery-free, skin-interfaced microfluidic/electronic systems for simultaneous electrochemical, colorimetric, and volumetric analysis of sweat, Sci. Adv. 5 (1) (2019), eaav3294.
[379] R. Chen, A. Canales, P. Anikeeva, Neural recording and modulation technologies, Nat. Rev. Mater. 2 (2) (2017) 1–16.
[380] S.N. Bhatia, D.E. Ingber, Microfluidic organs-on-chips, Nat. Biotechnol. 32 (8) (2014) 760–772.
[381] S.I. Park, D.S. Brenner, G. Shin, C.D. Morgan, B.A. Copits, H.U. Chung, M. Y. Pullen, K.N. Noh, S. Davidson, S.J. Oh, Soft, stretchable, fully implantable miniaturized optoelectronic systems for wireless optogenetics, Nat. Biotechnol. 33 (12) (2015) 1280–1286.
[382] A. Canales, X. Jia, U.P. Froriep, R.A. Koppes, C.M. Tringides, J. Selvidge, C. Lu, C. Hou, L. Wei, Y. Fink, Multifunctional fibers for simultaneous optical, electrical and chemical interrogation of neural circuits in vivo, Nat. Biotechnol. 33 (3) (2015) 277–284.
[383] E.A. Kiyatkin, Brain temperature fluctuations during physiological and pathological conditions, Eur. J. Appl. Physiol. 101 (2007) 3–17.
[384] A.R. Bain, L. Nybo, P.N. Ainslie, Cerebral vascular control and metabolism in heat stress, Compr. Physiol. 5 (3) (2011) 1345–1380.
[385] C. Childs, Human brain temperature: regulation, measurement and relationship with cerebral trauma: part 1, Br. J. Neurosurg. 22 (4) (2008) 486–496.
[386] S. Mrozek, F. Vardon, T. Geeraerts, Brain temperature: physiology and pathophysiology after brain injury, Anesthesiology research and practice (2012) 2012.
[387] E.A. Kiyatkin, Brain temperature and its role in physiology and pathophysiology: lessons from 20 years of thermorecording, Temperature 6 (4) (2019) 271–333.
[388] A. Dittmar, C. Gehin, G. Delhomme, D. Boivin, G. Dumont, C. Mott, Ieee in *A non invasive wearable sensor for the measurement of brain temperature*, in: E-And, 28th Annual International Conference of the IEEE-Engineering-In-Medicin, Biology-Society, New York, NY, 2006, p. 3994. New York, NY, Aug 30-Sep. 03.
[389] U. Izhar, L. Piyathilaka, D. Preethichandra, Sensors for brain temperature measurement and monitoring–A review, Neuroscience Informatics (2022), 100106.
[390] U. Kawoos, R.M. McCarron, C.R. Auker, M. Chavko, Advances in intracranial pressure monitoring and its significance in managing traumatic brain injury, Int. J. Mol. Sci. 16 (12) (2015) 28979–28997.
[391] N. Stocchetti, A.I. Maas, Traumatic intracranial hypertension, N. Engl. J. Med. 370 (22) (2014) 2121–2130.
[392] B. Mokri, The Monro-Kellie hypothesis - applications in CSF volume depletion, Neurology 56 (12) (2001) 1746–1748.
[393] W.H. Lee, G.D. Cha, D.H. Kim, Flexible and biodegradable electronic implants for diagnosis and treatment of brain diseases, Curr. Opin. Biotechnol. 72 (2021) 13–21.
[394] N. Carney, A.M. Totten, C. O'Reilly, J.S. Ullman, G.W. Hawryluk, M.J. Bell, S. L. Bratton, R. Chesnut, O.A. Harris, N. Kissoon, Guidelines for the management of severe traumatic brain injury, Neurosurgery 80 (1) (2017) 6–15.
[395] J. Zhong, M. Dujovny, H.K. Park, E. Perez, A.R. Perlin, F.G. Diaz, Advances in ICP monitoring techniques, Neurol. Res. 25 (4) (2003) 339–350.

[396] K.B. Evensen, P.K. Eide, Measuring intracranial pressure by invasive, less invasive or non-invasive means: limitations and avenues for improvement, Fluids Barriers CNS 17 (1) (2020) 1–33.
[397] P. Blanco, A. Abdo-Cuza, Transcranial Doppler ultrasound in neurocritical care, Journal of Ultrasound 21 (2018) 1–16.
[398] X. Zhang, J.E. Medow, B.J. Iskandar, F. Wang, M. Shokoueinejad, J. Koueik, J. G. Webster, Invasive and noninvasive means of measuring intracranial pressure: a review, Physiol. Meas. 38 (8) (2017) 143–182.
[399] M. Czosnyka, J.D. Pickard, Monitoring and interpretation of intracranial pressure, J. Neurol. Neurosurg. Psychiatr. 75 (6) (2004) 813–821.
[400] G.D. Cha, D. Kang, J. Lee, D.H. Kim, Bioresorbable electronic implants: history, materials, fabrication, devices, and clinical applications, Adv. Healthcare Mater. 8 (11) (2019).
[401] R. Li, H.T. Cheng, Y.W. Su, S.W. Hwang, L. Yin, H. Tao, M.A. Brenckle, D.H. Kim, F.G. Omenetto, J.A. Rogers, Y.G. Huang, An analytical model of reactive diffusion for transient electronics, Adv. Funct. Mater. 23 (24) (2013) 3106–3114.
[402] A. Silverman, N. Petersen. Physiology, cerebral autoregulation, StatPearls. Treasure Island (FL), StatPearls Publishing, 2023 Jan-.
[403] R.V. Immink, F.C. Pott, N.H. Secher, J.J. Van Lieshout, Hyperventilation, cerebral perfusion, and syncope, J. Appl. Physiol. 116 (7) (2014) 844–851.
[404] J. Astrup, B.K. Siesjö, L. Symon, Thresholds in cerebral ischemia-the ischemic penumbra, Stroke 12 (6) (1981) 723–725.
[405] R.S. Marshall, The functional relevance of cerebral hemodynamics: why blood flow matters to the injured and recovering brain, Curr. Opin. Neurol. 17 (6) (2004) 705–709.
[406] S.H. Friess, T.J. Kilbaugh, , Huh, J. W. J. C. c. r., practice, Advanced neuromonitoring and imaging in pediatric traumatic brain injury, Crit. Care. Res. Pract. 2012 (2012).
[407] T. Partington, A. Farmery, Intracranial pressure and cerebral blood flow, Anaesth. Intensive Care Med. 15 (4) (2014) 189–194.
[408] P. Brauer, E. Kochs, C. Werner, M. Bloom, R. Policare, S. Pentheny, H. Yonas, W. A. Kofke, Schulte am Esch, J., Correlation of transcranial Doppler sonography mean flow velocity with cerebral blood flow in patients with intracranial pathology, J. Neurosurg. Anesthesiol. 10 (2) (1998) 80–85.
[409] K.J. Busch, H. Kiat, M. Stephen, M. Simons, A. Avolio, M.K. Morgan, Cerebral hemodynamics and the role of transcranial Doppler applications in the assessment and management of cerebral arteriovenous malformations, J. Clin. Neurosci. 30 (2016) 24–30.
[410] H.S. Markus, Transcranial Doppler ultrasound, Br. Med. Bull. 56 (2) (2000) 378–388.
[411] S.S. Kazmi, L.M. Richards, C.J. Schrandt, M.A. Davis, A.K. Dunn, Expanding applications, accuracy, and interpretation of laser speckle contrast imaging of cerebral blood flow, J. Cerebr. Blood Flow Metabol. 35 (7) (2015) 1076–1084.
[412] T. Durduran, A.G. Yodh, Diffuse correlation spectroscopy for non-invasive, micro-vascular cerebral blood flow measurement, Neuroimage 85 (2014) 51–63.
[413] S. Tewolde, K. Oommen, D.Y. Lie, Y. Zhang, M.-C. Chyu, Epileptic seizure detection and prediction based on continuous cerebral blood flow monitoring–a review, Journal of healthcare engineering 6 (2) (2015) 159–178.
[414] P. Matz, L. Pitts, Monitoring in traumatic brain injury, Clin. Neurosurg. 44 (1997) 267–294.
[415] R.S. Shah, D.S. Jeyaretna, Cerebral vascular anatomy and physiology, Surgery 36 (11) (2018) 606–612.
[416] O.S. Akbik, A.P. Carlson, M. Krasberg, H. Yonas, The utility of cerebral blood flow assessment in TBI, Curr. Neurol. Neurosci. Rep. 16 (2016) 1–11.
[417] D. Roh, S. Park, Brain multimodality monitoring: updated perspectives, Curr. Neurol. Neurosci. Rep. 16 (6) (2016) 56.
[418] S.L. Bratton, R.M. Chestnut, J. Ghajar, F.F. McConnell Hammond, O.A. Harris, R. Hartl, G.T. Manley, A. Nemecek, D.W. Newell, G.X. Rosenthal, Brain oxygen monitoring and thresholds, J. Neurotrauma 24 (2007). Supplement 1), S-65-S-70.
[419] A. Bhatia, A.K. Gupta, Neuromonitoring in the intensive care unit. II. Cerebral oxygenation monitoring and microdialysis, Intensive Care Med. 33 (8) (2007) 1322–1328.
[420] R. Nangunoori, E. Maloney-Wilensky, M. Stiefel, S. Park, W. Andrew Kofke, J. M. Levine, W. Yang, P.D. Le Roux, Brain tissue oxygen-based therapy and outcome after severe traumatic brain injury: a systematic literature review, Neurocritical Care 17 (2012) 131–138.
[421] L.E. Bohman, J.M. Pisapia, M.R. Sanborn, S. Frangos, E. Lin, M. Kumar, S. Park, W.A. Kofke, M.F. Stiefel, P.D. LeRoux, J.M. Levine, Response of brain oxygen to therapy correlates with long-term outcome after subarachnoid hemorrhage, Neurocritical Care 19 (3) (2013) 320–328.
[422] M.F. Stiefel, A. Spiotta, V.H. Gracias, A.M. Garuffe, O. Guillamondegui, E. Maloney-Wilensky, S. Bloom, M.S. Grady, P.D. LeRoux, Reduced mortality rate in patients with severe traumatic brain injury treated with brain tissue oxygen monitoring, J. Neurosurg. 103 (5) (2005) 805–811.
[423] N. Tasneem, E.A. Samaniego, C. Pieper, E.C. Leira, H.P. Adams, D. Hasan, S. Ortega-Gutierrez, Brain multimodality monitoring: a new tool in neurocritical care of comatose patients, Crit. Care. Res. Pract. 2017 (2017).
[424] T.W.L. Scheeren, M.H. Kuizenga, H. Maurer, M. Struys, M. Heringlake, Electroencephalography and brain oxygenation monitoring in the perioperative period, Anesth. Analg. 128 (2) (2019) 265–277.
[425] E.W. Lang, M. Jaeger, Systematic and comprehensive literature review of publications on direct cerebral oxygenation monitoring, Open Crit. Care Med. J. 6 (1) (2013).
[426] A. Ledo, E. Fernandes, J.E. Quintero, G.A. Gerhardt, R.M. Barbosa, Electrochemical evaluation of a multi-site clinical depth recording electrode for monitoring cerebral tissue oxygen, Micromachines 11 (7) (2020).
[427] M.A. De Georgia, Brain tissue oxygen monitoring in neurocritical care, J. Intensive Care Med. 30 (8) (2015) 473–483.
[428] P. Yao, W. Guo, X. Sheng, D. Zhang, X. Zhu, In A portable multi-channel wireless NIRS device for muscle activity real-time monitoring, in: 36th Annual International Conference of the IEEE Engineering in Medicine and Biology Society, IEEE, 2014, pp. 3719–3722, 2014.
[429] M. Broom, A.M. Dunk, A.-L. E Mohamed, Predicting neonatal skin injury: the first step to reducing skin injuries in neonates, Health Serv. Insights 12 (2019), 1178632919845630.
[430] B. Blankertz, M. Tangermann, C. Vidaurre, S. Fazli, C. Sannelli, S. Haufe, C. Maeder, L.E. Ramsey, I. Sturm, G. Curio, The Berlin brain–computer interface: non-medical uses of BCI technology, Front. Neurosci. (2010) 198.
[431] J. Nortje, A.K. Gupta, The role of tissue oxygen monitoring in patients with acute brain injury, Br. J. Anaesth. 97 (1) (2006) 95–106.
[432] S.A. Zaidi, Utilization of an environmentally-friendly monomer for an efficient and sustainable adrenaline imprinted electrochemical sensor using graphene, Electrochim. Acta 274 (2018) 370–377.
[433] S.M. Gu, W. Wang, F.S. Wang, J.H. Huang, Neuromodulator and emotion biomarker for stress induced mental disorders, Neural Plast. 2016 (2016), 2609128.
[434] N. Coppede, G. Tarabella, M. Villani, D. Calestani, S. Iannotta, A. Zappettini, Human stress monitoring through an organic cotton-fiber biosensor, J. Mater. Chem. B 2 (34) (2014) 5620–5626.
[435] J. Strahler, S. Fischer, U.M. Nater, U. Ehlert, J. Gaab, Norepinephrine and epinephrine responses to physiological and pharmacological stimulation in chronic fatigue syndrome, Biol. Psychol. 94 (1) (2013) 160–166.